MATHEMATICAL MODELING OF INFECTIOUS DISEASES

BY

IFTIKHAR AHMED

DISSERTATION

Submitted in partial fulfillment of the requirements
for the degree of Doctor of Philosophy in Mathematics
in the Graduate College of the
University of Illinois at Urbana-Champaign, 2020

Urbana, Illinois

Doctoral Committee:

Professor Lee DeVille, Chair
Professor Zoi Rapti, Director of Research
Professor Vadim Zharnitsky
Professor Carla Cáceres

ABSTRACT

In this dissertation, we studied mathematical models of infectious diseases that consist of ordinary differential equations (ODEs) and partial differential equations (PDEs). An ODE model is formulated to describe the dynamics of wild mosquitoes when *Wolbachia*-infected female and male mosquitoes are introduced in the wild as a biological control, where we assume imperfect maternal transmission of *Wolbachia* to offspring and incomplete cytoplasmic incompatibility. In order to reduce the population of wild mosquitoes with minimal release of *Wolbachia*-infected mosquitoes in the wild, we develop an optimal control model. The optimal controls are found by using the Pontryagin's Maximum Principle. We also formulated an ODE optimal control model to describe the dynamics of dengue-infected humans when *Wolbachia*-infected mosquitoes are introduced in the wild along with efforts on educational campaigns to motivate individuals for using personal protection in order to reduce humans-mosquitoes. In this optimal control model, we also determined the most cost-effectiveness control strategy among different control interventions to reduce dengue infections in humans. In the host (*Daphnia*)– parasite (fungal spores) system, we study the disease dynamics of *Daphnia* in a water column where both algae and spores sink and diffuse. We formulated the*Daphnia*-spores-algae model using advection-diffusion partial differential equations (PDEs). We studied the effects of algal carrying capacity, sinking rates of algae and spores, and the water column maximum depth on the disease dynamics of *Daphnia*.

To my parents, for their love and support.

ACKNOWLEDGMENTS

This dissertation would not have been possible without the support of many people. First, I would like to thank my advisor, Zoi Rapti, for her guidance and great ideas on my research. Without her help and guidance, it would not have been possible to finish this dissertation. I would also like to thank my doctoral committee members Lee DeVille, Carla Cáceres, and Vadim Zharnitsky, for their time and guidance on my research. I am very appreciative of all the financial support I have received over the years, including the COMSATS fellowship for my MS program at the University of Illinois at Urbana-Champaign, Illini Campus Research Board grant RB14038, and National Science Foundation grant DUE-1129198. Thanks to my mother, father, brothers, and sisters for their love and support. Finally, I would like to thank my wife, Aarouj Ahmed, for her support, help, and taking care of my lovely daughters, Manaal and Mafaaz Ahmed, when I sit till late at night in the office and work on my dissertation.

TABLE OF CONTENTS

CHAPTER 1

INTRODUCTION

In this thesis, we develop and investigate mathematical models that consist of ordinary and partial differential equations to describe

1. the dynamics of wild mosquitoes when *Wolbachia*-infected mosquitoes are introduced in the wild as a biological control method,

2. optimal release of *Wolbachia*-infected mosquitoes in the wild to suppress the population of wild mosquitoes,

3. the transmission of dengue epidemic when *Wolbachia*-infected mosquitoes are used as a potential control measure,

4. optimal release of *Wolbachia*-infected mosquitoes in combination with educational campaign efforts for reducing dengue infections in humans,

5. the disease dynamics of *Daphnia* when both fungal spores and algae sink and diffuse in a water column.

In this chapter, we present background information on mosquito-borne diseases and *Daphnia* epidemics, along with terminologies and modeling techniques that we will use in subsequent chapters.

1.1 Mathematical models

Mathematical models are a useful tool to understand the spread of infectious diseases within-host and between hosts and vectors. Mathematical models can help to understand the

occurrences of outbreaks, the persistence of disease, and testing and comparing different intervention strategies for controlling infectious diseases. Three fundamental questions arise after an infected host is introduced into a susceptible population:

1. Does an epidemic occur?

2. If an epidemic occurs, then what proportion of the susceptible hosts get infected?

3. How does the infection spread with time and space?

Mathematical models can help to answer these questions. For example, whether a disease persists or not after introducing an infected individual into a susceptible population can be answered using the basic reproduction number $\mathscr{R}_0$. The basic reproduction number, $\mathscr{R}_0$, is defined as the average number of secondary infections produced by a single infected individual during the infectious period when introduce into a susceptible population [1].

1.1.1 Forward and backward bifurcations

In epidemic models, two phenomena, forward and backward bifurcations, usually arise depending on the value of $\mathscr{R}_0$. Generally, a disease invades if the basic reproduction number is greater than unity ($\mathscr{R}_0 > 1$) and dies out if $\mathscr{R}_0 < 1$ [1]. As the basic reproduction number increases through 1, there is an exchange of stability between the disease-free equilibrium and endemic equilibrium at $\mathscr{R}_0 = 1$, which is called forward (or transcritical) bifurcation [2, 3]. In the case of a forward bifurcation, a disease can not spread if $\mathscr{R}_0 < 1$. However, in various complex epidemic models, a stable endemic equilibrium may also exist when the basic reproduction number is less than one ($\mathscr{R}_0 < 1$). In this situation, the system can tend to a stable endemic equilibrium state when the basic reproduction number is less than one ($\mathscr{R}_0 < 1$). This phenomenon is called backward bifurcation. In the case of a forward bifurcation, it is sufficient to reduce the basic reproduction number below one ($\mathscr{R}_0 < 1$) to eradicate a disease but $\mathscr{R}_0 < 1$ is not sufficient, although necessary, to eradicate a disease in the case of the backward bifurcation. In epidemic models that exhibit the backward bifurcation phenomenon, It is necessary to reduce $\mathscr{R}_0$ well below one to control the disease epidemic. The backward bifurcation has been observed and studied in many infectious disease models [3–8].

1.1.2 Mathematical models for mosquito-borne diseases

Several types of models are used to study infectious diseases such as deterministic, stochastic, agent-based, and statistical models. In 1911, Ross [9] used a simple compartmental model to explain the relationship between the incidence of malaria in the number of mosquitoes and humans. Since then, deterministic models have been widely used to study the dynamics of mosquito-borne diseases. In deterministic models, a population is divided into different compartments (classes), and differential equations are used to express transition rates from one compartment to another compartment. For example, in mosquito-borne diseases models, the population of humans and mosquitoes is normally divided into the following compartments:

- Susceptible (S): This compartment represents the number of individuals that are not infected yet but can become infected in the future.
- Exposed (E): This compartment represents the number of individuals that are exposed to the disease, but they are not transmitting the disease to other susceptible individuals yet.
- Infected (I): This compartment represents the number of individuals that are infectious and can transmit the disease to other individuals.
- Recovered (R): This compartment represents the number of individuals who have been infected and recovered from the disease. There is no recovery compartment for mosquitoes since they do not recover from the disease due to the short life span.

Other types of compartment models have also been studied in the literature, for example SI, SIR, SIS, $SIRS$, $SEIR$ to name a few, and the choice of which compartments to include in a model depends on the disease under study. For example, we may ignore the exposed compartment in the model if the incubation period of a disease is very short. The flow diagram of a general $SEIR$ type compartmental model is shown in Figure (1.1) for mosquito-borne diseases.

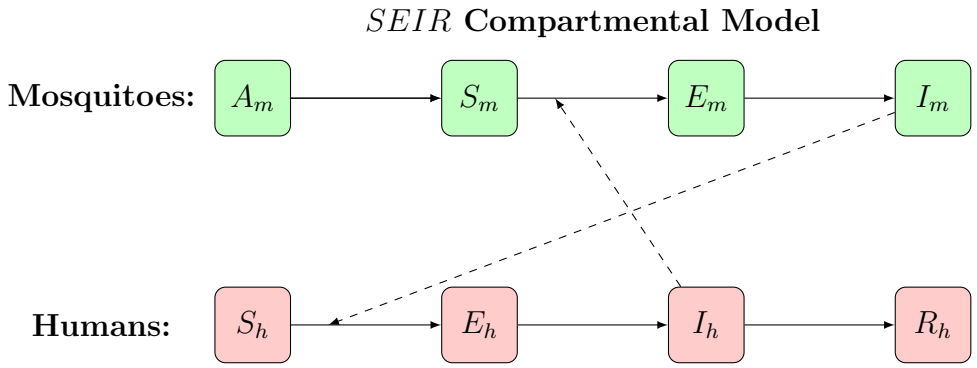

Figure 1.1: A general $SEIR$ compartmental model for mosquitoes borne diseases. The solid arrows show the rate of movement of mosquitoes and humans between two compartments. The dash arrows indicate paths of disease transmission between mosquitoes and humans. The subscript h is used for variables related to the human population, while the subscript m is used for variables related to the mosquitoes population.

1.2 Optimal control theory in epidemic models

Optimal control theory is a useful mathematical tool for assessing the effect of different intervention strategies in infectious disease models. For example, what fraction of people need to be vaccinated as time evolves to minimize the number of infected people and the cost of implementing the vaccination strategy? The desired goal (or objective) in optimal control problems depends on situations. For mosquito-borne disease models, the main goal is to minimize the number of infected individuals (humans) and mosquitoes along with minimizing the cost of implementing control strategies (for example, spraying, larvicide, use of bed nets to reduce contacts between humans and mosquitoes, etc.). We only explain the general theory of optimal control for a single ordinary differential equation (ODE), but it can be extended to a system of ODEs [10, 11]. The state of a system in terms of a single ODE is given by

$$\begin{cases} \frac{dy(t)}{dt} = f(y(t), t) \\ \text{with initial condition} \\ y(0) = y_0. \end{cases} \tag{1.1}$$

Now if the state of the system can be controlled through a variable $u(.)$ (called control variable), then the state equation (1.1) becomes

$$\begin{cases} \frac{dy(t)}{dt} &= f\left(y(t), u(t), t\right) \\ y(0) &= y_0, \end{cases} \tag{1.2}$$

where f is a continuously differentiable function. Note that the solution of the ODE (1.2) depends on the control variable $u(.)$ as well as on the the initial condition y_0. The control variable is usually constrained and let $u_{\max}$ denotes the upper bound on the control variable. The set $\mathcal{U} = \{u : [0, \infty) \to u_{\max} \mid u(.) \quad \text{measureable}\}$ denotes the collection of all admissible controls. Knowing the initial condition y_0 and the control trajectory $u(.)$ over the interval $[0, T]$, the state equation (1.2) can be integrated to get the state trajectory $y(.)$ over the same interval $[0, T]$. The goal of an optimal control problem is to determine a piecewise optimal control $u(.)$ and the associated state variable $y(.)$ on the interval $[0, T]$ that minimizes a given objective functional,

$$\begin{aligned} & J(y(.), u(.)) && = \min_u \textstyle\int_0^T g(y(t), u(t))\, dt, \\ & \text{subject to} && \\ & \tfrac{dy(t)}{dt} && = f\left(y(t), u(t)\right) \\ & y(0) = y_0 && \text{and} \quad y(T) \quad \text{free.} \end{aligned} \tag{1.3}$$

where $y(.)$ solves (1.2) for the control $u(.)$ and g is a given continuously differentiable function of the state variable (y), control variable u and time (t). We will denote the optimal control with $u^*(t)$ and the optimal trajectory, the solution of the state equation when $u = u^*$, with y^*.

The constraints on the controls (and possibly on the state variable as well) limit the values of the state variable at the final time T. Let χ denotes the set of possible values that can be reached when the state variable $y(t)$ and the control variable $u(t)$ satisfy imposed constraints. If there are no constraints on the state variable, then $y(T)$ is free, that is, the value of $y(T)$ is unrestricted at the final time T. The final time T is fixed for models that we consider in this dissertation. The objective is to find a control $u^*(.)$, which minimizes

the cost functional given in Eq. (1.3), that is

$$J(u^*) \leq J(u(.))$$

for all controls $u(.) \in \mathcal{U}$. The control $u^*(.)$ when it exists is called optimal control. The functions f and g are continuously differentiable functions in their arguments y and u. To show that an optimal control exists, we make use of the following theorem from Fleming and Rishel [12].

Theorem 1.1 (Existence of optimal control)**.** *1. The set of solutions of the state equation is not empty, i.e. there exists at least one pair* $(y(t), u(t))$ *that solves the state equations and satisfies the control constraints.*

2. *The set of admissible controls* $\mathcal{U}$ *is convex and closed.*

3. *The function* f*, which is the right hand side of the state equation* (1.2)*, is continuous, bounded from above by a sum of the state and control variables i.e.*

$$f(t, y(t), u(t) \leq c_1(1 + |y(t)| + |u(t)|).$$

4. f *can be written as linear function of the control i.e.*

$$f(t, x(t), u(t) = N(t, y(t)) + L(t, y(t))u.$$

5. $|f(t, y_1, u) - f(t, y, u)| \leq c_2|y_1 - y|(1 + |u|)$

6. *The integrand* $g(t, y, u)$ *in* (1.3) *is convex with respect to control and also satisfies* $g(t, y, u) \leq \alpha_1|u|^\alpha - \alpha_2$ *for some fixed* $\alpha_1 > 0$, $\alpha_2 \in \mathbb{R}$ *and* $\alpha > 1$.

Condition (i) implies that the problem is well-posed and is needed if the minimum problem is to make sense. Conditions (ii) and (iii) guarantees that the solution remains uniformly bounded for all t in the interval $[0, T]$. In condition (iv), the convexity of $f(t, y(t), u(t))$ is required for the existence of a minimum solution. If $f(t, y, u)$ is not convex then minimum

solution does not exist in general. In condition (v), Lipschitz continuity ensures that the system has a unique solution.

1.2.1 Characterization of controls

If the optimal control exists, that is all conditions of theorem (1.1) are satisfied, we use Pontryagin's Maximum Principle [13] to obtain the characterization of the optimal control in terms of the state and adjoint variables. Pontryagin's Maximum Principle converts the minimization of the objective functional subject to the state system into pointwise minimization of Hamiltonian with respect to the control variable. The Hamiltonian $\mathcal{H}$ is defined as

$$\mathcal{H} = \underbrace{g(y(t), u(t))}_{\text{integrand}} + \lambda_y \underbrace{f(y(t), u(t))}_{\text{r.h.s of the state equation}}, \tag{1.4}$$

where λ_x is the adjoint variable associated with the state x. Note that in the Hamiltonia $\mathcal{H}$, the first term denotes the integrand of the objective functional, while the adjoint variable λ_y is multiplied with the right-hand side of the associated state variable.

Theorem 1.2 (Pontryagin's Maximum Principle)**.** *Given an optimal control $u^*(t)$ and the corresponding state $y^*(t)$ of the system* (1.2)*, there exists a piecewise differentiable adjoint variable $\lambda_y : [0, T] \to \mathbb{R}$ satisfying*

$$\begin{aligned} \tfrac{d\lambda_y}{dt} &= -\tfrac{\partial \mathcal{H}}{\partial y}, \\ \lambda_y(T) &= 0, \end{aligned} \tag{1.5}$$

such that $\mathcal{H}(t, y^*(t), u(t), \lambda_y(t)) \leq \mathcal{H}(t, y^*(t), u^*(t), \lambda_y(t))$ for all admissible controls $u \in \mathcal{U}$ at each time t.

Further,

$$\frac{\partial^2 \mathcal{H}}{\partial u^2} > 0 \quad \text{at} \quad u^*.$$

The formula for the optimal control $u^*(t)$ in terms of the optimal trajectory $y^*(t)$ and the adjoint variable $\lambda_y(t)$ is known as the characterization of the optimal control. The

characterization is obtained by solving $\frac{\partial \mathcal{H}}{\partial u} = 0$ whenever $0 < u^*(t) < u_{\max}$ and using the bounds on u.

1.2.2 Optimality system

The differential equation for the state variable (1.2) with initial condition $y(0)$, the differential equation for the adjoint variable (1.5) with terminal condition $\lambda_y(T)$ along with the characterization of the optimal control u^* form the optimality system, and given below

$$\begin{array}{lrcl} \text{state equation:} & \frac{dy(t)}{dt} & = & f\left(y(t),\, u(t)\right), \\ \text{initial condition:} & y(0) & = & y_0, \\ \text{costate (adjoint) equation:} & \frac{d\lambda_y}{dt} & = & -\frac{\partial \mathcal{H}(t, y^*(t), u^*(t), \lambda_y(t))}{\partial y}, \\ \text{terminal (transversality) condition} & \lambda_y(T) & = & 0. \end{array} \tag{1.6}$$

Interpretation of $\lambda_y(t)$: The adjoint variable $\lambda_y(t)$ can be interpreted as the per unit change in the value of the objective functional for a small change in the optimal trajectory $y^*(t)$ at time t.

1.2.3 Numerical solution of the optimality system

In the optimality system (1.6), the state equation has initial condition y_0, while the adjoint equation has terminal condition $\lambda_y(T)$ (also called transversality condition). A system of differential equations where some variables have initial conditions and other variables have terminal conditions is known as a two-point boundary value problem. Since optimality system (1.6) is also a two-point boundary value problem and generally can not be solved analytically, we use forward-backward sweep method [10] for solving the optimality system numerically. The algorithm to solve the optimality system (1.6) using forward-backward sweep method [10] is as follows:

1. Initialize the control variable u with an initial guess.

2. Using the current value of u, integrate the state equation forward in time using the initial condition.

3. Using the current values of the state and control variables, integrate the adjoint equation backward in time using the terminal condition.

4. Using the current values of the state and adjoint variables, the control variable u is updated using the characterization.

5. Repeat the process until the following convergence criteria is satisfied.

$$\frac{y - oldy}{y} \leq \epsilon, \quad \frac{\lambda_y - old\lambda_y}{\lambda_y} \leq \epsilon, \quad \frac{u - oldu}{u} \leq \epsilon,$$

where ϵ denotes the required convergence tolerance.

1.3 Mosquito-borne diseases

Mosquitoes belong to the family of insects called *Diptera* (or flies) and cause millions of deaths every year due to diseases they carry and transmit to humans [14]. While there exist over 3,500 species of mosquitoes, *Anopheles*, *Aedes*, and *Culex* are known to be the vectors of some life-threatening mosquito-borne diseases such as dengue, yellow fever, Chikungunya, West Nile virus, Zika, and malaria [15]. The four stages of a mosquito lifecycle include eggs, larvae, pupae, and adults. In the first stage, adult female mosquitoes lay eggs in stagnant water. These eggs can survive even at low temperatures, and their development depends on the ambient temperature. In the second stage, larvae emerge from eggs and feed on microorganisms present in the standing water. In the third stage, the larvae developed into pupae that continue to develop until the adult mosquitoes emerge from their skin and leave the water. After leaving the water, the adult mosquitoes start mating roughly once per day. Only female mosquitoes bite for blood to produce eggs. Once eggs are fully developed, female mosquitoes lay eggs on water surface. Male mosquitoes feed on flowers' nectar and other plant juices [14]. Thus, only female adult infected mosquitoes transmit the virus to humans through bites.

Among mosquito-borne diseases, dengue has grown significantly around the world in recent years. It is now endemic in 128 countries, with roughly 50-100 million reported cases annually

[16]. Two vectors, *Aedes albopictus* and *Aedes aegypti* , transmit the virus to humans through bites, but *Aedes aegypti* is considered the primary vector. Dengue exists in two forms called Dengue Fever (DF) and Dengue Hemorrhagic Fever (DHF) [17]. Dengue Hemorrhagic may evolve to a more severe case called Dengue Shock Syndrome (DSS) [17]. Dengue fever exists in four distinct serotypes known as DENV1, DENV2, DENV3, and DENV4 [17]. If a person get infected with one particular serotype of dengue, he/she gets life-long immunity against that serotype only and the immunity against all other serotypes of dengue is temporary and more susceptible for developing DHF. There is no vaccine available yet in the market for dengue neither for some other widespread diseases such as West Nile virus, yellow fever, and Zika. Therefore, the control measures of these diseases rely on controlling mosquitoes. Traditional mosquitoes control methods, such as removal of mosquitoes breeding sites and the use of insecticides, have proven not to be very useful due to the development of mosquitoes resistance against the pesticides [18]. Instead of these traditional methods, biological control methods are being used and tested to remove or suppress the population of wild mosquitoes. One such biological control method is the transinfection of *Aedes aegypti* mosquitoes with *Wolbachia* strains and then released in the wild to suppress the population of wild *Aedes aegypti* mosquitoes.

1.3.1 Why transinfecting *Aedes aegypti* mosquitoes with *Wolbachia* strains?

Wolbachia, which is maternally transmitted to offspring, is a bacterium which is naturally present in more than 60% of all insect species [19] including *Aedes albopictus* [20]. *Aedes aegypti* is known to be among the insect species that does not have *Wolbachia* present in them naturally. *Aedes aegypti* mosquitoes can be transinfected with different strains of *Wolbachia* and then released in different locations where *Wolbachia* infected mosquitoes interact with wild mosquitoes and grow. *Aedes aegypti* mosquitoes, when transinfected with a particular strain of *Wolbachia*, have the following advantages:

1. *Wolbachia* reduces the lifespan of mosquitoes,

2. *Aedes aegypti* mosquitoes when transinfected with *wMel*, *wMelPop*, and wAlbB strains

of *Wolbachia* [21] can block the transmission of dengue, yellow fever, Chikungunya, and Zika viruses [22–24],

3. incomplete cytoplasmic incompatibility (CI) is the probability of producing no offspring if a *Wolbachia*-free female mosquito mates with *Wolbachia*-infected male mosquitoes. However, *Wolbachia*-infected female mosquitoes are not affected by the cytoplasmic incompatibility phenomena and produce both *Wolbachia* infected and uninfected offspring when mating with either *Wolbachia*-infected male or *Wolbachia*-uninfected male.

4. *Wolbachia* can be passed on to the next generation, allowing the *Wolbachia*-infected mosquitoes to suppress the population of wild mosquitoes.

Due to these advantages of *Wolbachia*-infected mosquitoes over wild mosquitoes, *Wolbachia*-infected mosquitoes are being used to control widespread arbovirus diseases such as yellow fever, dengue, Chikungunya, and Zika [22–24]. *Aedes aegypti* mosquitoes, when transinfected with the *wMelPop* strain, have high fitness cost and reduced lifespan as compare to when transinfected with *wMel* strain of *Wolbachia*. Due to lower fitness cost and high maternal transmission associated with the *wMel* strain of *Wolbachia*, *wMel* transinfected *Aedes aegypti* mosquitoes have been released in Australia for field trials [25]. *Wolbachia*-infected mosquitoes are also being tested in Vietnam, Australia, and Brazil as a biological control to reduce the dengue infection [25–29].

1.4 Mathematical models of *Daphnia* epidemics

Daphnia, also called water fleas, are freshwater zooplankton found in lakes and ponds. *Daphnia* has been used as a model organism for research studies in different fields such as eco-toxicology, ecology, behavior ecology, developmental biology, evolutionary biology, evolutionary genetics, physiology, and comparative morphology [30,31]. Some of the reasons why *Daphnia* is an attractive model organism are the following.

- They are available and can be collected from ponds, puddles, and lakes.

- They are relatively easy to handle in a laboratory due to their size and can be analyzed under a microscope.
- They have short lives and reproduction cycles compared to other microscopic crustaceans.
- Transparent body/shell structure of susceptible *Daphnia* makes it easy to study/analyze various body parts such as heart and the reproductive system.
- *Daphnia* has a vital role in aquatic food webs because they are the primary grazers of algae, bacteria, and fungi and also prey to juvenile fish.
- Clonal reproduction and maternal lines.

1.4.1 How do *Daphnia* become sick?

Daphnia are filter-feeders, and susceptible *Daphnia* (*Daphnia dentifera*) get infected by accidentally ingesting fungal spores (*Metschnikowia bicuspidata*) that are distributed in a water column [32]. These fungal spores are needle-like in shape and puncture the gut wall of the host. The spores are released back in the water column upon the death of an infected *Daphnia* where they can infect more susceptible *Daphnia* . Also, the infection reduces the life span and fecundity of the hosts due to their resistance against the pathogens. The outer shell of a *Daphnia* is transparent but becomes opaque when infected, and hence has a higher risk of predation. A general schematic of the model is shown in Figure 1.2.

1.4.2 Previous *Daphnia* epidemic models

In previous models [32, 33], the interaction among *Daphnia*, spores, and algae has been studied using coupled ordinary differential equations. Hall et al. [33] discussed an ODE model of the *Daphnia*-fungal-fish system. Cáceres et. al [32] developed and analyzed an ODE model that incorporates algal resource and a competitor, *Daphnia pulicaria*, along with hosts and spores. In a water column, the spores and algae can also move randomly due to the temperature gradient and the wind on the water surface. They can even sink due to

the higher weight density than water. The dynamics of spores and algae in the presence of diffusion and advection (sinking) is then modeled using advection-diffusion partial differential equations.

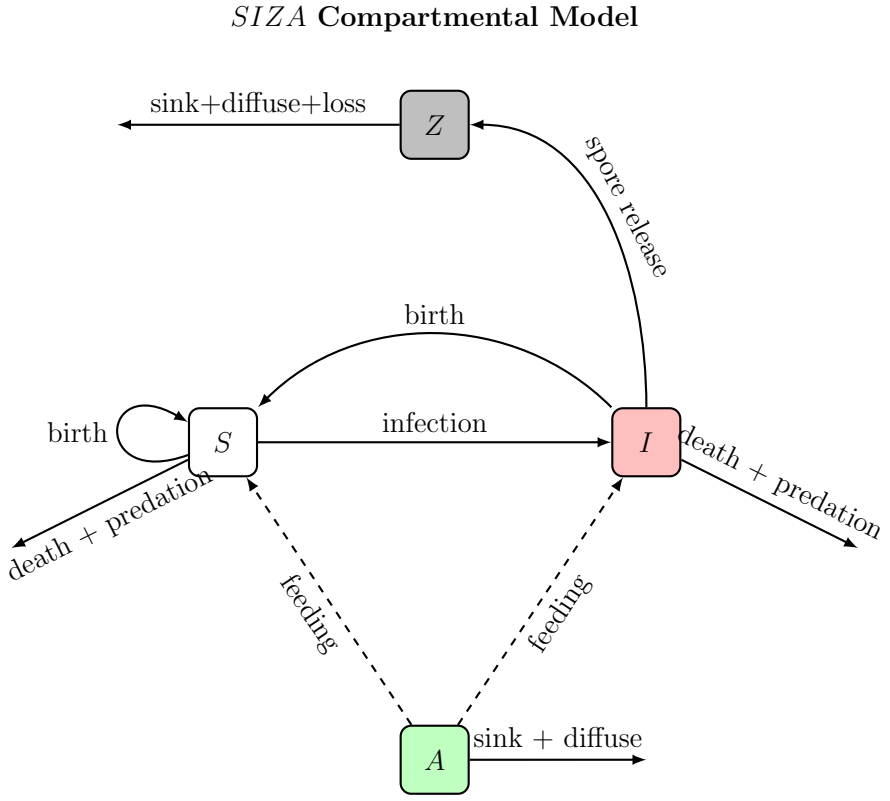

Figure 1.2: Flow diagram of susceptible *Daphnia* (S), infected *Daphnia* (I), spores (Z), and algae (A) compartmental model.

1.5 Dissertation layout

The layout of this dissertation is as follows. In chapter 2, we formulate a compartmental model to describe the dynamics of wild mosquitoes when *Wolbachia*-infected mosquitoes are released in the wild as a biological control method to suppress the population of wild mosquitoes. We then formulate an optimal control model where we consider the release of *Wolbachia*-infected mosquitoes as control variables and discuss optimal releasing strategies of the *Wolbachia*-infected mosquitoes in the wild. Chapter 3 describes the transmission dynamics of dengue virus into humans when *Wolbachia*-infected mosquitoes are introduced

in the wild as a potential control method for controlling the transmission of dengue infections in humans. We discuss the existence of different disease (dengue)-free equilibria and their stability properties in terms of $\mathcal{R}_0$. In chapter 4, we develop and analyze an optimal control dengue epidemic model. In this model, we consider two control variables; the release rate of *Wolbachia*-infected mosquitoes and the use of educational campaigns to reduce human-vector contact. The most cost-effectiveness strategy is then determined among the combination of different control interventions. Chapter 5 describes the disease dynamics of *Daphnia* when both algae and spores sink and diffuse in a water column. We use advection-diffusion-reaction partial differential equations to describe the dynamics of algae and spores. In the Appendix A, we define important terms and state theorems use in this dissertation and the stability of dengue-free equilibrium points, found in chapter 3, is discussed in Appendix B.

CHAPTER 2

OPTIMAL RELEASING OF *WOLBACHIA*-INFECTED MOSQUITOES TO SUPPRESS WILD *AEDES AEGYPTI* MOSQUITOES

2.1 Introduction

Several mathematical models including deterministic ordinary differential equation models [34–42], delay differential equation models [43, 44], stochastic models [45], and spatial models [46–48] have been studied to understand the dynamics and spread of *Wolbachia*-infected mosquitoes in wild mosquitoes. However, in most these models perfect (100%) maternal transmission is assumed. But in a recent study [49] it has been demonstrated that at a high temperature (80 - 98^oF) maternal transmission is not perfect in *Aedes aegypti* mosquitoes. Also, the cytoplasmic incompatibility is not complete and depends on the strain of *Wolbachia* [36]. Recently Zheng et al. [50–52] considered imperfect maternal transmission but considered perfect cytoplasmic incompatibility in their model. Farkas and Hinow [53] considered a single sex model in which they incorporated different mortality and fertility rates in individuals. A model that incorporates the following, has not been considered yet:

- all key state variables such as immature mosquitoes (eggs, larva, and pupa), adult mosquitoes including both female and male mosquitoes (two-sex),
- imperfect maternal transmission,
- incomplete cytoplasmic incompatibility (CI),
- and different death and density dependent growth rates for *Wolbachia*-infected and uninfected female mosquitoes.

To fill this gap, we first propose a more general compartmental model without controls that incorporates aquatic stages (eggs, larva, pupa) for *Wolbachia*-infected and *Wolbachia*-

uninfected immature mosquitoes, adult mosquitoes including both female and male (two-sex) mosquitoes, imperfect maternal transmission, incomplete cytoplasmic incompatibility, and density dependent growth rate for *Wolbachia* infected and uninfected female mosquitoes. We further extend the model by considering the release of *Wolbachia*-infected mosquitoes in the wild as time-dependent control variables and discuss different releasing strategies for *Wolbachia*-infected mosquitoes using optimal control theory.

2.2 Mathematical model

First, we develop an uncontrolled two-sex mosquito population model in which we divide the population of *Wolbachia*-uninfected (WU) and *Wolbachia*-infected ((WI) mosquitoes into two stages: (i) aquatic stage that includes eggs, larva, and pupa and (ii) adult stage that includes adult female and male mosquitoes. We denote the number of *Wolbachia*-uninfected immature, adult female, and adult male mosquitoes by A_n, F_n, and M_n, respectively. Similarly, A_w, F_w, and M_w represent the number of *Wolbachia*-infected immature, adult female, and adult male mosquitoes, respectively. To model the density-dependent fecundity rate, we consider the following cases when a female mosquito mates randomly with male mosquitoes and produces offspring.

- *Wolbachia*-free offspring are produced when a *Wolbachia*-free female mates with *Wolbachia*-free male mosquitoes.

- Due to incomplete cytoplasmic incompatibility (CI), *Wolbachia*-free offspring are also produced with probability $1 - \alpha$ when a *Wolbachia*-free female mates with *Wolbachia*-infected male mosquitoes, where α measures the probability of the cytoplasmic incompatibility.

- Due to imperfect maternal transmission, *Wolbachia*-infected as well as *Wolbachia*-free offspring are produced in a certain proportion when a *Wolbachia*-infected female mosquito mates with either *Wolbachia*-infected or *Wolbachia*-uninfected male mosquitoes.

The fecundity rates of *Wolbachia*-free and *Wolbachia*-infected females are denoted by ρ_n and ρ_w, respectively. The maturation rates of *Wolbachia* uninfected and infected immature mosquitoes are denoted by γ_n and γ_w, respectively. The death rates of *Wolbachia*-free immature, adult females, and adult males are denoted by μ_{na}, μ_n, and μ_m, respectively, whereas the death rates of immature and adult mosquitoes infected with *Wolbachia* are denoted by μ_{wa}, μ_w, and μ_m, respectively. A proportion τ of immature mosquitoes are female and $1-\tau$ are male mosquitoes. K represents the carrying capacity of immature mosquitoes and ϵ_w denotes the probability of the vertical transmission. The schematic of the *Wolbachia* model is shown in Figure 2.1. In the model, the subscript n stands for *Wolbachia*-free and w for *Wolbachia*-infected mosquitoes.

The resulting model reads as follow:

$$\begin{aligned}
\frac{dA_n}{dt} &= \rho_n F_n \frac{M_n}{M_n+M_w}\left(1-\frac{A_n+A_w}{K}\right) \\
&\quad + (1-\alpha)\rho_n F_n \frac{M_w}{M_n+M_w}\left(1-\frac{A_n+A_w}{K}\right) \\
&\quad + \rho_w\left(1-\epsilon_w\right)F_w\left(1-\frac{A_n+A_w}{K}\right) - (\gamma_n+\mu_{na})A_n, && \text{(2.1a)}\\
\frac{dF_n}{dt} &= \tau\gamma_n A_n - \mu_n F_n, && \text{(2.1b)}\\
\frac{dM_n}{dt} &= (1-\tau)\gamma_n A_n - \mu_m M_n, && \text{(2.1c)}\\
\frac{dA_w}{dt} &= \rho_w\epsilon_w F_w\left(1-\frac{A_n+A_w}{K}\right) - (\gamma_w+\mu_{wa})A_w, && \text{(2.1d)}\\
\frac{dF_w}{dt} &= \tau\gamma_w A_w - \mu_w F_w, && \text{(2.1e)}\\
\frac{dM_w}{dt} &= (1-\tau)\gamma_w A_w - \mu_m M_w. && \text{(2.1f)}
\end{aligned}$$

From equation (2.1b) it follows that

$$\frac{d}{dt}F_n = \tau\gamma_n A_n - \mu_n F_n \le \tau\gamma_n K - \mu_n F_n \qquad (\text{if} \quad A_n \le K),$$

$$0 \le F_n(t) \le \frac{\tau\gamma_n K}{\mu_n} + \left(F_n(0) - \frac{\gamma_n K}{\mu_n}\right)e^{-\mu_n t}.$$

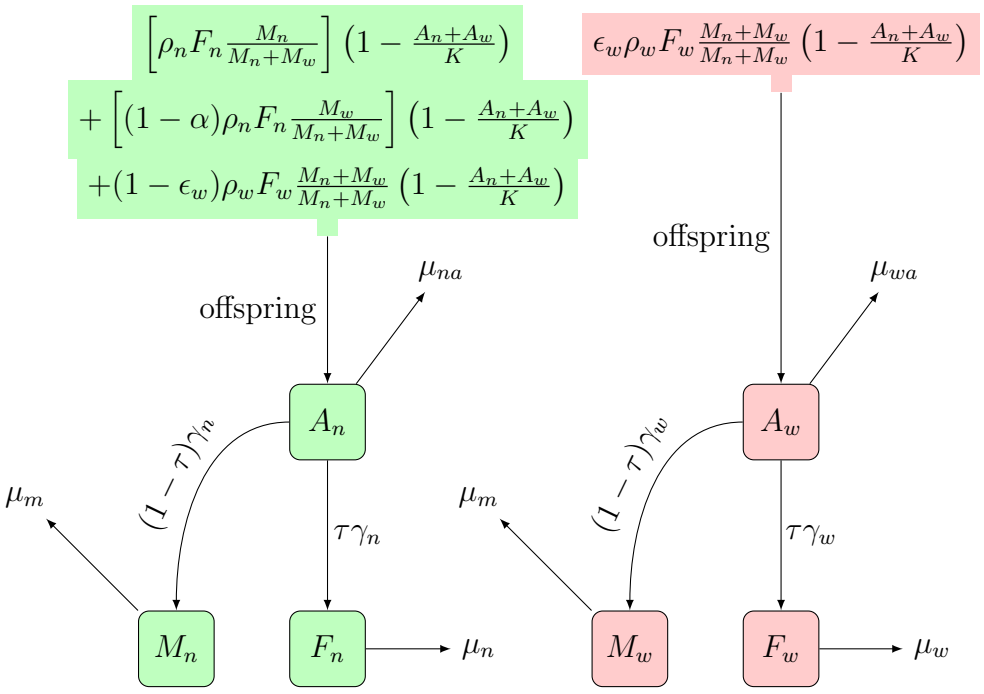

Figure 2.1: A schematic of the model (2.1). The subscripts n and w are used to denote the population and parameters of the *Wolbachia*-uninfected (wild) and *Wolbachia*-infected mosquitoes, respectively.

Thus,

$$0 \leq F_n(t) \leq \frac{\tau\gamma_n K}{\mu_n} \qquad \text{as t} \to \infty.$$

Similarly, (2.1c) implies

$$0 \leq M_n(t) \leq \frac{(1-\tau)\gamma_n K}{\mu_m} \qquad \text{as t} \to \infty.$$

From equation (2.1e), it follows that

$$\frac{d}{dt}F_w = \tau\gamma_w A_w - \mu_w F_w \leq \tau\gamma_w K - \mu_w F_w \qquad (\text{if} \quad A_w \leq K),$$

$$0 \leq F_w(t) \leq \frac{\tau\gamma_w K}{\mu_w} + \left(F_w(0) - \frac{\gamma_w K}{\mu_w}\right) e^{-\mu_w t}.$$

Table 2.1: Description of variables and parameters used in model (2.1).

Symbol	Description	Value	Unit	Source
Variables:				
A_n	*Wolbachia*-uninfected aquatic stage of mosquitoes	...		
F_n	*Wolbachia*-uninfected adult female mosquitoes	...		
M_n	*Wolbachia*-uninfected adult male mosquitoes	...		
A_w	*Wolbachia*-infected aquatic stage of mosquitoes	...		
F_w	*Wolbachia*-infected adult female mosquitoes	...		
M_w	*Wolbachia*-infected adult male mosquitoes	...		
t	Time	...	days	
Parameters:				
ρ_n	Reproduction rate of *Wolbachia*-free female mosquitoes	2	day^{-1}	[37]
ρ_w	Reproduction rate of *Wolbachia*-infected female mosquitoes	$0.95 \times \rho_n$	day^{-1}	[37]
τ	Fraction of female offspring	[0, 1]		
ϵ_w	Probability of maternal transmission	[0, 1]	—	
α	Strength of cytoplasmic incompatibility	$0.9, 0.95, 1.0$		[36]
μ_{na}	Death rate of *Wolbachia*-free immature (aquatic stage) mosquitoes	1/8	day^{-1}	[37]
μ_{wa}	Death rate of *Wolbachia*-infected immature mosquitoes	1/8	day^{-1}	[37]
μ_n	Death rate of *Wolbachia*-free female mosquitoes	1/16	day^{-1}	[37]
μ_w	Death rate of *Wolbachia*-infected female mosquitoes	1.5/16	day^{-1}	[37]
μ_m	Death rate of *Wolbachia* uninfected and infected male mosquitoes	1/10.5	day^{-1}	[41]
γ_n	Maturation rate of *Wolbachia*-uninfected immature mosquitoes	1/10	day^{-1}	[37]
γ_w	Maturation rate of *Wolbachia*-infected immature mosquitoes	1/10	day^{-1}	[37]
K	Carrying capacity of immature mosquitoes	2×10^4	—	assumed

Thus,

$$0 \leq F_w(t) \leq \frac{\tau\gamma_w K}{\mu_w} \qquad \text{as t} \to \infty.$$

Similarly,

$$0 \leq M_w(t) \leq \frac{(1-\tau)\gamma_w K}{\mu_m} \qquad \text{as t} \to \infty.$$

Now consider the region $\mathcal{D}$:

$$\mathcal{D} = \left\{ \begin{array}{l} (A_n, F_n, M_n, A_w, F_w, M_w) \in \mathcal{R}^6 : \\ 0 \leq A_n + A_w \leq K, 0 \leq F_n \leq \frac{\tau\gamma_n}{\mu_n} K, \\ 0 \leq M_n \leq \frac{(1-\tau)\gamma_n}{\mu_m} K, \\ 0 \leq F_w \leq \frac{\tau\gamma_w}{\mu_w} K, 0 \leq M_w \leq \frac{(1-\tau)\gamma_w}{\mu_m} K \end{array} \right\}. \tag{2.2}$$

From equations (2.1a)-(2.1f) $A_n = 0 \Rightarrow \frac{dA_n}{dt} \geq 0$, $F_n = 0 \Rightarrow \frac{dF_n}{dt} \geq 0$, $M_n = 0 \Rightarrow \frac{dM_n}{dt} \geq 0$, $A_w = 0 \Rightarrow \frac{dA_w}{dt} \geq 0$, $F_w = 0 \Rightarrow \frac{dF_w}{dt} \geq 0$, $M_w = 0 \Rightarrow \frac{dM_w}{dt} \geq 0$, Thus, $\mathcal{D}$ is positively invariant, that is if a solution starts in $\mathcal{D}$, it remains in $\mathcal{D}$ for all $t > 0$, for the system (2.1a)-(2.1f).

2.3 Local stability of the *Wolbachia*-free equilibrium (WFE) point

2.3.1 *Wolbachia*-free equilibrium point

The *Wolbachia*-free equilibrium point is obtained after setting $A_w = F_w = M_w = 0$ in the system of equations (2.1a)-(2.1f) and solving the resulting system of algebraic equations. The only biologically realistic *Wolbachia*-free equilibrium point is

$$E_1 = (A_{1n}, S_{1n}, M_{1n}, 0, 0, 0)\,,$$

where

$$\begin{aligned} A_{1n} &= K(1 - \frac{1}{\mathscr{R}_{0n}}), \\ S_{1n} &= \frac{\tau\gamma_n}{\mu_n} K(1 - \frac{1}{\mathscr{R}_{0n}}), \\ M_{1n} &= \frac{(1-\tau)\gamma_n}{\mu_{mn}} K(1 - \frac{1}{\mathscr{R}_{0n}}), \\ \mathscr{R}_{0n} &= \tau \frac{\gamma_n}{\gamma_n + \mu_{na}} \frac{\rho_n}{\mu_n}. \end{aligned}$$

Since $A_{1n} > 0$ so it requires $\mathscr{R}_{0n} > 1$.Thus, the population of *Wolbachia*-free (wild) mosquitoes exists only if $\mathscr{R}_{0n} > 1$. In terms of biology, $\mathscr{R}_{0n}$ denotes the total number of

female offspring produced by a *Wolbachia*-uninfected female mosquito during its lifetime. The term makes sense since the term $\frac{\rho_n}{\mu_n}$ stands for the total eggs produce during the lifespan of an adult wild female mosquito. These eggs go through different aquatic phases and survive in aquatic phase with probability $\frac{\gamma_n}{\gamma_n+\mu_{na}}$ and finally developed as female adult mosquitoes with probability τ. If $\mathscr{R}_{0n} < 1$, then there will be no mosquitoes (i.e. trivial equilibrium point).

2.3.2 *Wolbachia* basic reproduction number $\mathscr{R}_0^{wolb}$

The *Wolbachia* basic reproduction number ($\mathscr{R}_0^{wolb}$) for the model (2.1) is calculated using the next generation matrix approach [1, 54, 55]. The spectral radius (the largest absolute eigenvalue) of the matrix $\mathcal{F}\mathcal{V}^{-1}$ gives $\mathscr{R}_0^{wolb}$.

To calculate $\mathscr{R}_0^{wolb}$ for the model (2.1), we consider the state equations that correspond to the state variables A_w, F_w, and M_w, and then write the corresponding system of differential equations as

$$\frac{d}{dt}\left[A_w, F_w, M_w\right]^T = F - V, \tag{2.3}$$

where $F = \begin{pmatrix} \rho_w \epsilon_w F_w \left(1 - \frac{A_n + A_w}{K}\right) \\ 0 \\ 0 \end{pmatrix}$ and $V = \begin{pmatrix} (\gamma_w + \mu_{wa}) A_w \\ \mu_w F_w - \tau \gamma_w A_w \\ \mu_m M_w - (1-\tau)\gamma_w A_w \end{pmatrix}$. The matrices $\mathcal{F}$ and $\mathcal{V}$ are defined as

$$\mathcal{F} := \left[\frac{\partial F_i(y_0)}{\partial y_j}\right], \qquad \mathcal{V} := \left[\frac{\partial V_i(y_0)}{\partial y_j}\right], \tag{2.4}$$

where F_i denotes the rate of new infections in the compartment i and V_i represents the rate of infections transfer out of compartment i. The point y_0 represents a disease-free equilibrium point, and y_j represents the number of infected individuals in the compartment j. For our model, the transmission matrix $\mathcal{F}$ and transfer matrix $\mathcal{V}$ at the *Wolbachia*-free equilibrium point $E_1 = (A_{1n}, M_{1n}, M_{1n}, 0, 0, 0)$ are:

$$\mathcal{F} = \begin{pmatrix} 0 & \frac{\epsilon_w \rho_w}{\mathscr{R}_{0n}} & 0 \\ 0 & 0 & 0 \\ 0 & 0 & 0 \end{pmatrix}, \qquad \mathcal{V} = \begin{pmatrix} \gamma_w + \mu_{wa} & 0 & 0 \\ -\tau\gamma_w & \mu_w & 0 \\ -(1-\tau)\gamma_w & 0 & \mu_m \end{pmatrix}.$$

The next generation matrix, denoted by $\mathcal{F}\mathcal{V}^{-1}$, is

$$\mathcal{F}\mathcal{V}^{-1} = \begin{pmatrix} \frac{\epsilon_w \tau \gamma_w \rho_w}{\mathscr{R}_{0n}(\gamma_w+\mu_{wa})\mu_w} & \frac{\epsilon_w \rho_w}{\mathscr{R}_{0n}\mu_w} & 0 \\ 0 & 0 & 0 \\ 0 & 0 & 0 \end{pmatrix}.$$

After simplifying, the largest absolute eigenvalue of the next generation matrix is

$$\rho(\mathcal{F}\mathcal{V}^{-1}) = \frac{\epsilon_w \tau \rho_w \gamma_w}{\mu_w(\gamma_w + \mu_{wa})} \frac{\mu_n(\gamma_n + \mu_{na})}{\tau \rho_n \gamma_n} = \frac{\mathscr{R}_{0w}}{\mathscr{R}_{0n}},$$

where $\mathscr{R}_{0w} = \frac{\tau \epsilon_w \rho_w}{\mu_w} \frac{\gamma_w}{\gamma_w + \mu_{wa}}$ and denotes the number of female *Wolbachia*-infected offspring produced by a *Wolbachia*-infected female during its lifespan ($\epsilon_w \rho_w / \mu_w$) that survived in the aquatic stage with probability $\frac{\gamma_w}{\gamma_w + \mu_{wa}}$ and developed as female adult mosquitoes with probability τ. Therefore, the basic reproduction number $\mathscr{R}_0^{wolb}$ is

$$\mathscr{R}_0^{wolb} := \frac{\epsilon_w \tau \rho_w \gamma_w}{\mu_w(\gamma_w + \mu_{wa})} \frac{\mu_n(\gamma_n + \mu_{na})}{\tau \rho_n \gamma_n} = \frac{\mathscr{R}_{0w}}{\mathscr{R}_{0n}}. \tag{2.5}$$

Interpretation of $\mathscr{R}_0^{wolb}$: *Wolbachia* basic reproduction number $\mathscr{R}_0^{wolb}$ given in (2.5) is the ratio of the WI female offspring produced by a WI female during her lifespan to the WU female offspring produced by a WU female during her lifespan.

2.3.3 Endemic equilibrium points

We calculate the endemic equilibrium points for complete vertical transmission (i.e., $\epsilon_w = 1$) as well as for incomplete vertical transmission (i.e., $0 < \epsilon_w < 1$). (See appendix B for the stability analysis of the *Wolbachia*-free equilibrium point $E_1 = (A_{1n}, F_{1n}, F_{1n}, 0, 0, 0)$.)

Case 1: Complete vertical transmission ($\epsilon_w = 1$)

When the vertical transmission is perfect, that is $\epsilon_w = 1$, then there is only one endemic

equilibrium point that corresponds to the existence of *Wolbachia*-infected mosquitoes only and is given by

$$E_2 = (0, 0, 0, A^*_{2w}, F^*_{2w}, M^*_{2w}),$$

where

$$\begin{aligned}
A^*_{2w} &= K(1 - \frac{1}{\mathscr{R}_{0w}}), \\
F^*_{2w} &= \frac{\tau\gamma_w}{\mu_w} K(1 - \frac{1}{\mathscr{R}_{0w}}), \\
M^*_{2w} &= \frac{(1-\tau)\gamma_w}{\mu_{mw}} K(1 - \frac{1}{\mathscr{R}_{0w}}), \\
\mathscr{R}_{0w} &= \tau\rho_w \frac{\gamma_w}{\gamma_w + \mu_{wa}} \frac{1}{\mu_w}.
\end{aligned}$$

Since $A^*_{2w} > 0$ which requires $\mathscr{R}_{0w} > 1$. The equilibrium point E_2 exists only when $\epsilon_w = 1$ and $\mathscr{R}_{0w} > 1$. Biologically, $\mathscr{R}_{0w}$ denotes the number of *Wolbachia*-infected female offspring produced by a *Wolbachia*-infected female during its lifetime.

Case 2: Incomplete vertical transmission $(0 < \epsilon_w < 1)$

For incomplete vertical transmission $(0 < \epsilon_w < 1)$, the endemic equilibrium points are given by

$$A^*_n = \frac{K}{1+\eta}\left(1 - \frac{1}{\mathscr{R}_{0w}}\right), \tag{2.6}$$

$$F^*_n = \frac{\tau\gamma_n}{\mu_n} A^*_n, \tag{2.7}$$

$$M^*_n = \frac{(1-\tau)\gamma_n}{\mu_m} A^*_n, \tag{2.8}$$

$$A^*_w = \eta A^*_n, \tag{2.9}$$

$$F^*_w = \frac{\tau\gamma_w}{\mu_w} A^*_w, \tag{2.10}$$

$$M^*_w = \frac{(1-\tau)\gamma_w}{\mu_m} A^*_w, \tag{2.11}$$

where $\eta := \frac{A^*_w}{A^*_n}$ and denotes the positive solutions of the following quadratic equation

$$\psi_1\eta^2 + \psi_2\eta + \frac{1}{\mathscr{R}_0^{wolb}} - 1 = 0, \tag{2.12}$$

where

$$\begin{aligned}\psi_1 &= \frac{1-\epsilon_w}{\epsilon_w}\frac{\gamma_w}{\gamma_n}\frac{\gamma_w+\mu_{wa}}{\gamma_n+\mu_{na}},\\ \psi_2 &= \frac{1-\epsilon_w}{\epsilon_w}\frac{\gamma_w+\mu_{wa}}{\gamma_n+\mu_{na}}-\frac{\gamma_w}{\gamma_n}+(1-\alpha)\frac{\gamma_w}{\gamma_n}\mathscr{R}_0^{wolb}.\end{aligned}$$

Depending on the parameter values, Eq. (2.12) has zero, one, or two positive solutions.

$$\eta_1 = \frac{-\psi_2+\sqrt{\psi_2^2-4\psi_1(\frac{1}{\mathscr{R}_0^{wolb}}-1)}}{2\psi_1}$$

$$\eta_2 = \frac{-\psi_2-\sqrt{\psi_2^2-4\psi_1(\frac{1}{\mathscr{R}_0^{wolb}}-1)}}{2\psi_1}$$

Table 2.2: Existence of positive endemic equilibrium points

Parameter values		Endemic equilibrium values
$\mathscr{R}_0^{wolb}>1$	$\psi_2<0$	η_1
	$\psi_2>0$	η_1
$\mathscr{R}_0^{wolb}=1$	$\psi_2<0$	η_1
$\mathscr{R}_0^{wolb}=\mathscr{R}_{cr}$	$\psi_2<0$	$\eta_1=\eta_2=\frac{-\psi_2}{2\psi_1}$
$\mathscr{R}_{cr}<\mathscr{R}_0^{wolb}<1$	$\psi_2<0$	η_1, η_2
$\mathscr{R}_0^{wolb}<\mathscr{R}_{cr}$	$\psi_2>0$	nonexistence
	$\psi_2<0$	nonexistence

The results in Table 2.2 indicate that the system exhibits backward bifurcation and the critical value above which the backward bifurcation occurs is given by

$$\mathscr{R}_{cr} = \frac{4\psi_1}{\psi_2^2+4\psi_1}.$$

In Table 2.2, we summarize the existence of positive endemic equilibrium that depend on the value of $\mathscr{R}_0^{wolb}$. For $\mathscr{R}_{cr}<\mathscr{R}_0^{wolb}<1$, there exist two positive endemic equilibrium points,

namely:

$$\eta_1 = \frac{1}{2\psi_1}\left(-\psi_2 + \sqrt{\psi_2^2 - 4\psi_1(\frac{1}{\mathscr{R}_0^{wolb}} - 1)}\right), \tag{2.13}$$

$$\eta_2 = \frac{1}{2\psi_1}\left(-\psi_2 - \sqrt{\psi_2^2 - 4\psi_1(\frac{1}{\mathscr{R}_0^{wolb}} - 1)}\right). \tag{2.14}$$

Only one globally stable endemic equilibrium point exists for $\mathscr{R}_0^{wolb} > 1$.

2.4 Backward bifurcation analysis

In this section, we prove the existence of the backward bifurcation phenomena theoretically using Center Manifold theory [56]. We take γ_w as a bifurcation parameter and then by setting $\mathscr{R}_0^{wolb} = 1$ and solving for γ_w, we get

$$\gamma_w^* = \frac{\rho_n\gamma_n\mu_w(\gamma_w + \mu_{wa})}{\rho_w\gamma_w\mu_n(\gamma_n + \mu_{na}}. \tag{2.15}$$

Let $J_{E_1}^{\gamma_w^*}$ represents the Jacobian of the system of equations (2.1a)-(2.1f) at the *Wolbachia*-free equilibrium (WFE) point E_1 with $\gamma_w = \gamma_w^*$ and is given by

$$J_{E_1}^{\gamma_w^*} = \begin{pmatrix} -(\gamma_n + \mu_{na}) + J_1 & \frac{\rho_n}{\mathscr{R}_{0n}} & 0 & J_1 & \frac{(1-\epsilon_w)\rho_w}{\mathscr{R}_{0n}} & \frac{-\tau\mu_{mn}\rho_n}{\mathscr{R}_{0n}(1-\tau)\mu_n} \\ \tau\gamma_n & -\mu_n & 0 & 0 & 0 & 0 \\ (1-\tau)\gamma_n & 0 & -\mu_{mn} & 0 & 0 & 0 \\ 0 & 0 & 0 & -(\gamma_w + \mu_{wa}) & \frac{\epsilon_w\rho_w}{\mathscr{R}_{0n}} & 0 \\ 0 & 0 & 0 & \tau\gamma_w & -\mu_w & 0 \\ 0 & 0 & 0 & (1-\tau)\gamma_w & 0 & -\mu_m \end{pmatrix},$$

where

$$J_1 = \frac{(1 - \mathscr{R}_{0n})\tau\gamma_n\rho_n}{\mu_n\mathscr{R}_{0n}}.$$

The system (2.1a)-(2.1f) has a non-hyperbolic equilibrium point when $\gamma_w = \gamma_w^*$ (i.e., $\mathscr{R}_0^{wolb} = 1$). Thus, the linearized system of (2.1a)-(2.1f) at E_1 and $\gamma_w = \gamma_w^*$ has one eigenvalue equal 0 and all other eigenvalues with negative real part. Hence, center manifold theory [6, 57, 58] can be used to discuss the dynamics of the system (2.1a)-(2.1f) near the bifurcation point

$\gamma_w = \gamma_w^*$. To analyze the dynamics of the model (2.1a)-(2.1f) near the bifurcation point $\gamma_w = \gamma_w^* \quad (\mathscr{R}_0^{wolb} = 1)$, we make use of the theorem 4.1 proved in [6]. To use the theorem 4.1 in [6], we need to calculate the right and left eigenvectors of the Jacobian matrix at the zero eigenvalue. Let $\mathbf{w} = (w_1, w_2, w_3, w_4, w_5, w_6)$ denotes the right eigenvector of the Jacobian matrix $J_{E_1}^{\gamma_w^*}$ at the zero eigenvalue and is given by

$$\begin{aligned}
w_1 &= \frac{\tau\rho_n\left(\gamma_n^2\mu_m\mu_w\tau\rho_n^2 - \mu_m\mu_n(\kappa_1\mu_w + \kappa_2)\right))}{\gamma_w\kappa_3(1-\tau)\left(1 - \frac{1}{\mathscr{R}_{0n}}\right)}, \\
w_2 &= \frac{\mu_m\tau\left(\mu_n\kappa_1 + \kappa_2\right) - \gamma_n^2\mu_w\tau\rho_n^2}{\mu_n\gamma_w\kappa_3(1-\tau)\left(1 - \frac{1}{\mathscr{R}_{0n}}\right)}, \\
w_3 &= \frac{\mu_n\left(\mu_w\kappa_1 + \kappa_2\right) - \gamma_n^2\mu_w\tau\rho_n^2}{\gamma_w\kappa_3\left(1 - \frac{1}{\mathscr{R}_{0n}}\right)}, \\
w_4 &= \frac{\mu_m\mu_n(\gamma_n + \mu_{na})}{\gamma_n\mu_{wa}\rho_n\tau(1-\tau)}\left(\frac{\tau\epsilon_w\rho_w}{\mu_w} - R_{on}\right), \\
w_5 &= \frac{\tau\mu_m}{\mu_w(1-\tau)}, \\
w_6 &= 1,
\end{aligned} \tag{2.16}$$

where

$$\kappa_1 = \gamma_n^2 - \gamma_w\mu_{na} - \gamma_n(2\gamma_w + \mu_{wa} - \mu_{na}))\rho_n, \tag{2.17}$$

$$\kappa_2 = \gamma_w\mu_n(\gamma_n + \mu_n a)\rho_w, \tag{2.18}$$

$$\kappa_3 = \gamma_n\mu_w\rho_n^2. \tag{2.19}$$

Let $\mathbf{v} = (v_1, v_2, v_3, v_4, v_5, v_6)$ be the left eigenvector of $J_{E_1}^{\gamma_w^*}$ at the zero eigenvalue and its components are given by

$$v_1 = v_2 = v_3 = 0, \quad v_4 = \frac{\tau\gamma_n\mu_w\rho_n}{\epsilon_w\rho_w\mu_n(\gamma_n + \mu_{na})}, \quad v_5 = 1, \quad v_6 = 0. \tag{2.20}$$

Now following the results proved in [6], the local bifurcation analysis near $\gamma_w = \gamma_w^*$ is

determined by the sign of a and b where

$$m = \sum_{k,i,j}^{6} v_k w_i w_j \frac{\partial^2 f_k}{\partial y_i \partial y_j}(y_0, \phi), \tag{2.21}$$

$$n = \sum_{k,i}^{6} v_k w_i \frac{\partial^2 f_k}{\partial y_i \partial \epsilon_w}(y_0, \phi), \tag{2.22}$$

and y_0 denotes the equilibrium point which in our case is E_1 and ϕ represents the bifurcation parameter which is γ_w^* in our case. After calculating the partial derivatives and keeping only the nonzero terms, m and n defined in (2.21) and (2.22) take the following form

$$\begin{aligned} m &= v_4 w_1 w_5 \frac{\partial^2 f_4}{\partial A_n \partial F_w}(E_1, \gamma_w^*) + v_4 w_4 w_5 \frac{\partial^2 f_4}{\partial A_w \partial F_w}(E_1, \gamma_w^*), \\ &\quad + v_4 w_5 w_1 \frac{\partial^2 f_4}{\partial F_w \partial A_n}(E_1, \gamma_w^*) + v_4 w_4 w_5 \frac{\partial^2 f_4}{\partial F_w \partial A_w}(E_1, \gamma_w^*) \end{aligned} \tag{2.23}$$

$$n = v_4 w_5 \frac{\partial^2 f_4}{\partial F_w \partial \gamma_w}(E_1, \gamma_w^*). \tag{2.24}$$

Substituting the values of w_i and v_i, where $i = 1, \ldots, 6$, from Eqs. (2.16) and (2.20) in Eqs. (2.23) and (2.24) and simplifying we get

$$m = \frac{2\mu_m^2(\mathcal{G}_0 - (1-\epsilon_w))}{K(1-\tau)^2\gamma_n \mathcal{G}_0 \tau (1 - \frac{1}{\mathscr{R}_{0n}})}, \tag{2.25}$$

$$n = \frac{\mu_m \left[(\gamma_n \mu_w \rho_n - \epsilon_w \mu_n(\gamma_n + \mu_{na})\rho_w\right]^2 \tau}{\gamma_n \epsilon_w \mu_n (\gamma_n + \mu_{na}) \mu_w \mu_{wa} \rho_n \rho_w (1-\tau)}, \tag{2.26}$$

where $\mathcal{G}_0 = \frac{\rho_n}{\mu_n} / \frac{\rho_w}{\mu_w}$. In terms of biology $\mathcal{G}_0$ represents the ratio of eggs produced by a WU female mosquito to eggs produced by a WI female mosquito during their lifespan. From Eq. (2.26), it is clear that $n > 0$. Thus, it is the sign of m that matters. $m > 0$ if $\mathcal{G}_0 > (1 - \epsilon_w)$ and $m < 0$ when $\mathcal{G}_0 < (1 - \epsilon_w)$. Thus, we have the following theorem

Theorem 2.1. *The model* (2.1a)-(2.1f) *exhibits a backward bifurcation at* $\gamma_w = \gamma_w^*$ *(i.e.* $\mathscr{R}_0^{wolb} = 1$*) when* $\mathcal{G}_0 > (1 - \epsilon_w)$.

In Figure (2.2), we also numerically confirmed that the model (2.1a)-(2.1f) exhibits the backward bifurcation phenomenon when the conditions of the Theorem 2.1 hold.

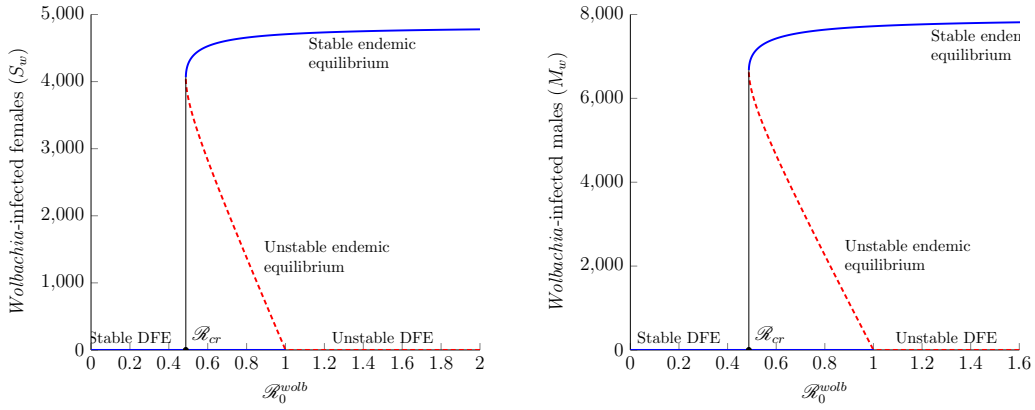

Figure 2.2: Backward bifurcation when $\epsilon_w = 0.9$, $\mu_w = 0.09$, $\rho_w = 1.9$ and all other parameter values follow Table (2.1). Corresponding to these parameter values $\mathscr{R}_0^{wolb} = 0.57$, $\mathscr{R}_{cr} = 0.48$, and $m = 0.1579 > 0$.

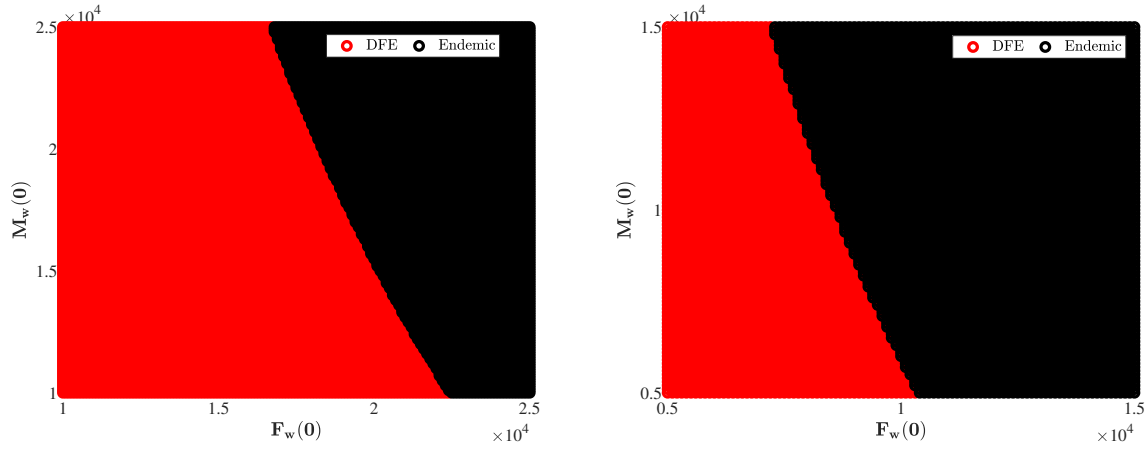

(a) $\epsilon_w = 0.9$ and $\alpha = 0.95$ (b) $\epsilon_w = 0.95$ and $\alpha = 1$

Figure 2.3: Region of attraction when the initial conditions $A_n(0)$, $F_n(0)$, $M_n(0)$ are fixed.

2.5 Optimal control model

Motivation: The following observations in the uncontrolled model (2.1) motivate us towards formulating an optimal control model.

- The uncontrolled model (2.1) has two positive endemic equilibria (stable and unstable) when $\mathscr{R}_0^{wolb} < 1$, which means that it is possible for *Wolbachia*-infected mosquitoes to persist even if $\mathscr{R}_0^{wolb} < 1$ but a large number of *Wolbachia*-infected mosquitoes is required to be released initially.

- The results in Figure 2.5 show that the *Wolbachia* basic reproduction number, de-

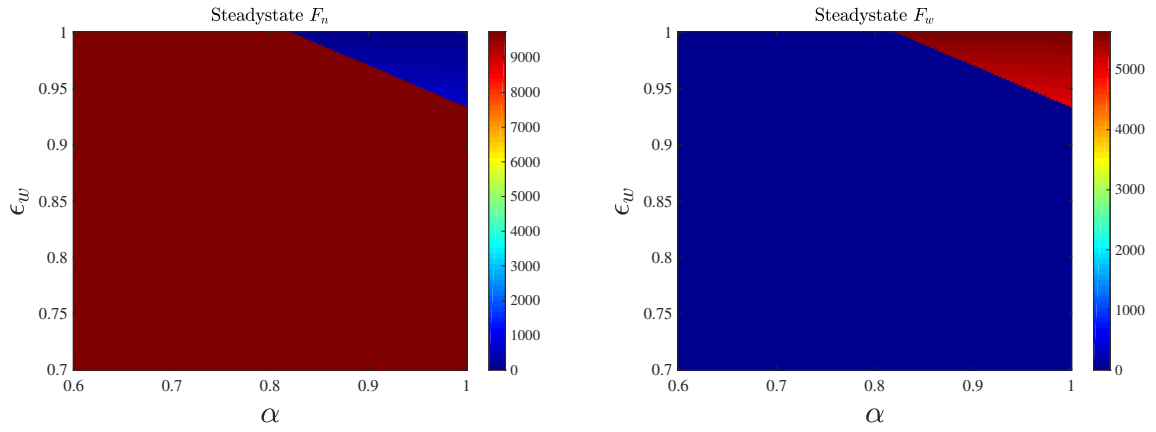

Figure 2.4: Effects of ϵ_w and α on steady states when the initial release of *Wolbachia*-infected mosquitoes is $F_w(0) = M_w(0) = 10,000$

noted with $\mathscr{R}_0^{wolb}$, remains below one for parameter values that are biologically feasible. Therefore, the initial release of *Wolbachia*-infected mosquitoes is critical if we want *Wolbachia*-infected mosquitoes to persist and suppress the population of the wild mosquitoes. If the initial release of *Wolbachia*-infected mosquitoes is not large enough, *Wolbachia*-infected mosquitoes will not persist and die out.

The above-mentioned observations suggest that an initial release of *Wolbachia*-infected mosquitoes is important for *Wolbachia*-infected mosquitoes to persist and suppress the wild mosquitoes population. If an initial release of *Wolbachia*-infected mosquitoes is below a certain threshold value, they will not persist in the system. Thus, there is a need to develop a mathematical model that ensures the persistence of *Wolbachia* infection in wild regardless of the initial release number of *Wolbachia*-infected mosquitoes in the wild. To achieve this goal, we extend the model (2.1a) - (2.1f) by considering time-dependent control variables $u_1(t)$ and $u_2(t)$ in the WI female and male compartments, respectively. We also notice that authors in [39, 40] studied optimal control models for releasing *Wolbachia*-infected mosquitoes, but they simplified the models by considering only female mosquitoes (single-sex) along with perfect maternal transmission and complete cytoplasmic incompatibility. Also, the models in [39, 40] considered feedback control that depends on the current population of female mosquitoes, which is not realistic due to the difficulty of counting female mosquitoes. In our model, the control variable $u_1(t)\colon [0, T] \mapsto u_{1max}$ denotes the release rate of WI female

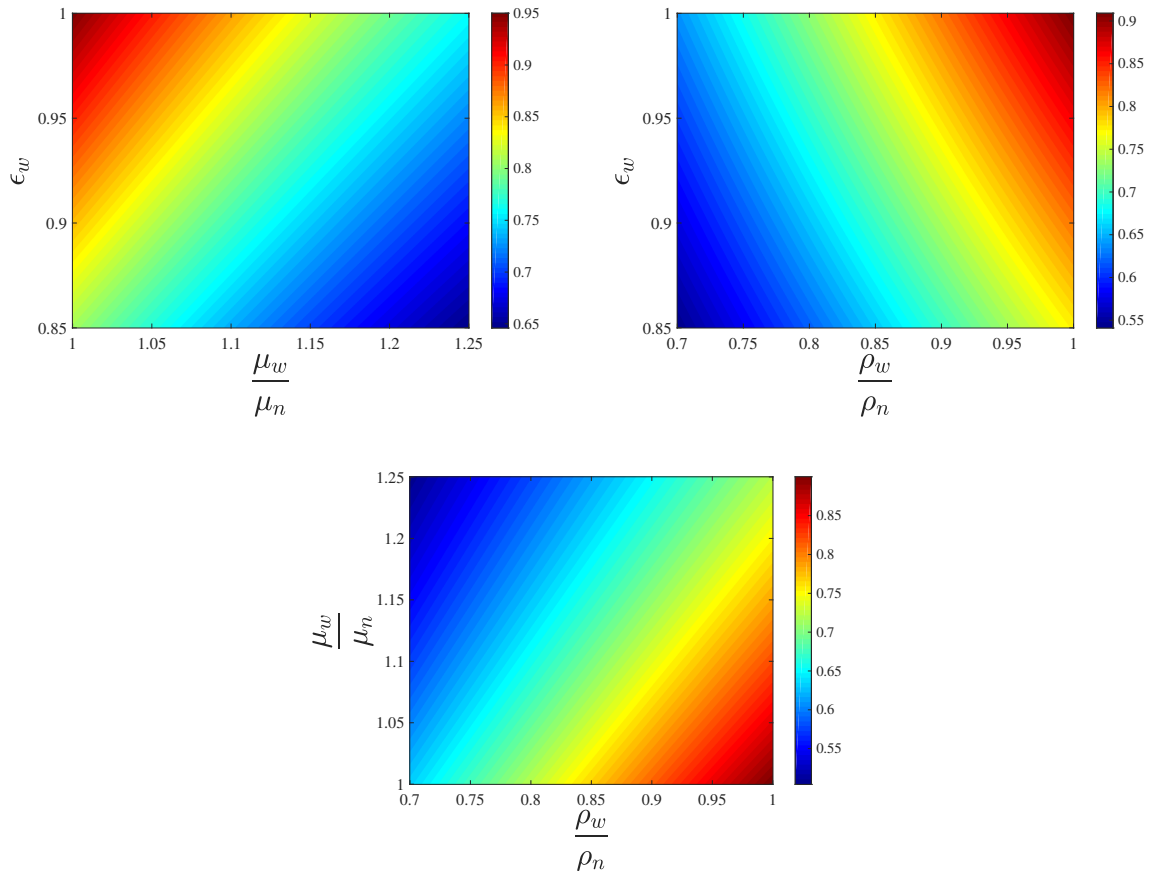

Figure 2.5: $\mathscr{R}_0^{wolb}$ values for different parameters space. On the top left panel (a) values of $\mathscr{R}_0^{wolb}$ for $\left(\epsilon_w, \frac{\mu_w}{\mu_n}\right)$– space, on the top right panel (b) values of $\mathscr{R}_0^{wolb}$ for $\left(\epsilon_w, \frac{\rho_w}{\rho_n}\right)$–space, and on the bottom panel (c) values of $\mathscr{R}_0^{wolb}$ for $\left(\frac{\rho_w}{\rho_n}, \frac{\mu_w}{\mu_n}\right)$–space.

mosquitoes, while the control variable $u_2(t)\colon [0,T] \mapsto u_{2max}$ represents the release rate of WI male mosquitoes. The upper bounds on the maximum release rate per day of WI female and male mosquitoes are denoted with u_{1max} and u_{2max}, respectively. With these control variables in the *Wolbachia*-infected female and male compartments, the new system reads as follows:

$$\frac{dA_n}{dt} = \rho_n F_n \frac{M_n}{M_n + M_w}\left(1 - \frac{A_n + A_w}{K}\right) + (1-\alpha)\rho_n F_n \frac{M_w}{M_n + M_w}\left(1 - \frac{A_n + A_w}{K}\right) + \rho_w (1-\epsilon_w) F_w \left(1 - \frac{A_n + A_w}{K}\right) - (\gamma_n + \mu_{na})A_n, \tag{2.27a}$$

$$\frac{dF_n}{dt} = \tau\gamma_n A_n - \mu_n F_n, \tag{2.27b}$$

$$\frac{dM_n}{dt} = (1-\tau)\gamma_n A_n - \mu_{mn} M_n, \tag{2.27c}$$

$$\frac{dA_w}{dt} = \rho_w \epsilon_w F_w \left(1 - \frac{A_n + A_w}{K}\right) - (\gamma_w + \mu_{wa})A_w, \tag{2.27d}$$

$$\frac{dF_w}{dt} = u_1(t) + \tau\gamma_w A_w - \mu_w F_w, \tag{2.27e}$$

$$\frac{dM_w}{dt} = u_2(t) + (1-\tau)\gamma_w A_w - \mu_m M_w. \tag{2.27f}$$

with the initial conditions

$$A_n(0) \geq 0, \quad F_n(0) \geq 0, \quad M_n(0) \geq 0, \tag{2.28}$$

$$A_w(0) = 0, \quad F_w(0) = 0, \quad M_w(0) = 0. \tag{2.29}$$

and with

$$0 \leq u_1 \leq u_{1max} \quad \text{and} \qquad 0 \leq u_2 \leq u_{2max}.$$

The objective of the optimal control model is to minimize the population of wild female mosquitoes along with the cost associated with the production and release of WI female and male mosquitoes on the time interval $[0, T]$, which is also in line with other studies [39, 40, 59, 60]. Thus, we define the objective functional as

$$J(u_1, u_2) = \min_{u_1,\, u_2 \in \mathcal{U}} \int_0^T B_1 F_n + \frac{1}{2}\left(B_2 u_1^2 + B_3 u_2^2\right)\, dt, \tag{2.30}$$

subject to the system (2.27a)-(2.27f) and (2.2). The set $\mathcal{U}$ of admissible controls is defined

$$\mathcal{U} := \left\{ \begin{array}{l} (u_1(t),\, u_2(t)) \mid 0 \leq u_1(t) \leq u_{1max}, \quad 0 \leq u_2(t) \leq u_{2max}, \\ u_1 \text{ and } u_2 \text{ are measurable} \quad \forall t \in [0,\, T]. \end{array} \right\} \tag{2.31}$$

The term $B_1 F_n$ in the functional (2.30) represents the social cost (for examples hospitalization, screening, testing, etc.) due to female mosquito bites whereas the terms $B_2 u_1$ and $B_2 u_2$ denote the marginal cost of producing and releasing WI female and male mosquitoes, respectively. The weight constants B_i are positive and describe the relative importance of the state variable F_n and control variables $u_1(t)$ and $u_2(t)$. Since the cost associated with the production and release of WI female and male mosquitoes is the same, we take $B_2 = B_3$. Also, we consider quadratic cost on the control variables $u_1(t)$ and $u_2(t)$, which is the simplest and widely used nonlinear representation of controls cost in epidemic models and consistent with previous studies [7,10,39,40,59–63]. Thus, our goal is to find the optimal release of the *Wolbachia*-infected female $u_1^*(t)$ and *Wolbachia*-infected male $u_2^*(t)$ mosquitoes that minimize the objective functional (2.30), i.e.

$$J(u_1^*, u_2^*) = \min_{u_1,\, u_2 \in \mathcal{U}} J(u_1, u_2), \tag{2.32}$$

where $\mathcal{U}$ is the control set defined in (2.31).

2.6 Existence of controls

To prove that the optimal control pair (u_1^*, u_2^*) exists, we make use of results from [12] and also stated in chapter (1).

Theorem 2.2. *Suppose the objective functional*

$$J(u_1, u_2) = \min_{u_1,\, u_2 \in \mathcal{U}} \int_0^T B_1 F_n + \frac{B_2}{2} \left(u_1^2 + u_2^2\right)\, dt$$

where $(u_1,\, u_2) \in \mathcal{U}$ *are measurable functions subject to the dynamical system* (2.27a)-(2.27f)

along with the initial conditions (2.28) *and* (2.29) *and* (2.2)*, then there exists an optimal control pair* (u_1^*, u_2^*) *such that* $J(u_1^*, u_2^*) = \min_{u_1,\, u_2 \in \mathcal{U}} J(u_1, u_2)$.

Proof.

1. The set of controls and the corresponding state variables is not empty because the solutions to the state equations are a priori bounded and the state equations are continuous and Lipschitz in the state variables, hence there is a unique solution corresponding to every admissible control in $\mathcal{U}$.

2. The control set $\mathcal{U}$ is closed and convex by definition.

3. The right hand side of the system (2.27a)-(2.27f) can be written as the sum of linear functions in the control and state variables by observing linear dependence of the state equations on the controls u_1 and u_2.

4. The integrand of the objective functional, defined in (2.30), is convex with respect to control variables due to the quadratic nature of the controls.

5. The integrand of the objective functional (2.30) is bounded below.

$$\begin{aligned} L(t, F_n, M_n, u_1, u_2) &= B_1 F_n + \tfrac{B_2}{2}\,(u_1^2 + u_2^2) \\ &\geq B_2(u_1^2 + u_2^2) \\ &\geq c_3 \left(\textstyle\sum_{j=1}^{2} |u_i|^2\right)^{\frac{\beta}{2}} - c_4, \end{aligned}$$

where the last inequality is satisfied if we take $c_3 = B_2$, $\beta = 2$, and $c_4 > 0$.

□

2.7 Necessary conditions of the control

Since it is a constrained problem, we use the Pontryagin's maximum principle [13], which converts the system (2.27a)-(2.27f) and the objective functional (2.30) into a problem of minimizing the Hamiltonian point-wise with respect to the control variables u_1 and u_2.

Theorem 2.3. *If* $(u_1^*,\, u_2^*)$ *is an optimal control pair corresponding to the states* A_n^*, F_n^*, M_n^*, A_w^*, F_w^* *and* M_w^* *which minimize the objective functional* $J(u_1,\, u_2)$*, then there exists adjoint*

variables $\lambda_i \quad i \in \{A_n, F_n, M_n A_w, F_w, M_w\}$ *which satisfy:*

$$\begin{aligned}
\frac{d\lambda_{A_n}}{dt} &= -\frac{\partial \mathcal{H}}{\partial A_n} \\
&= \gamma_n(\lambda_{A_n} - \tau\lambda_{F_n} - (1-\tau)\lambda_{M_n}) + \frac{\lambda_{A_n}\rho_n}{K}\frac{F_n M_n}{(M_n + M_w)} \\
&\quad + \frac{\rho_w F_w}{K}(\epsilon_w \lambda_{A_w} + (1-\epsilon_w)\lambda_{A_n}) + \mu_{na}\lambda_{A_n} \\
\frac{d\lambda_{F_n}}{dt} &= -\frac{\partial \mathcal{H}}{\partial F_n} \\
&= -B_1 + \mu_n \lambda_{F_n} - \lambda_{A_n}\rho_n \left(1 - \frac{A_n + A_w}{K}\right)\frac{M_n}{M_n + M_w} \\
\frac{d\lambda_{M_n}}{dt} &= -\frac{\partial \mathcal{H}}{\partial M_n} \\
&= \mu_m \lambda_{M_n} - \lambda_{A_n}\rho_n \left(1 - \frac{A_n + A_w}{K}\right)\frac{F_n M_n}{(M_n + M_w)^2} \qquad (2.33) \\
\frac{d\lambda_{A_w}}{dt} &= -\frac{\partial \mathcal{H}}{\partial A_w} \\
&= \frac{\rho_n \lambda_{A_n}}{K}\frac{F_n M_n}{M_n + M_w} + \frac{(1-\epsilon_w)\rho_w \lambda_{A_n}}{K} F_w \\
&\quad + (\gamma_w + \mu_{wa})\lambda_{A_w} + \frac{\epsilon_w \rho_w \lambda_{A_w}}{K} F_w - (1-\tau)\gamma_w \lambda_{M_w} - \tau\gamma_w \lambda_{F_w} \\
\frac{d\lambda_{F_w}}{dt} &= -\frac{\partial \mathcal{H}}{\partial F_w} \\
&= \mu_w \lambda_{F_w} - \rho_w \left(\epsilon_w \lambda_{A_w} + (1-\epsilon_w)\lambda_{A_n}\right)\left(1 - \frac{A_n + A_w}{K}\right) \\
\frac{d\lambda_{M_w}}{dt} &= -\frac{\partial \mathcal{H}}{\partial M_w} \\
&= \mu_m \lambda_{M_w} + \lambda_{A_n}\rho_n \left(1 - \frac{A_n + A_w}{K}\right)\frac{F_n M_n}{(M_n + M_w)^2}
\end{aligned}$$

with the terminal (also called transversality) conditions

$$\lambda_i(T) = 0 \quad \textit{where} \quad i \in \{A_n, F_n, M_n A_w, F_w, M_w\}\,. \qquad (2.34)$$

Furthermore, the characterization of optimal control variables u_1^* and u_2^* are given by

$$\begin{aligned} u_1^* &= \max\left\{0, \min\{-\frac{\lambda_{F_w}}{B_2}, u_{1max}\}\right\} \\ u_2^* &= \max\left\{0, \min\{-\frac{\lambda_{M_w}}{B_2}, u_{2max}\}\right\}. \end{aligned}$$

Proof. The Hamiltonian $\mathcal{H}$ is given by

$$\begin{aligned} \mathcal{H} &= B_1 F_n + \tfrac{1}{2}\left(B_2 u_1^2 + B_2 u_2^2\right) \\ &\quad + \lambda_{A_n}\tfrac{dA_n}{dt} + \lambda_{F_n}\tfrac{dF_n}{dt} + \lambda_{M_n}\tfrac{dM_n}{dt} + \lambda_{A_w}\tfrac{dA_w}{dt} + \lambda_{F_w}\tfrac{dF_w}{dt} + \lambda_{M_w}\tfrac{dM_w}{dt} \end{aligned}$$

Differentiating $\mathcal{H}$ with respect to the control variables, u_1 and u_2, and setting equal to zero, we get

$$u_1^* = -\frac{\lambda_{F_w}}{B_2}, \quad u_2^* = -\frac{\lambda_{M_w}}{B_2}.$$

Now using the bounds on the control varialbes u_1 and u_2, we have

$$u_1^* = \begin{cases} 0 & \text{if} \quad -\frac{\lambda_{F_w}}{B_2} < 0 \\ -\frac{\lambda_{F_w}}{B_2} & \text{if} \quad 0 < -\frac{\lambda_{F_w}}{B_2} < u_{1max} \\ u_{1max} & \text{if} \quad -\frac{\lambda_{F_w}}{B_2} > u_{1max} \end{cases} \tag{2.35}$$

$$u_2^* = \begin{cases} 0 & \text{if} \quad -\frac{\lambda_{M_w}}{B_2} < 0 \\ -\frac{\lambda_{M_w}}{B_2} & \text{if} \quad 0 < -\frac{\lambda_{M_w}}{B_2} < u_{2max} \\ u_{2max} & \text{if} \quad -\frac{\lambda_{M_w}}{B_2} > u_{2max}. \end{cases} \tag{2.36}$$

Writing (2.35) and (2.36) in compact notation, we get the following characterization of control variables

$$\begin{aligned} u_1^* &= \max\left\{0, \min\{-\frac{\lambda_{F_w}}{B_2}, u_{1\max}\}\right\} \\ u_2^* &= \max\left\{0, \min\{-\frac{\lambda_{M_w}}{B_2}, u_{2\max}\}\right\}. \end{aligned}$$

□

Finally, optimality system is given by

State Equations:

$$\begin{cases} \frac{dA_n}{dt} &= \rho_n F_n \frac{M_n}{M_n+M_w}\left(1-\frac{A_n+A_w}{K}\right) \\ & \quad +(1-\alpha)\rho_n F_n \frac{M_w}{M_n+M_w}\left(1-\frac{A_n+A_w}{K}\right) \\ & \quad +\rho_w\left(1-\epsilon_w\right)F_w\left(1-\frac{A_n+A_w}{K}\right)-(\gamma_n+\mu_{na})A_n, \\ \frac{dF_n}{dt} &= \tau\gamma_n A_n-\mu_n F_n, \\ \frac{dM_n}{dt} &= (1-\tau)\gamma_n A_n-\mu_m M_n, \\ \frac{dA_w}{dt} &= \rho_w\epsilon_w(F_w)\left(1-\frac{A_n+A_w}{K}\right)-(\gamma_w+\mu_{wa})A_w, \\ \frac{dF_w}{dt} &= u_1^*(t)+\tau\gamma_w A_w-\mu_w F_w, \\ \frac{dM_w}{dt} &= u_2^*(t)+(1-\tau)\gamma_w A_w-\mu_m M_w, \\ A_n(0) &\geq 0 \quad , \quad F_n(0)\geq 0,\ M_n(0)\geq 0 \\ A_w(0) &= 0, \quad F_w(0)=0, \quad M_w(0)=0. \end{cases} \tag{2.37}$$

Adjoint (co-state) Equations:

$$\begin{cases} \frac{d\lambda_{A_n}}{dt} &= \gamma_n(\lambda_{A_n}-\tau\lambda_{F_n}-(1-\tau)\lambda_{M_n})+\frac{\lambda_{A_n}\rho_n}{K}\frac{F_nM_n}{(M_n+M_w)} \\ & \quad +\frac{\rho_w F_w}{K}(\epsilon_w\lambda_{A_w}+(1-\epsilon_w)\lambda_{A_n})+\mu_{na}\lambda_{A_n} \\ \frac{d\lambda_{F_n}}{dt} &= -B_1+\mu_n\lambda_{F_n}-\lambda_{A_n}\rho_n\left(1-\frac{A_n+A_w}{K}\right)\frac{M_n}{M_n+M_w} \\ \frac{d\lambda_{M_n}}{dt} &= \mu_m\lambda_{M_n}-\lambda_{A_n}\rho_n\left(1-\frac{A_n+A_w}{K}\right)\frac{F_nM_n}{(M_n+M_w)^2} \\ \frac{d\lambda_{A_w}}{dt} &= \frac{\rho_n\lambda_{A_n}}{K}\frac{F_nM_n}{M_n+M_w}+\frac{(1-\epsilon_w)\rho_w\lambda_{A_n}}{K}F_w+(\gamma_w \\ & \quad +\mu_{wa})\lambda_{A_w}+\frac{\epsilon_w\rho_w\lambda_{A_w}}{K}F_w-(1-\tau)\gamma_w\lambda_{M_w}-\tau\gamma_w\lambda_{F_w} \\ \frac{d\lambda_{F_w}}{dt} &= \mu_w\lambda_{F_w}-\rho_w\left(\epsilon_w\lambda_{A_w}+(1-\epsilon_w)\lambda_{A_n}\right)\left(1-\frac{A_n+A_w}{K}\right) \\ \frac{d\lambda_{M_w}}{dt} &= \mu_m\lambda_{M_w}+\lambda_{A_n}\rho_n\left(1-\frac{A_n+A_w}{K}\right)\frac{F_nM_n}{(M_n+M_w)^2} \\ \lambda_i(T) &= 0 \quad \text{where} \quad i=\{A_n,F_n,M_n,A_w,F_w,M_w\}. \end{cases} \tag{2.38}$$

2.8 Numerical results and discussion

Due to non-linearity and complexity of the control dynamical system (2.37) and (2.38), we solve the control system numerically and present the results of the simulations in this section.

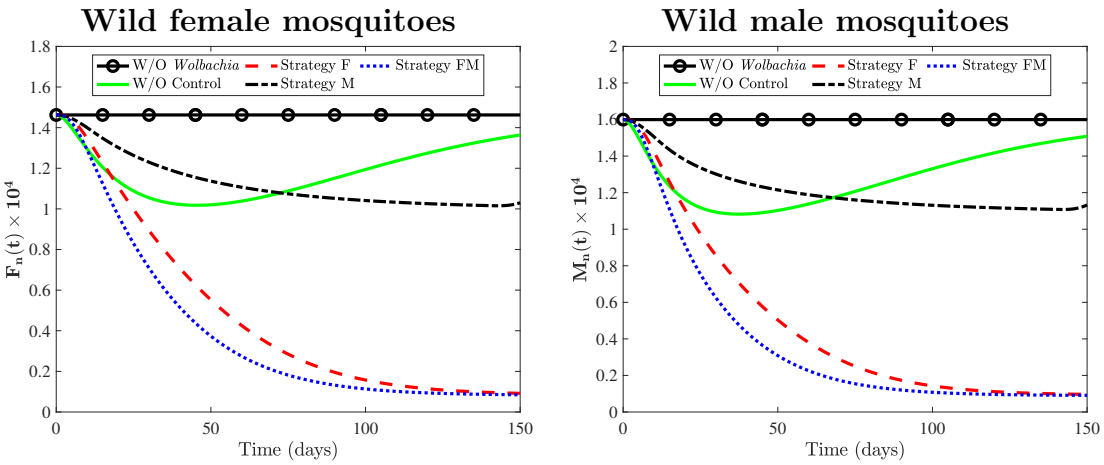

(a) (b)

Figure 2.6: Dynamics of wild female mosquitoes (left panel) and male mosquitoes (right panel) population when *Wolbachia*-infected mosquitoes are released using different strategies. The solid circled line shows the steady state of wild mosquitoes in the absence of *Wolbachia*-infected mosquitoes.

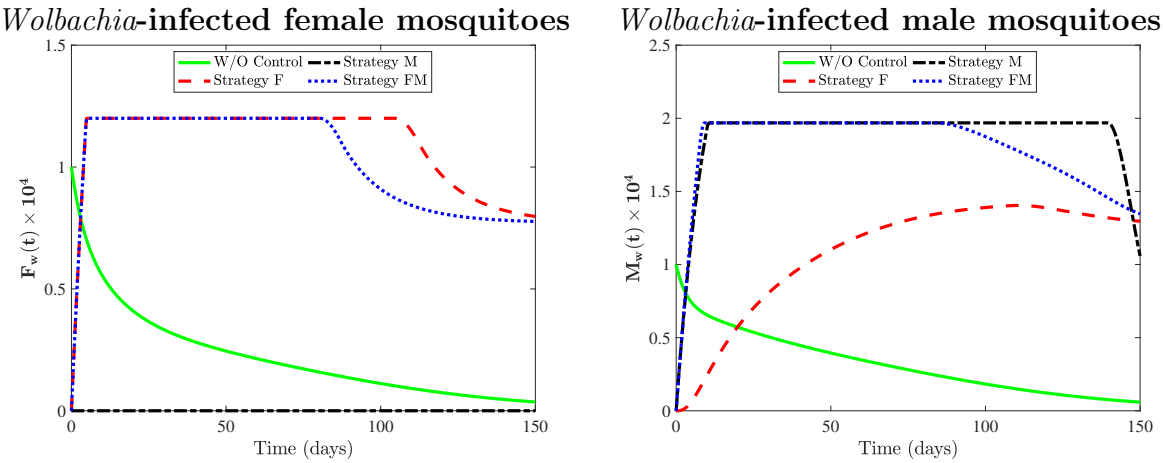

(a) (b)

Figure 2.7: Dynamics of *Wolbachia*-infected female (left panel) and male (right panel) mosquitoes when different strategies are implemented for releasing *Wolbachia*-infected mosquitoes in the wild.

For solving the control system numerically, we assume that initially there are no *Wolbachia*-infected mosquitoes present and the population of wild mosquitoes is at the equilibrium states, that is

$$A_n(0) = K(1 - \frac{1}{\mathscr{R}_{0n}}), \qquad F_n(0) = \frac{\tau\gamma_n}{\mu_n}A_n(0), \qquad M_n(0) = \frac{(1-\tau)\gamma_n}{\mu_n}A_n(0),$$

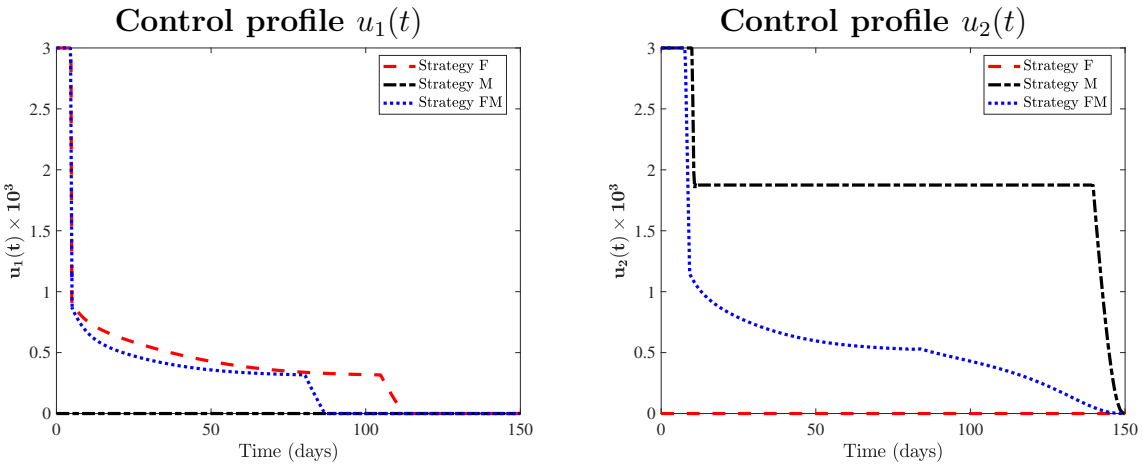

(a) (b)

Figure 2.8: The trajectories of the optimal controls $u_1^*(t)$ (left panel) and $u_2^*(t)$ (right panel) for different control strategies.

$$A_w(0) = 0, \qquad F_w(0) = 0, \text{and} \qquad M_w(0) = 0.$$

Thus, the state equations (2.37) in the optimal control system are defined at the initial time (initial conditions) whereas the costate equations (2.38) are defined at the terminal time (terminal conditions). We solve the control system (2.37) and (2.38) numerically using the forward-backward sweep method and the algorithm discussed in Section 1.2.3 of chapter 1. In all simulations, we choose parameter values given in Table (2.1). In our optimal control problem, our top priority is to decrease the number of wild female mosquitoes F_n; hence we need to take high values for the weight constant B_1 associated with F_n and in our simulations we set $B_1 = 5$. For the weight constant B_2, we consider $B_2 = \frac{1}{10^3}$, where 10^3 is used to balance all the terms in the objective functional (2.30). In all simulations, we consider $T = 150$ days (5 months). To study the effects of releasing *Wolbachia*-infected mosquitoes on the population of wild mosquitoes, we investigate the following releasing strategies of *Wolbachia*-infected mosquitoes:

1. **Strategy F:** When only *Wolbachia*-infected female mosquitoes are released (i.e. $u_1 \neq 0$ and $u_2 = 0$).

2. **Strategy M:** When only *Wolbachia*-infected male mosquitoes are released (i.e. $u_2 \neq 0$ and $u_1 = 0$).

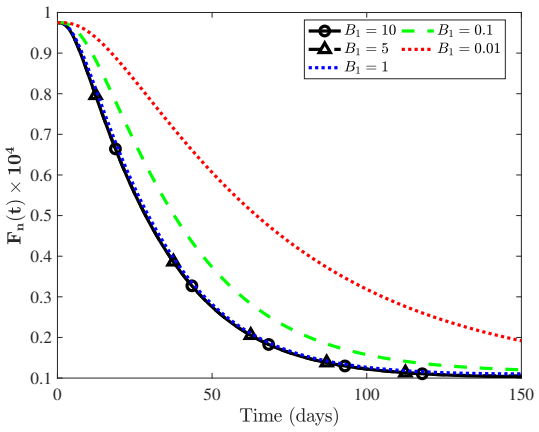

Dynamics of F_n for low values of B_1

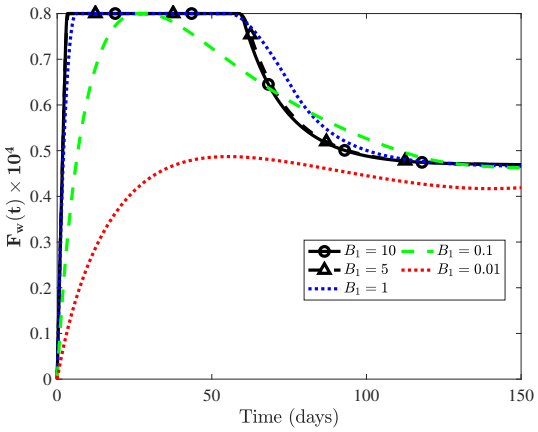

Dynamics of F_w for low values of B_1

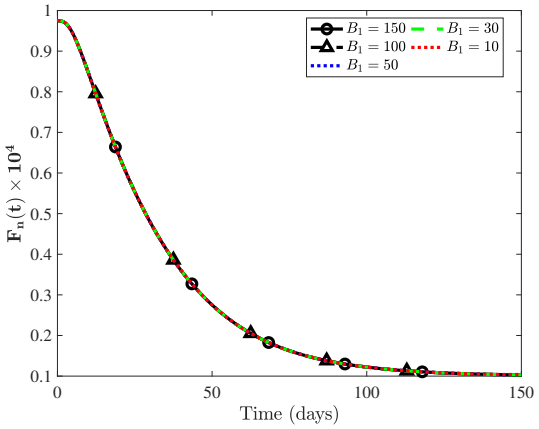

Dynamics of F_n for high values of B_1

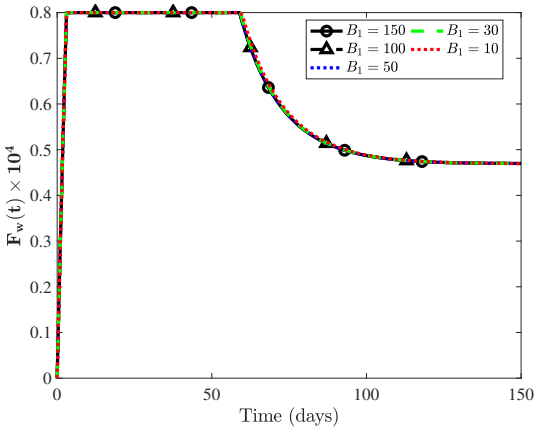

Dynamics of F_w for high values of B_1

Figure 2.9: Dynamics of wild female mosquitoes (left panel) and *Wolbachia*-infected female mosquitoes (right panel) under different weight constant B_1 and fixed $B_2 = 0.001$. The upper bound on $u_{1_{max}}$ and $u_{2_{max}}$ is 3000.

3. **Strategy FM:** When both *Wolbachia*-infected female and male mosquitoes are released (i.e. $u_1 \neq 0$ and $u_2 \neq 0$).

The numerical results for the number of *Wolbachia*-uninfected female mosquitoes (left panel) and *Wolbachia*-uninfected male mosquitoes (right panel) are shown in Figure 2.6 when *Wolbachia*-infected mosquitoes are released according to the above mentioned strategies. The black solid circle line in Figure 2.6 represents the wild mosquitoes population in the absence of *Wolbachia*-infected mosquitoes and the green solid line shows the dynamics when *Wolbachia*-infected mosquitoes are released initially only (i.e. no controls). The dotted and dashed lines show the dynamics of *Wolbachia*-free mosquitoes when

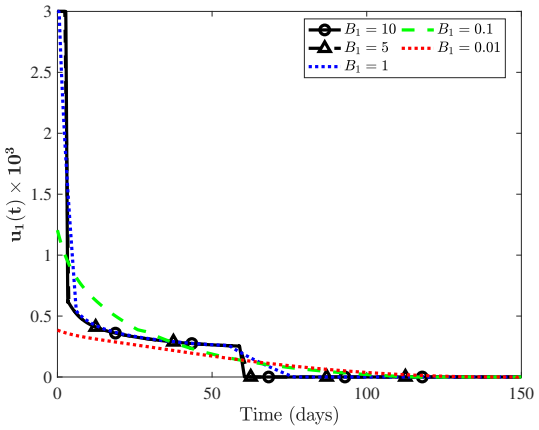

Control profile $u_1(t)$ for low values of B_1.

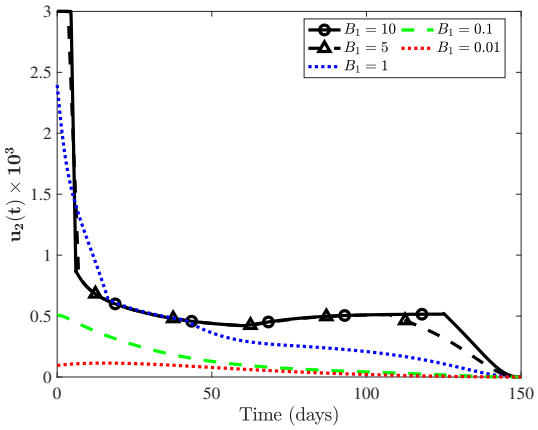

Control profile $u_2(t)$ for low values of B_1.

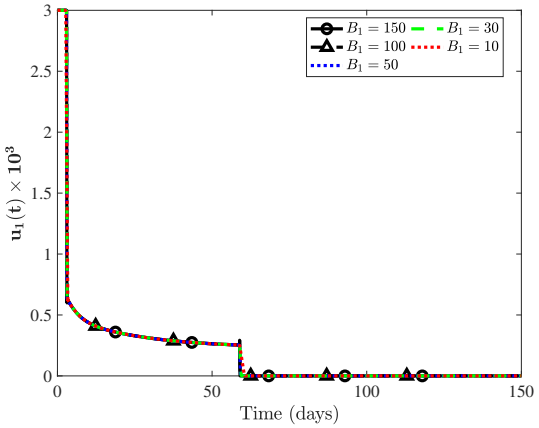

Control profile $u_1(t)$ for high values of B_1.

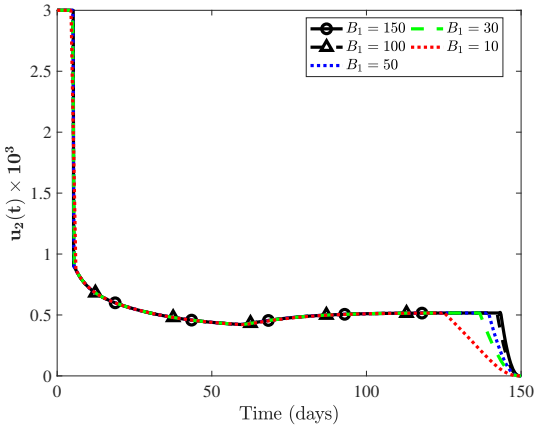

Control profile $u_2(t)$ for high values of B_1.

Figure 2.10: Trajectories of the optimal controls u_1^* and u_2^* under different weight constant B_1 and fixed $B_2 = 0.001$.

Wolbachia-infected mosquitoes are released according to the three different strategies. The numerical results in Figure 2.6 manifest that the number of wild mosquitoes is large in the absence of *Wolbachia*-infected mosquitoes (black solid circle line) whereas the wild mosquitoes population decreases when *Wolbachia*-infected mosquitoes are released using any of the above mentioned strategies. However, the results in Figure 2.6 show that the population of wild mosquitoes does not decrease significantly when only *Wolbachia*-infected male mosquitoes are released (i.e. when strategy 1 is applied only) and the population of wild mosquitoes decreases significantly when both, female and male, *Wolbachia*-infected mosquitoes are released into wild (i.e. when strategy 3 is applied). The results in Figure 2.6 also demonstrate that the population of wild mosquitoes decreases more when *Wolbachia*-infected female

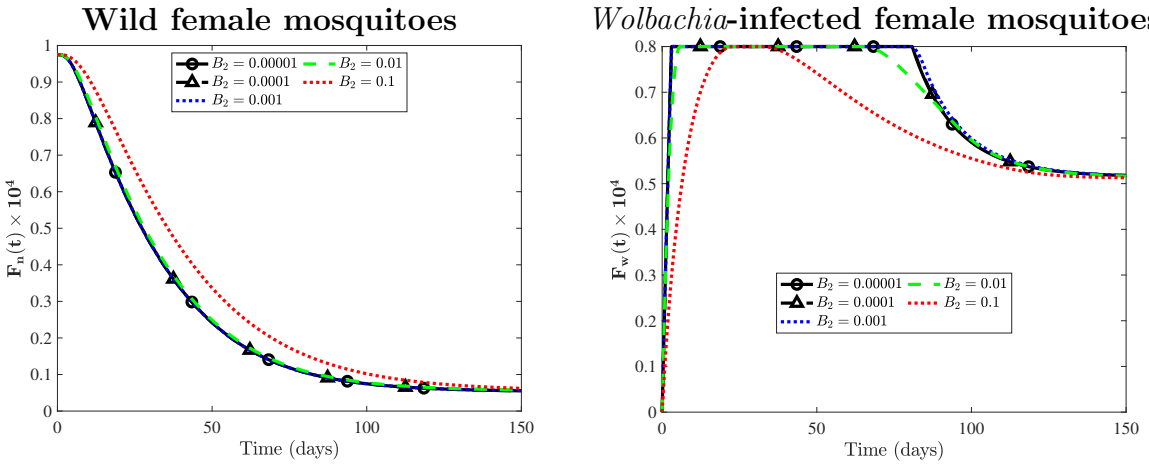

Figure 2.11: Dynamics of wild female mosquitoes (left panel) and *Wolbachia*-infected female mosquitoes (right panel) under different weight constant B_2 while $B_1 = 10$ is fixed. The upper bound on $u_{1_{max}}$ and $u_{2_{max}}$ is 3000.

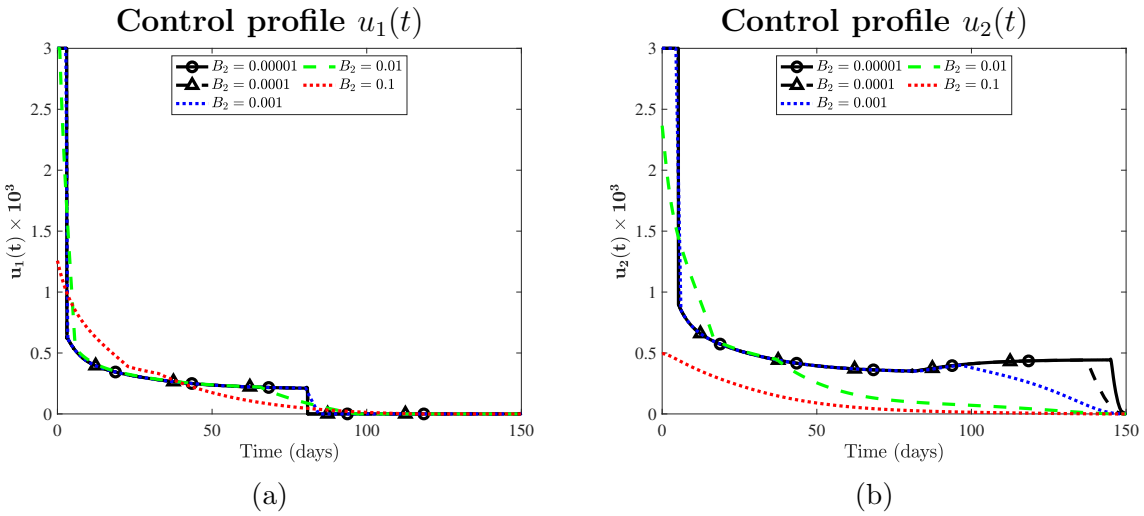

Figure 2.12: Trajectories of the optimal controls u_1^* and u_2^* under different weight constant B_2 while $B_1 = 10$ is fixed.

mosquitoes are released alone (i.e. under strategy 2) compare to the strategy 1. The optimal control trajectories in the left panel of Figure 2.8 also show that smaller numbers of *Wolbachia*-infected female mosquitoes are required to release under strategy 3 and is also in favor of humans since female mosquitoes are the one who bite for the blood meal and thus are nuisance for humans. The numerical results in Figures 2.6 and 2.8 show that strategy 3 (i.e. releasing both female and male *Wolbachia*-infected mosquitoes) is more effective in

reducing wild mosquitoes population compare to the other two strategies. Under strategy 3, the total number of *Wolbachia*-infected female and male required to release is 3.5×10^3 and 8.1×10^3, respectively. The evolution of *Wolbachia*-infected female and male mosquitoes as a function of time is also shown in Figure 2.7 when different control strategies are implemented for releasing *Wolbachia*-infected mosquitoes.

2.8.1 Effects of weight constants B_1 and B_2

The effects of the weight constants B_1(social cost) and B_2 (production and releasing cost of *Wolbachia*-infected mosquitoes) are also studied for different values of the weight constants B_1 and B_2. Since strategy 3 seems more promising in terms of cost and effectiveness, we only study the effects of the weight constants, B_1 and B_2, when *Wolbachia*-infected mosquitoes are released under strategy 3. The results in Figure 2.9 show the evolution of wild female mosquitoes when $B_2 = 0.001$ is fixed and B_1 is varied. The upper bound for both controls is also kept constant at 3000. The results in Figure **??** show that when the weight constant is the smallest (i.e. $B_1 = 0.01$), reduction in the number of wild female mosquitoes is small compare to when high values of B_1 are used. However, the results in Figure 2.9 show that increasing the values of B_1 beyond 5 do not change the dynamics of wild female mosquitoes much but only increase the total cost to implement the strategy. The trajectories of the optimal controls, $u_1^*(t)$ and $u_2^*(t)$, are also shown in Figure 2.10 for different values of B_1.

In Figure 2.11, time series plots for wild (left panel) and *Wolbachia*-infected (right panel) female mosquitoes are shown when B_1 is fixed and B_2 is varied. The results in Figure 2.11 show that the population of wild female mosquitoes is small for smaller values of B_2 (i.e. when production and releasing cost of *Wolbachia*-infected mosquitoes is cheap) and reduction in the number of wild female mosquitoes is small for larger values of B_2 (i.e. when production and releasing cost of *Wolbachia*-infected mosquitoes is expensive).

2.9 Conclusion

In this chapter, we considered both uncontrolled and controlled models to study the population dynamics of wild and *Wolbachia*-infected mosquitoes. To fill the gap in the existing models on *Wolbachia*, we considered a more general model that incorporates key biological parameters such as imperfect maternal transmission, incomplete cytoplasmic incompatibility, and density dependent birth rates along with aquatic, female, and male compartments for both group of mosquitoes population. Using the next generation matrix approach, we found an analytic expression for the basic reproduction number, $\mathscr{R}_0^{wolb}$, and studied stability properties of the *Wolbachia*-free equilibrium point for the uncontrolled model. The existence of backward bifurcation phenomena when $\mathscr{R}_0^{wolb} < 1$ along with the observation that $\mathscr{R}_0^{wolb}$ remains below one for biological feasible parameter values led us to consider an optimal control model to ensure persistence of *Wolbachia*-infected mosquitoes in the wild. We studied three different releasing strategies for *Wolbachia*-infected mosquitoes in the controlled model and compared the numerical results with those obtained from the uncontrolled model. The numerical results show that releasing both *Wolbachia*-infected female and male mosquitoes in the wild is the best optimal releasing strategy because when this strategy is implemented it keeps the population of wild mosquitoes at the minimum level and *Wolbachia*-infected mosquitoes at a higher level. The numerical results also indicate that lower number of *Wolbachia*-infected mosquitoes are required to release when both *Wolbachia*-infected female and male mosquitoes are introduced in the wild to combat with wild mosquitoes. The effects of weight constant B_1, which measures the social cost due to mosquitoes bite, are also studied and the numerical results show that a higher number mosquitoes infected with *Wolbachia* are required to release for longer time period when the social cost is more expensive (i.e. when B_1 increases). The numerical results also show that a lower number of mosquitoes that are infected with *Wolbachia* is required to release for high values of the production and releasing cost of the *Wolbachia*-infected mosquitoes (i.e. when B_2 increases).

CHAPTER 3

CONTROLLING DENGUE EPIDEMICS THROUGH *WOLBACHIA*-INFECTED MOSQUITOES

Dengue, a vector-borne disease, is now endemic in more than 100 countries in the world and approximately 50-100 million cases are reported every year including tropical and subtropical regions [16]. Dengue virus is transmitted to humans via a bite of infectious mosquitoes. *Aedes aegypti* and *Aedes albopictus* are the two vectors that transmit the virus to humans through bites, but *Aedes aegypti* mosquitoes transmit the virus to humans mostly. Dengue exists in two forms called Dengue Fever (DF) and Dengue Hemorrhagic Fever (DHF) [17]. Dengue Hemorrhagic may evolve to a more severe case called Dengue Shock Syndrome (DSS) [17]. Dengue fever exists in four distinct serotypes known as DENv1, DENv2, DENv3, and DENv4 [17]. A person infected with one serotype gets life-long immunity against that particular serotype, but only temporary immunity against all other serotypes and becomes more susceptible to develop DHF. In [64], it is observed that a particular strain of *Wolbachia* blocks the transmission of virus for a particular serotype of dengue, but it is not clear yet that a particular strain of *Wolbachia* effectively blocks the virus transmission against all dengue serotypes.

3.1 Mathematical model

Several mathematical models have been proposed in the presence of *Wolbachia* [35, 38, 53, 65, 66]. Hancock et al. [65] studied a mathematical model to understand the population dynamics in the presence of *Wolbachia*-carrying mosquitoes. Chan and Kim [67] developed a reaction-diffusion model to study the spread of *Wolbachia* in the mosquitoes population. Ndii et al. [37] formulated a compartmental model by considering aquatic and adult classes for *Wolbachia*-infected and non-*Wolbachia* mosquitoes. They showed that only for perfect

maternal transmission, *Wolbachia*-infected mosquitoes alone persist. Ndii et al. [38] developed a compartmental model for the transmission of dengue in the presence of *Wolbachia*. In this chapter, we develop a dengue epidemic model which is an extension of the model (2.1) formulated in chapter (2). In this model, we also consider human population and divide human population into SEIR compartments and mosquito population into SEI compartments. After including human compartments in the model (2.1), the dengue model reads as follows:

$$\begin{aligned}
\frac{dA_n}{dt} &= \rho_n(S_n + E_n + I_n)\frac{M_n}{M_n + M_w}\left(1 - \frac{A_n + A_w}{K}\right) \\
&\quad + (1-\alpha)\rho_n(S_n + E_n + I_n)\frac{M_w}{M_n + M_w}\left(1 - \frac{A_n + A_w}{K}\right) \\
&\quad + \rho_w\left(1 - \epsilon_w\right)\left(S_w + E_w + I_w\right)\left(1 - \frac{A_n + A_w}{K}\right) \\
&\quad - (\gamma_n + \mu_{na})A_n, \qquad (3.1a)\\
\frac{dS_n}{dt} &= \tau\gamma_n A_n - \mu_n S_n - \frac{a_n\beta_{hn}I_h}{N_h}S_n, \qquad (3.1b)\\
\frac{dE_n}{dt} &= \frac{a_n\beta_{hn}I_h}{N_h}S_n - \beta_n E_n - \mu_n E_n, \qquad (3.1c)\\
\frac{dI_n}{dt} &= \beta_n E_n - \mu_n I_n, \qquad (3.1d)\\
\frac{dM_n}{dt} &= (1-\tau)\gamma_n A_n - \mu_m M_n, \qquad (3.1e)\\
\frac{dA_w}{dt} &= \rho_w\epsilon_w(S_w + E_w + I_w)\left(1 - \frac{A_n + A_w}{K}\right) - (\gamma_w + \mu_{wa})A_w, \qquad (3.1f)\\
\frac{dS_w}{dt} &= \tau\gamma_w A_w - \mu_w S_w - \frac{a_w\beta_{hw}I_h}{N_h}S_w, \qquad (3.1g)\\
\frac{dE_w}{dt} &= \frac{a_w\beta_{hw}I_h}{N_h}S_w - \beta_w E_w - \mu_w E_w, \qquad (3.1h)\\
\frac{dI_w}{dt} &= \beta_w E_w - \mu_w I_w, \qquad (3.1i)\\
\frac{dM_w}{dt} &= (1-\tau)\gamma_w A_w - \mu_m M_w, \qquad (3.1j)
\end{aligned}$$

$$\frac{dS_h}{dt} = \mu_h N_h - \mu_h S_h - \frac{a_n \beta_{nh} I_n}{N_h} S_h - \frac{a_w \beta_{wh} I_w}{N_h} S_h, \tag{3.2a}$$

$$\frac{dE_h}{dt} = \frac{a_n \beta_{nh} I_n}{N_h} S_h + \frac{a_w \beta_{wh} I_w}{N_h} S_h - \mu_h E_h - \theta_h E_h, \tag{3.2b}$$

$$\frac{dI_h}{dt} = \theta_h E_h - \mu_h I_h - \beta_h I_h, \tag{3.2c}$$

$$\frac{dR_h}{dt} = \beta_h I_h - \mu_h R_h. \tag{3.2d}$$

In the model (3.1), we assume homogeneous mixing between mosquitoes and hosts (humans). The schematic of the model (3.1) is shown in Figure 3.1. The mosquito population is divided into two groups: *Wolbachia*-free mosquitoes (i.e. wild mosquitoes) and *Wolbachia*-infected mosquitoes. Each mosquito group is further divided into four compartments: aquatic stages (A_n, A_w), susceptible (S_n, S_w), exposed (exposed to dengue virus but not yet infectious) (E_n, E_w), and infectious (can transmit dengue virus to humans) (I_n, I_w). In both mosquito groups, the aquatic compartments A_n and A_w include eggs, larva, and pupa stages. Total non-*Wolbachia* adult female mosquitoes population is $F_n = S_n + E_n + I_n$ and total *Wolbachia*-infected adult female mosquitoes population is $F_w = S_w + E_w + I_w$.

The host (humans) population is also divided into four compartments: susceptible (S_h), exposed (E_h), infectious (I_h), and recovered (R_h). In this model, we assume constant total host population $N_h = S_h + E_h + I_h + R_h$. Each host class decreases due to natural mortality at a rate μ_h. The susceptible class (S_h) increases due to births at a rate of μ_h and decreases after being bitten by dengue infectious mosquitoes, either *Wolbachia*-infected or *Wolbachia*-uninfected, with a rate of $a_n \beta_{nh} I_n / N_h$ and $a_w \beta_{wh} I_w / N_h$, respectively, where β_{nh} is the transmission probability from non-*Wolbachia* dengue infected female mosquitoes to humans and β_{wh} is the transmission probability from *Wolbachia*-infected and dengue infected female mosquitoes to humans. Exposed people become infectious at a rate of θ_h. Infectious people either die at rate μ_h or recover at a rate of β_h. The decrease in recovery class is due to death at rate μ_h.

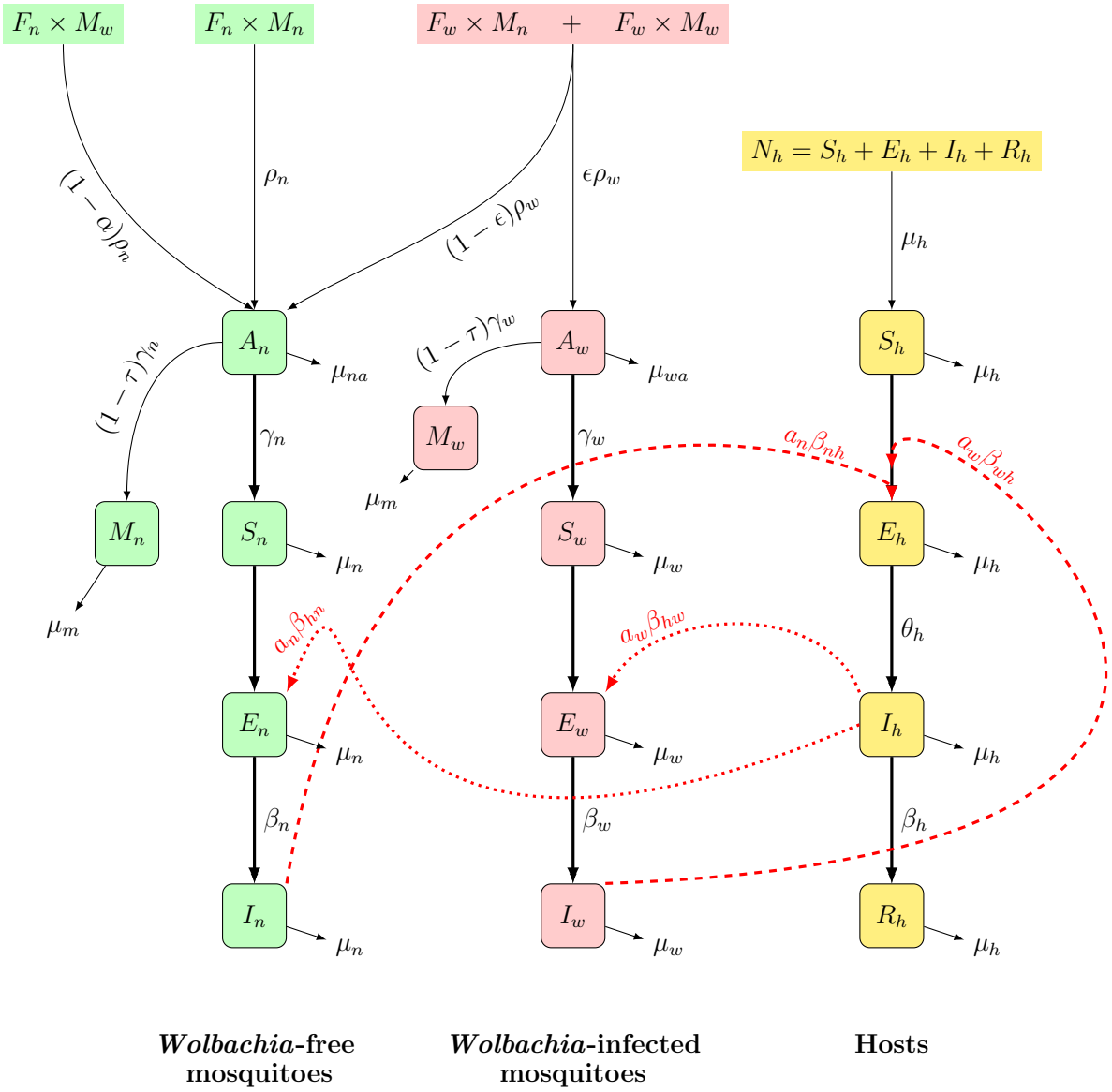

Figure 3.1: A flow diagram of the compartmental model for the transmission of dengue virus in presence of *Wolbachia*-infected mosquitoes along with wild mosquitoes. The subscripts n, w, and h are used to denote the population of wild mosquitoes, *Wolbachia*-infected mosquitoes, and humans, respectively.

Table 3.1: Description of variables and parameters used in the model (3.1). The other parameters are the same as explained in chapter (2).

Symbol	Description	Value	Unit	Source
Variables:				
S_h	Number of susceptible humans	...		
E_h	Number of humans which are exposed to dengue virus but not yet infectious	...		
I_h	Number of humans infected with dengue virus	...		
R_h	Number of humans recovered from dengue	...		
A_n	*Wolbachia*-uninfected population in aquatic stage	...		
S_n	Number of *Wolbachia*-uninfected susceptible female mosquitoes	...		
E_n	Number of *Wolbachia*-uninfected exposed female mosquitoes	...		
I_n	Number of *Wolbachia*-uninfected infectious female mosquitoes	...		
M_n	Number of *Wolbachia*-uninfected Male mosquitoes	...		
A_w	*Wolbachia*-infected population in aquatic stage	...		
S_w	Number of *Wolbachia*-infected susceptible female mosquitoes	...		
E_w	Number of *Wolbachia*-infected exposed female mosquitoes	...		
M_w	Number of *Wolbachia*-infected male mosquitoes	...		
t	Time	...	Days	
Parameters:				
$1/\mu_h$	Average life span of humans	$1/(70*364)$	days	[68]
$1/\theta_h$	Intrinsic incubation period	5	days	[68]
$1/\beta_h$	Infectious period	7	days	[68]
a_n	average number of bites of Wolbachia-free female mosquitoes	0.63	day^{-1}	[38]
a_w	average number of bites of Wolbachia-infected female mosquitoes	$0.95a_n$	day^{-1}	[38]
β_{nh}	Transmission probability from a dengue infected host to *Wolbachia*-uninfected female	0.26	...	[38]
β_{wh}	Transmission probability from a dengue infected host to *Wolbachia*-infected female	0.13	...	[38]
β_{hn}	Transmission probability from a dengue infected *Wolbachia*-free female to hosts	0.26	...	[38]
β_{hw}	Transmission probability from a dengue infected *Wolbachia*-infected female to hosts	0.26	...	[38]
β_n	Extrinsic incubation period for *Wolbachia*-uninfected	10	days	[38]
β_w	Extrinsic incubation period for *Wolbachia*-infected	10	days	[38]

To check that model (3.1) is well-posed, we define the following region $\mathcal{D}$:

$$\mathcal{D} = \left\{ \begin{array}{l} (A_n, S_n, E_n, I_n, M_n, A_w, S_w, E_w, I_w, M_w, S_h, E_h, I_h, R_h) \in \mathcal{R}_+^{14} : \\ A_n + A_w \leq K, S_n + E_n + I_n \leq \frac{\gamma_n}{\mu_n} K, M_n \leq \frac{\gamma_n K}{\mu_m}, \\ S_w + E_w + I_w \leq \frac{\gamma_w}{\mu_w} K, M_w \leq \frac{\gamma_w K}{\mu_m}, \\ S_h + E_h + I_h + R_h \leq N_h \end{array} \right\}$$

From equations (3.1a)-(3.1e) $A_n = 0 \Rightarrow \frac{dA_n}{dt} \geq 0$, $S_n = 0 \Rightarrow \frac{dS_n}{dt} \geq 0$, $E_n = 0 \Rightarrow \frac{dE_n}{dt} \geq 0$, $I_n = 0 \Rightarrow \frac{dI_n}{dt} \geq 0$, $M_n = 0 \Rightarrow \frac{dM_n}{dt} \geq 0$. Similarly from equations (3.1f)-(3.1j) $A_w = 0 \Rightarrow \frac{dA_w}{dt} \geq 0$, $S_w = 0 \Rightarrow \frac{dS_w}{dt} \geq 0$, $E_w = 0 \Rightarrow \frac{dE_w}{dt} \geq 0$, $I_w = 0 \Rightarrow \frac{dI_w}{dt} \geq 0$, and $M_w = 0 \Rightarrow \frac{dM_w}{dt} \geq 0$. Equations (3.2a)-(3.2d) yield $S_h = 0 \Rightarrow \frac{dS_h}{dt} \geq 0$, $E_h = 0 \Rightarrow \frac{dE_h}{dt} \geq 0$, $I_h = 0 \Rightarrow \frac{dI_h}{dt} \geq 0$, $R_h = 0 \Rightarrow \frac{dR_h}{dt} \geq 0$. Thus, $\mathcal{D}$ is positively invariant, that is if a solution starts in $\mathcal{D}$, it remains in $\mathcal{D}$ for all $t > 0$, for the system (3.1a)-(3.2d).

3.2 Dengue-free equilibrium points

Disease(dengue)-free equilibrium points are obtained by setting $E_n = I_n = E_w = I_w = E_h = I_h = R_h = 0$ in the system (3.1a)-(3.2d) and solving the resulting system of equations. In the absence of dengue, the equilibria of the system (3.1a)-(3.2d) are:

1. Host only equilibrium point $E_0 = (0, 0, 0, 0, 0, 0, 0, 0, S_{h0}, 0, 0, 0, 0)$.

2. Host and wild mosquitoes only *Wolbachia*
   $E_1 = (A_{1n}^*, S_{1n}^*, 0, 0, M_{1n}^*, 0, 0, 0, 0, 0, S_{h0}, 0, 0, 0)$,
   where $S_{h0} = N_h$ represents total human population and

$$A_{1n}^* = K(1 - \frac{1}{\mathscr{R}_{0n}}), \quad S_{1n}^* = \frac{\tau\gamma_n}{\mu_n} A_{1n}^*, \quad M_{1n}^* = \frac{(1-\tau)\gamma_n}{\mu_{mn}} A_{1n}^*, \tag{3.3}$$

   where $\mathscr{R}_{0n} = \tau\rho_n \frac{\gamma_n}{\gamma_n + \mu_{na}} \frac{1}{\mu_n}$ is defined in Chapter 2 and represents the total number of female offspring produced by a single *Wolbachia*-uninfected female mosquito during its lifespan. Thus, the disease-free equilibrium point (E_1) persists only if $\mathscr{R}_{0n} > 1$.

3. Host with *Wolbachia*-infected mosquitoes only:

   When maternal transmission is 100% (i.e. $\epsilon_w = 1$), then the disease-free equilibrium point is

$$E_2 = (0, 0, 0, 0, 0, A^*_{2w}, S^*_{2w}, 0, 0, M^*_{2w}, S_{h0}, 0, 0, 0)\,,$$

   where $S_{h0} = N_h$ is the total number of human population, $A^*_{2w} = K(1 - \frac{1}{\epsilon_w R_{0w}})$, $S^*_{2w} = \frac{\tau\gamma_w}{\mu_w} A^*_{2w}$, and $M^*_{2w} = \frac{(1-\tau)\gamma_w}{\mu_{mw}} A^*_{2w}$. $A^*_{2w} > 0$ requires $R_{0w} > 1$, where $\mathscr{R}_{0w} = \tau\rho_w \frac{\gamma_w}{\gamma_w + \mu_{wa}} \frac{1}{\mu_w}$ is *Wolbachia*-infected offspring number which gives total number of female offspring produced by a *Wolbachia*-infected female during its lifetime. Thus, for *Wolbachia*-infected population to persist only $\mathscr{R}_{0w} > 1$ and $\epsilon_w = 1$.

4. Host with *Wolbachia*-infected and wild mosquitoes:

$$E_3 = (A^*_n, S^*_n, 0, 0, M^*_n, A^*_w, S^*_w, 0, 0, M^*_w, S_{h0}, 0, 0, 0)\,,$$

   where A^*_n, S^*_n, M^*_n, A^*_w, S^*_w, and M^*_w are defined in chapter (2) Eqns. (2.6) – (2.11).

3.3 Dengue basic reproduction number $\mathscr{R}_0^{deng}$

In this section, we compute the basic reproduction number ($\mathscr{R}_0^{deng}$) for the dengue epidemic model when *Wolbachia*-infected mosquitoes are introduced in the wild as biological control to reduce dengue infections in humans. To calculus $\mathscr{R}_0^{deng}$, we use the next generation matrix approach proposed by Diekmann et al. [54]. We write the system (3.1a)-(3.2d) in matrix form and linearize the equations that correspond to exposed and infected classes about the dengue-free equilibrium (DFE). The linearized matrix can be decompose into two matrices $\mathcal{F}$ and $\mathcal{V}$, where $\mathcal{F}$ denotes the transmission part and $\mathcal{V}$ denotes the transition part. The next generation matrix $\mathcal{F}\mathcal{V}^{-1}$ is given by

$$\mathcal{FV}^{-1} = \begin{pmatrix} 0 & 0 & \Omega_1\frac{\beta_n}{(\beta_n+\mu_n)} & \Omega_1 & \Omega_2\frac{\beta_w}{(\beta_w+\mu_w)} & \Omega_2 \\ 0 & 0 & 0 & 0 & 0 & 0 \\ \Omega_3\frac{\theta_h}{\theta_h+\mu_h} & \Omega_3 & 0 & 0 & 0 & 0 \\ 0 & 0 & 0 & 0 & 0 & 0 \\ \Omega_4\frac{\theta_h}{\theta_h+\mu_h} & \Omega_4 & 0 & 0 & 0 & 0 \\ 0 & 0 & 0 & 0 & 0 & 0 \end{pmatrix},$$

where $\Omega_1 = \frac{a_n\beta_{nh}}{\mu_n N_h}S_{h0}$, $\Omega_2 = \frac{a_w\beta_{wh}}{\mu_w N_h}S_{h0}$, $\Omega_3 = \frac{a_n\beta_{hn}}{(\beta_h+\mu_h)}\frac{S_n^*}{N_h}$, and $\Omega_4 = \frac{a_w\beta_{hw}}{(\beta_h+\mu_h)}\frac{S_w^*}{N_h}$.

Dengue basic reproduction number $\mathscr{R}_0^{deng}$ is the spectral radius of the next generation matrix $\mathcal{FV}^{-1}$ and given by

$$\mathscr{R}_0^{deng} = \sqrt{\underbrace{\frac{a_n\beta_{nh}}{\mu_n}\frac{\beta_n}{\beta_n+\mu_n}\frac{S_{h0}}{N_h}\frac{a_n\beta_{hn}}{\beta_h+\mu_h}\frac{\theta_h}{\theta_h+\mu_h}\frac{S_n^*}{N_h}}_{\mathscr{R}_{0n}^{deng}} + \underbrace{\frac{a_w\beta_{wh}}{\mu_w}\frac{\beta_w}{\beta_w+\mu_w}\frac{S_{h0}}{N_h}\frac{a_w\beta_{hw}}{\beta_h+\mu_h}\frac{\theta_h}{\theta_h+\mu_h}\frac{S_w^*}{N_h}}_{\mathscr{R}_{0w}^{deng}}}. \tag{3.4}$$

The first term $\mathscr{R}_{0n}^{deng}$ in (3.4) denotes the basic reproduction number of the dengue model when only wild mosquitoes persist, while the second term $\mathscr{R}_{0w}^{deng}$ denotes the basic reproduction number when only *Wolbachia*-infected mosquitoes persist. The basic reproduction number $\mathscr{R}_0^{deng}$ in (3.4) represents when *Wolbachia*-uninfected and *Wolbachia*-infected coexist. It is worth mentioning here that the basic reproduction number $\mathscr{R}_0^{deng}$ depends on the values of S_{h0}, S_n^*, and S_w^* for the particular dengue-free equilibrium point under consideration (i.e. either E_1, E_2, or E_3).

Interpretation of $\mathscr{R}_0^{deng}$:

Note that the term $\frac{a_n\beta_{nh}}{\mu_n}\frac{\beta_n}{\beta_n+\mu_n}\frac{S_{h0}}{N_h}$ denotes the number of infections produced by a single dengue infected wild female mosquitoes during its lifespan when bite susceptible humans, while the term $\frac{a_n\beta_{hn}}{\beta_h+\mu_h}\frac{\theta_h}{\theta_h+\mu_h}\frac{S_n^*}{N_h}$ represents the number of infections produced due to a single infectious human when bitten by susceptible *Wolbachia*-uninfected adult female mosquitoes. The terms $\frac{a_w\beta_{wh}}{\mu_w}\frac{\beta_w}{\beta_w+\mu_w}\frac{S_{h0}}{N_h}$ and $\frac{a_w\beta_{hw}}{\beta_h+\mu_h}\frac{\theta_h}{\theta_h+\mu_h}\frac{S_w^*}{N_h}$ have similar interpretation but for *Wolbachia*-infected mosquitoes.

3.4 Stability analysis of the dengue-free equilibrium points

In this section, we discuss the local and global asymptotic stability of the disease-free equilibrium point E_1.

3.4.1 Local asymptotic stability of the dengue-free equilibrium point E_1

The Jacobian of the system (3.1a)-(3.2d) at the dengue-free equilibrium point

$$E_1 = (A_n^*, S_n^*, 0, 0, M_n^*, 0, 0, 0, 0, 0, S_{h0}, 0, 0, 0)$$

is given by:

$$J_{E_1} = \begin{pmatrix}
J_0 & J_1 & J_1 & J_1 & 0 & -\frac{\rho_n S_n^*}{K} & J_2 & J_2 & J_2 & J_3 & 0 & 0 & 0 & 0 \\
\gamma_n\tau & -\mu_n & 0 & 0 & 0 & 0 & 0 & 0 & 0 & 0 & 0 & 0 & -\frac{a_n\beta_{hn}S_n^*}{N_h} & 0 \\
0 & 0 & -\beta_n-\mu_n & 0 & 0 & 0 & 0 & 0 & 0 & 0 & 0 & 0 & \frac{a_n\beta_{hn}S_n^*}{N_h} & 0 \\
0 & 0 & \beta_n & -\mu_n & 0 & 0 & 0 & 0 & 0 & 0 & 0 & 0 & 0 & 0 \\
(1-\tau)\gamma_n & 0 & 0 & 0 & -\mu_{mn} & 0 & 0 & 0 & 0 & 0 & 0 & 0 & 0 & 0 \\
0 & 0 & 0 & 0 & -\gamma_w-\mu_{wa} & J_4 & J_4 & J_4 & 0 & 0 & 0 & 0 & 0 & 0 \\
0 & 0 & 0 & 0 & \tau\gamma_w & -\mu_w & 0 & 0 & 00 & 0 & & 0 & 0 & 0 \\
0 & 0 & 0 & 0 & 0 & 0 & 0 & -\beta_w-\mu_w & 0 & 0 & 0 & 0 & 0 & 0 \\
0 & 0 & 0 & 0 & 0 & 0 & 0 & \beta_w & -\mu_w & 0 & 0 & 0 & 0 & 0 \\
0 & 0 & 0 & 0 & 0 & (1-\tau)\gamma_w & 0 & 0 & 0 & -\mu_{mw} & 0 & 0 & 0 & 0 \\
0 & 0 & 0 & -J_5 & 0 & 0 & 0 & 0 & -J_6 & 0 & -\mu_h & 0 & 0 & 0 \\
0 & 0 & 0 & J_5 & 0 & 0 & 0 & 0 & J_6 & 0 & 0 & -\mu_h-\theta_h & 0 & 0 \\
0 & 0 & 0 & 0 & 0 & 0 & 0 & 0 & 0 & 0 & 0 & \theta_h & -\beta_h-\mu_h & 0 \\
0 & 0 & 0 & 0 & 0 & 0 & 0 & 0 & 0 & 0 & 0 & 0 & \beta_h & -\mu_h
\end{pmatrix},$$

where $J_0 = -\frac{K(\gamma_n+\mu_{na})+\rho_n S_n^*}{K}$, $J_1 = \rho_n\left(1-\frac{A_n^*}{K}\right)$, $J_2 = \rho_w(1-\epsilon_w)$, $J_3 = -\rho_n\left(1-\frac{A_n^*}{K}\right)\frac{S_n^*}{M_n^*}$, $J_4 = \epsilon_w\rho_w$, $J_5 = a_n\beta_{nh}$, and $J_6 = a_w\beta_{wh}$.

Eigenvalues of the Jacobian matrix J_{E_1} are $-\mu_h, -\mu_w, -\mu_{mn}, -\mu_{mw}, -(\beta_w+\mu_w)$ and the roots of the following equations:

$$\lambda^2 + \alpha_1\lambda + \alpha_2 = 0, \tag{3.5}$$

$$\lambda^2 + \alpha_3\lambda + \alpha_4 = 0, \tag{3.6}$$

$$\lambda^4 + \alpha_5\lambda^3 + \alpha_6\lambda^2 + \alpha_7\lambda + \alpha_8 = 0, \tag{3.7}$$

where

$$
\begin{aligned}
\alpha_1 &= \gamma_w + \mu_w + \mu_{wa}, \\
\alpha_2 &= \frac{\epsilon_w \tau \rho_w \gamma_w}{\mathscr{R}_{0n}} \left(\frac{\mathscr{R}_{0n}}{\mathscr{R}_{0w}} - 1 \right), \\
\alpha_3 &= \gamma_n + \mu_n + \mu_{na} + \frac{\tau \rho_n \gamma_n}{\mu_n} \left(1 - \frac{1}{\mathscr{R}_{0n}} \right), \\
\alpha_4 &= \tau \gamma_n \rho_n \left(1 - \frac{1}{\mathscr{R}_{0n}} \right), \\
\alpha_5 &= \beta_h + \beta_n + 2(\mu_h + \mu_n) + \theta_h, \\
\alpha_6 &= (\beta_h + \mu_h)(\theta_h + \mu_h) + (\beta_h + \theta_h + 2\mu_h)(\beta_n + 2\mu_n) + (\beta_n + \mu_n)\mu_n, \\
\alpha_7 &= (\beta_h + \mu_h)(\theta_h + \mu_h)(\beta_n + 2\mu_n) + (\beta_h + \theta_h + 2\mu_h)(\beta_n + \mu_n)\mu_n, \\
\alpha_8 &= \mu_n(\beta_h + \mu_h)(\mu_h + \theta_h)(\beta_n + \mu_n)(1 - (\mathscr{R}_0^{deng})^2).
\end{aligned}
$$

Using Routh-Hurwitz criteria, we find that roots of (3.5) have negative real part if all the coefficients of (3.5) are positive. Clearly, α_1 is positive and α_2 is positive if $\mathscr{R}_{0n} > \mathscr{R}_{0w}$. Thus, Eq. (3.5) has roots with negative real part if $\mathscr{R}_{0n} > \mathscr{R}_{0w}$. Similarly, Eq. (3.6) has roots with negative real part if $\mathscr{R}_{0n} > 1$. Again by using Routh-Hurwitz criteria for (3.7), its roots have negative real provided $\alpha_5 > 0$, $\alpha_6 > 0$, $\alpha_7 > 0$, $\alpha_8 > 0$, and $\alpha_5\alpha_6\alpha_7 > \alpha_8\alpha_5^2$. Clearly, α_5, α_6, and α_7 are positive while α_8 is positive if $\mathscr{R}_0^{deng} < 1$. Now following [69], $\alpha_5\alpha_6\alpha_7 > \alpha_8\alpha_5^2$ is satisfied if $\mathscr{R}_0^{deng} < 1$. Thus, if $\mathscr{R}_{0n} > \max\{1, \mathscr{R}_{0w}\}$ and $\mathscr{R}_0^{deng} < 1$, all eigenvalues of J_{E1} have negative real part. Therefore, E_1 is locally asymptotically stable for $\mathscr{R}_{0n} > \max\{1, \mathscr{R}_{0w}\}$ and $\mathscr{R}_0^{deng} < 1$.

Theorem 3.1. *If $\mathscr{R}_{0n} > \max\{1, \mathscr{R}_{0w}\}$ and $\mathscr{R}_0^{deng} < 1$ then the dengue-free equilibrium point $E_1 = (A_{1n}^*, S_{1n}^*, 0, 0, M_{1n}^*, 0, 0, 0, 0, 0, N_h, 0, 0, 0)$ is locally asymptotically stable.*

3.4.2 Global asymptotic stability of the DFE

To prove the global asymptotic stability of dengue (disease)-free equilibria, we make use of a result from Kamgang and Sallet [70]. Using the property of a disease-free equilibrium, we

can rewrite the system (3.1a)-(3.2d) as

$$\left.\begin{aligned} \dot{y}_s &= A_1(y)\,(y_s - y_{\mathrm{DFE},s}) + A_{12} y_i, \\ \dot{y}_i &= A_2(y) y_i, \end{aligned}\right\} \tag{3.8}$$

where y_s represents the state of different compartments of non-transmitting individuals (e.g. susceptible, recovered) and y_i represents the state of compartment of different transmitting individuals (e.g. infected, exposed). For our model, $y_s = (A_n, S_n, M_n, A_w, S_w, M_w, S_h, R_h)^T$, $y_i = (E_n, I_n, E_w, I_w, E_h, I_h)^T$, $y = (y_s, y_i)$, and $y_{DFE} = (A^*_{1n}, S^*_{1n}, 0, 0, M^*_{1n}, 0, 0, 0, 0, 0, S_{h0}, 0, 0)$. The matrices A_1, A_{12}, and A_2 are given by:

$$A_1(y) = \begin{pmatrix} -\frac{\rho_n S^*_{1n}}{K} - (\gamma_n + \mu_{na}) & \zeta_1 & 0 & -\frac{\rho_n S^*_{1n}}{K} & \zeta_2 & -\rho_n \frac{S^*_{1n}}{M^*_{1n}}\left(1 - \frac{An^*_{1n}}{K}\right) & 0 & 0 \\ \tau\gamma_n & -\mu_n & 0 & 0 & 0 & 0 & 0 & 0 \\ (1-\tau)\gamma_n & 0 & -\mu_{mn} & 0 & 0 & 0 & 0 & \\ 0 & 0 & 0 & -(\gamma_w + \mu_{wa}) & \zeta_2 & 0 & 0 & 0 \\ 0 & 0 & 0 & \tau\gamma_w & -\mu_w & 0 & 0 & 0 \\ 0 & 0 & 0 & (1-\tau)\gamma_w & 0 & -\mu_{mw} & 0 & 0 \\ 0 & 0 & 0 & 0 & 0 & 0 & -\mu_h & 0 \\ 0 & 0 & 0 & 0 & 0 & 0 & 0 & -\mu_h \end{pmatrix},$$

$$A_{12}(y) = \begin{pmatrix} \zeta_3 & \zeta_3 & (1-\epsilon_w)\zeta_4 & (1-\epsilon_w)\zeta_4 & 0 & 0 \\ 0 & 0 & 0 & 0 & 0 & -\frac{a_n \beta_{hn} S_n}{N_h} \\ 0 & 0 & 0 & 0 & 0 & 0 \\ 0 & 0 & \epsilon_w\zeta_4 & \epsilon_w\zeta_4 & 0 & -\frac{a_w \beta_{hw} S_w}{N_h} \\ 0 & 0 & 0 & 0 & 0 & 0 \\ 0 & 0 & 0 & 0 & 0 & -\frac{a_w \beta_{hw} S_w}{N_h} \\ 0 & -\frac{a_n \beta_{nh} S_h}{N_h} & 0 & -\frac{a_w \beta_{wh} S_h}{N_h} & 0 & 0 \\ 0 & 0 & 0 & 0 & 0 & \beta_h \end{pmatrix},$$

$$A_2(y) = \begin{pmatrix} -(\beta_n + \mu_n) & 0 & 0 & 0 & 0 & \frac{a_n \beta_{hn} S_n}{N_h} \\ \beta_n & -\mu_n & 0 & 0 & 0 & 0 \\ 0 & 0 & -(\beta_w + \mu_w) & 0 & 0 & \frac{a_w \beta_{hw} S_w}{N_h} \\ 0 & 0 & \beta_w & -\mu_w & 0 & 0 \\ 0 & \frac{a_n \beta_{nh} S_h}{N_h} & 0 & \frac{a_w \beta_{wh} S_h}{N_h} & -(\mu_h + \theta_h) & 0 \\ 0 & 0 & 0 & 0 & \theta_h & -(\mu_h + \beta_h) \end{pmatrix},$$

where

$$\begin{aligned}
\zeta_1 &= \rho_n\left(1-\frac{An_{1n}^*}{K}\right),\\
\zeta_2 &= \rho_w(1-\epsilon_w)\left(1-\frac{An_{1n}^*}{K}\right),\\
\zeta_3 &= \frac{\rho_n M_n}{M_n+M_w}\left(1-\frac{A_n+A_w}{K}\right),\\
\zeta_4 &= \rho_w\left(1-\frac{A_n+A_w}{K}\right).
\end{aligned}$$

The matrix A_2 is a Metzler matrix since all its off-diagonal entries are non-negative. The eigenvalues of A_1 are real and negative; hence the system $y_s = A_1(y)\,(y_s - y_{\mathrm{DFE},s})$ is globally asymptotically stable (GAS) at the dengue-free equilibrium point E_1.
Now we define a bounded set G:

$$\mathcal{G} = \left\{ \begin{array}{l}
(A_n, S_n, E_n, I_n, M_n, A_w, S_w, E_w, I_w, M_w, S_h, E_h, I_h, R_h) \in \mathcal{R}_+^{14}|\\
A_n \le K, S_n \le \frac{\gamma_n}{\mu_n}K, E_n \le \frac{\gamma_n}{\mu_n}K, I_n \le \frac{\gamma_n}{\mu_n}K, M_n \le \frac{\gamma_n}{\mu_{mn}}K,\\
A_w \le K, S_w \le \frac{\gamma_w}{\mu_w}K, E_w \le \frac{\gamma_w}{\mu_w}K, I_w \le \frac{\gamma_w}{\mu_w}K, M_w \le \frac{\gamma_w}{\mu_{mw}}K,\\
S_h \le N_h, E_h \le N_h, I_h \le N_h, R_h \le N_h,\\
S_n + E_n + I_n \le \frac{\gamma_n}{\mu_n}K,\\
S_w + E_w + I_w \le \frac{\gamma_w}{\mu_w}K, S_h + E_h + I_h + R_h = N_h.
\end{array} \right\}$$

We now state a theorem proved by Kamgang and Sallet [70] which we will use for our model to discuss the global asymptotic stability of the disease free equilibrium point E_1.

Theorem 3.2. *[70] Let $\mathcal{G} \subset \mathcal{N} = \mathcal{R}_+^8 \times \mathcal{R}_+^6$ be a bounded set with nonempty interior. The system* (3.8) *is of class C^1 defined on $\mathcal{N}$. If*

1. *$\mathcal{G}$ is positively invariant relative to* (3.8).

2. *The system $\dot{y}_1 = A_1(y)\,(y_1 - y_{DFE,1})$ is globally asymptotically stable (GAS) at y_{DFE}.*

3. *For any $y \in \overline{\mathcal{G}}$, the matrix $A_2(y)$ is Metzler irreducible.*

4. *There exists a matrix* $\overline{A}_2$*, which is an upper bound of the set* $\mathcal{M} = \left\{A_2(y) \in \mathcal{M}_6(\mathcal{R}) \,|y \in \overline{\mathcal{G}}\right\}$ *with the property that if* $\overline{A}_2 \in \mathcal{M}$*, for any* $\overline{y} \in \overline{\mathcal{G}}$*, such that* $A_2(\overline{y}) = \overline{A}_2$*, then* $\overline{\mathbf{y}} \in \mathcal{R}^7_+ \times \{0\}$.

5. *The stability modulus of* $\overline{A}_2$ *satisfies* $\alpha\left(\overline{A}_2\right) \leq 0$.

Then the DFE is GAS in $\overline{\mathcal{G}}$.

Now we verify all the assumptions of the theorem. Assumptions (1-3) are obvious. The upper bound, $\overline{A}_2$, of the set of matrices $\mathcal{M}$ is given by

$$\overline{A}_2 = \begin{pmatrix} -(\beta_n+\mu_n) & 0 & 0 & 0 & 0 & \frac{a_n\beta_{hn}\overline{S}_n}{N_h} \\ \beta_n & -\mu_n & 0 & 0 & 0 & 0 \\ 0 & 0 & -(\beta_w+\mu_w) & 0 & 0 & \frac{a_w\beta_{hw}S_w}{N_h} \\ 0 & 0 & \beta_w & -\mu_w & 0 & 0 \\ 0 & \frac{a_n\beta_{nh}\overline{S}_h}{N_h} & 0 & \frac{a_w\beta_{wh}\overline{S}_h}{N_h} & -(\mu_h+\theta_h) & 0 \\ 0 & 0 & 0 & 0 & \theta_h & -(\mu_h+\beta_h) \end{pmatrix},$$

To check the condition (5) in the theorem (3.2), we use a lemma which is also proved in [70].

Lemma 3.1. *[70] Let* M *be a square Metzler matrix written in block form* $M = \begin{pmatrix} A & B \\ C & D \end{pmatrix}$*, with* A *and* D *square matrices.* M *is Metzler stable if and only if matrices* A *and* $D - CA^{-1}B$ *are Metzler stable.*

In our case, we have $A = \begin{pmatrix} -(\beta_w+\mu_n) & 0 & 0 & 0 \\ \beta_n & -\mu_n & 0 & 0 \\ 0 & 0 & -(\beta_w+\mu_w) & 0 \\ 0 & 0 & \beta_w & -\mu_w \end{pmatrix}$, $B = \begin{pmatrix} 0 & \frac{a_n\beta_{hn}\overline{S}_n}{N_h} \\ 0 & 0 \\ 0 & 0 \\ 0 & 0 \end{pmatrix}$, $C = \begin{pmatrix} 0 & \frac{a_n\beta_{nh}\overline{S}_h}{N_h} & 0 & \frac{a_w\beta_{wh}\overline{S}_h}{N_h} \\ 0 & 0 & 0 & 0 \end{pmatrix}$, and $D = \begin{pmatrix} -(\mu_h+\theta_h h) & 0 \\ \theta_h & -(\mu_h+\beta_h). \end{pmatrix}$. A is Metzler and stable since all diagonal elements are negative, all off diagonal elements are positive, and all eigenvalues are negative.

$D - CA^{-1}B = \begin{pmatrix} -(\mu_h+\theta_h) & \frac{a_n^2\beta_{nh}\beta_{hn}\beta_n}{\mu_n(\beta_n+\mu_n)}\frac{\overline{S}_h}{N_h}\frac{\overline{S}_n}{N_h} \\ \theta_h & -(\beta_h+\mu_h) \end{pmatrix}$.

Clearly the matrix $D - CA^{-1}B$ is Metzler, and it is also stable if

$(\mu_h + \theta_h)(\beta_h + \mu_h) > \theta_h \left(\frac{a_n^2 \beta_{nh} \beta_{hn} \beta_n}{\mu_n(\beta_n + \mu_n)} \frac{\overline{S}_h}{N_h} \frac{\overline{S}_n}{N_h} \right)$.

Thus, $D - CA^{-1}B$ is stable if $\mathscr{R}_{\text{cd}}^2 < 1$, where

$$\mathscr{R}_{\text{cd}}^2 = \frac{a_n \beta_{nh}}{\mu_n} \frac{\beta_n}{\beta_n + \mu_n} \frac{\overline{S}_h}{N_h} \frac{a_n \beta_{hn}}{\beta_h + \mu_h} \frac{\theta_h}{\theta_h + \mu_h} \frac{\overline{S}_n}{N_h} \ . \tag{3.9}$$

Thus, $\mathscr{R}_{\text{cd}}^2 < 1$ gives the necessary condition for the DFE to be globally asymptotic stable(GAS).

Since the matrix $\overline{A}_2$ is not obtained at DFE, the condition we obtained for the DFE to be GAS is not $\mathscr{R}_0^{deng}$. The relationship between $\mathscr{R}_0^{deng}$ and $\mathscr{R}_{\text{cd}}$ is given by:

$$\mathscr{R}_{\text{cd}}^2 = \frac{K \gamma_n N_h}{\mu_n S_{h_0} S_{n_0}} \mathscr{R}_0^{deng} \geq \mathscr{R}_0^{deng}.$$

Theorem 3.3. *If $\mathscr{R}_{0n} > \max\{1, \mathscr{R}_{0w}\}$ and $\mathscr{R}_0^{deng} \leq \mathscr{R}_{cd} < 1$ then the dengue-free equilibrium point*
$E_1 = (A_{1n}^*, S_{1n}^*, 0, 0, M_{1n}^*, 0, 0, 0, 0, 0, S_{h0}, 0, 0, 0)$ *is globally asymptotically stable in $\mathcal{G}$.*

Using the same analysis for the disease-free equilibrium point E_2, we have the following result

Theorem 3.4. *If $\mathscr{R}_{0w} > 1$ and $\mathscr{R}_0^{deng} \leq \mathscr{R}_{cd}^2 < 1$ then the dengue-free equilibrium point*
$E_2 = (0, 0, 0, 0, 0, A_{2w}^*, S_{2w}^*, 0, 0, M_{2w}^*, S_{h0}, 0, 0, 0)$ *is globally asymptotically stable in $\mathcal{G}$.*

Remark 3.1. *It is worth mentioning here that both $\mathscr{R}_0^{deng}$ and $\mathscr{R}_{cd}$ depend on K through S_{n0}, so it was important to consider the aquatic stage in the model. Lowering the value of K can be used as controlling strategy to reduce the number of dengue infections.*

3.5 Numerical results and discussion

To study the effects of maternal transmission ϵ_w, incomplete and complete cytoplasmic incompatability on the dynamics of dengue disease, we numerically solve the model (3.1) using the parameters values given in Table (3.1).

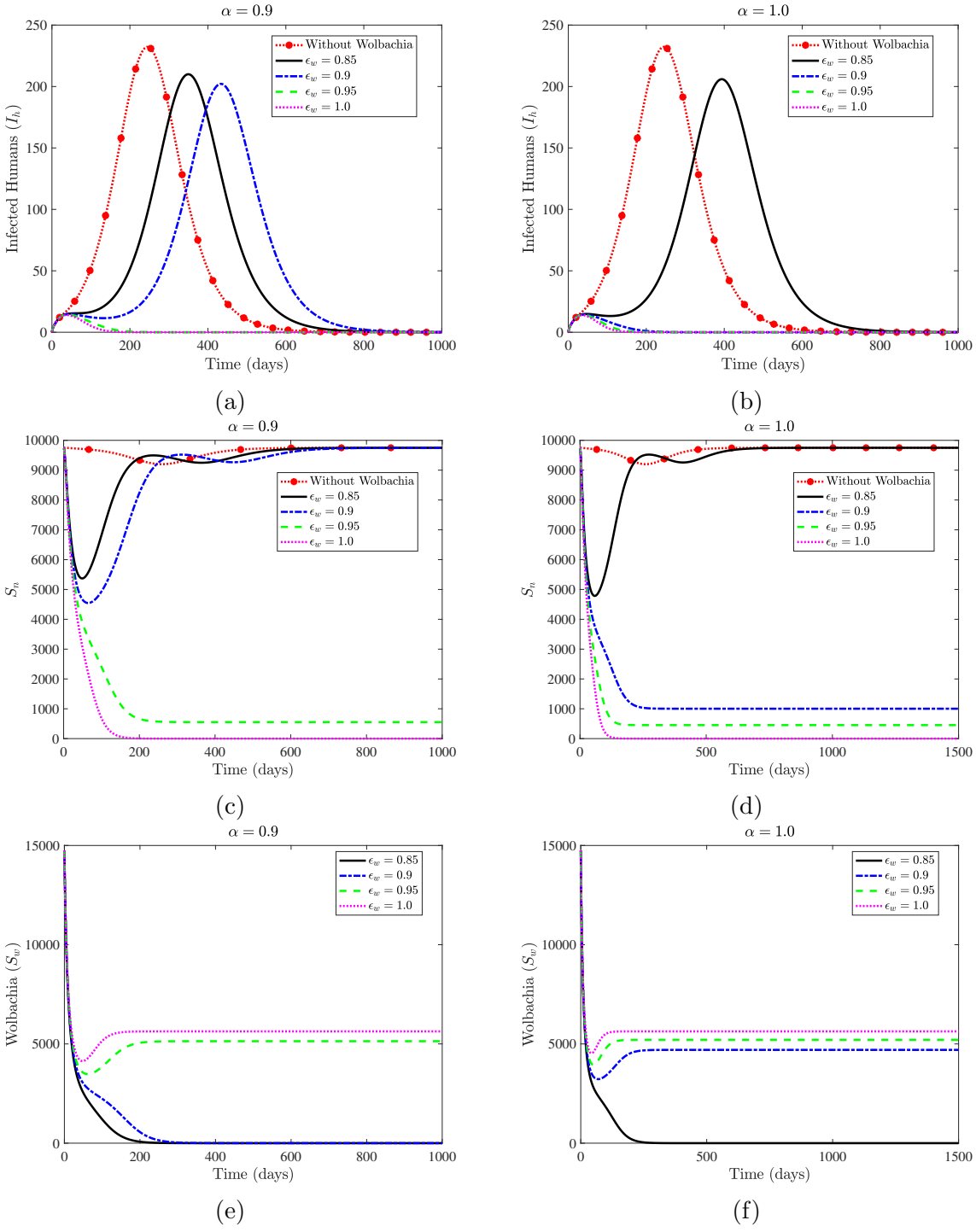

Figure 3.2: The dynamics of the infected humans (top panels), *Wolbachia*-free susceptible female mosquitoes (middle panels), *Wolbachia*-infected susceptible female mosquitoes (bottom panels) for different values of maternal transmission ϵ_w and strength of cytoplasmic incompatibility α. The plots in the left panels correspond to $\alpha = 0.9$, while the plots in the right panels correspond to complete cytoplasmic incompatibility $\alpha = 1.0$. The effects on the dynamics for different values of ϵ_w are shown within each panel.

Figures (3.2a) and (3.2b) illustrate the effects on the dynamics of the infected humans under different values of vertical transmission ϵ_w and α. In Figures (3.2a) and (3.2b), we first observe significant decrease in the number of infected humans compare to when only wild mosquitoes persist when $\epsilon \geq 0.95$. However, when $\alpha 0.9$ (left panels) there is no significant difference in the number of infected humans when $\epsilon_w = 0.9$ compare to when only wild mosquitoes persist in the wild. However, for complete cytoplasmic incompatabilty $\alpha = 1$(right panels), there is significant decrease in the number of infected humans when $\epsilon_w = 0.9$. The results of these graphs reveal that when cytoplasmic incompatibility is not complete, higher vertical transmission of *Wolbachia*-infected female to its offspring is required to eradicate dengue epidemic. can also be seen when we compare Figure anFor the case of perfect vertical transmission $\epsilon_w = 1$, we observe no significant difference in the number of infected humans for different values of α. The numerical results in Figure (3.2) also reveal that the peak (maximum infections) is shifted to the right as we increase the values of ϵ_w from 0.85 to 0.9 when $\alpha = 0.9$. This shift of the peak is expected since *Wolbachia*-infected female mosquitoes spend more time in the exposed class compare to non-*Wolbachia* female mosquitoes.

3.6 Conclusion

We formulated a model to study the transmission of dengue virus to humans when *Wolbachia*-infected mosquitoes are released in the wild as a biological control method to suppress the population of wild mosquitoes. We found and derive conditions for the existence of three dengue-free equilibria: host and *Wolbachia*-uninfected only, host and *Wolbachia*-infected provided the maternal transmission is complete, and host along with coexistence of *Wolbachia*-free and *Wolbachia*-infected mosquitoes. We also calculated the basic reproduction number and discussed the global asymptotic stability of the disease-free equilibria. The effects of the cytoplasmic incompatibility (CI) and the maternal transmission on the dynamics of disease infection in humans have been studied numerically. The results indicate a higher reduction in the number of infected humans for high values of ϵ_w α. Overall, there is significant reduction in the number of dengue infected humans in the presence of

Wolbachia-infected. Also the reduction in the number of dengue infections depend both on α and ϵ_w; a higher reduction for higher values of α and ϵ_w. Our numerical results suggest that introduction of *Wolbachia* in the wild as a biological control method for dengue disease is a promising approach to eradicate dengue.

CHAPTER 4

OPTIMAL RELEASE OF *WOLBACHIA*-INFECTED MOSQUITOES FOR A DENGUE EPIDEMIC MODEL

4.1 Introduction

Many models have been studied that incorporate optimal control models that include only a single control strategy such as insecticide spraying [71–73], Sterile Insect Technique (SIT) [74]. Some models also considered combinations of different types of vector controls such as the combined effects of insecticide spraying with personal protection measures [75] or educational campaigns [76–78], the use of insecticide spraying along with larvicides and SIT [59, 79–81], or along with vaccination [82].

In this chapter, we extend the model (3.1) developed in chapter 3 and formulate an optimal control epidemic model of dengue by considering continuous release of *Wolbachia*-infected mosquitoes in the wild and through educational campaigns that promote awareness for using personal protection (e.g., bed nets, mosquito repellents) to limit the humans-vectors contact.

4.2 Optimal control model

We formulate an optimal control model by considering the following time-dependent control variables in the model (3.1) formulated in chapter 3. The control variables $u_1(t)\colon [0,T] \mapsto u_{1max}$ and $u_2(t)\colon [0,T] \mapsto u_{2max}$ represent the investment in production and release of *Wolbachia*-infected female mosquitoes $u_1(t)$ and male mosquitoes $u_2(t)$, respectively. The control variable $u_3(t)\colon [0,T] \mapsto u_{3max} \leq 1$ denotes the percentage reduction of disease transmission to humans due to educational campaigns for motivating individuals to use personal protection, such as bed nets and mosquito repellents, in order to minimize female mosquitoes bite on humans. Therefore, in the presence of time-dependent control u_3, the force of in-

fection between humans and mosquitoes will decrease by a factor of $1 - u_3(t)$. The upper bounds u_{1max} and u_{2max} on control variables u_1 and u_2, respectively, denote the maximum number of *Wolbachia*-infected mosquitoes that can be produced and released per day, whereas $0 \leq u_{3max} < 1$ stands for the maximum efficiency of educational campaigns in reducing disease transmission. In the presence of controls u_1, u_2 and u_3, the new model reads:

$$\begin{aligned}
\frac{dA_n}{dt} &= \rho_n F_n \frac{M_n}{M_n + M_w}\left(1 - \frac{A_n + A_w}{K}\right) \\
&\quad + (1-\alpha)\rho_n F_n \frac{M_w}{M_n + M_w}\left(1 - \frac{A_n + A_w}{K}\right) \\
&\quad + \rho_w (1 - \epsilon_w) F_w \left(1 - \frac{A_n + A_w}{K}\right) - (\gamma_n + \mu_{na})A_n, && \text{(4.1a)} \\
\frac{dS_n}{dt} &= \tau\gamma_n A_n - \mu_n S_n - \frac{a_n(1-u_3)\beta_{hn} I_h}{N_h} S_n, && \text{(4.1b)} \\
\frac{dE_n}{dt} &= \frac{a_n(1-u_3)\beta_{hn} I_h}{N_h} S_n - \beta_n E_n - \mu_n E_n, && \text{(4.1c)} \\
\frac{dI_n}{dt} &= \beta_n E_n - \mu_n I_n, && \text{(4.1d)} \\
\frac{dM_n}{dt} &= (1-\tau)\gamma_n A_n - \mu_m M_n, && \text{(4.1e)} \\
\frac{dA_w}{dt} &= \rho_w \epsilon_w F_w \left(1 - \frac{A_n + A_w}{K}\right) - (\gamma_w + \mu_{wa})A_w, && \text{(4.1f)} \\
\frac{dS_w}{dt} &= u_1(t) + \tau\gamma_w A_w - \mu_w S_w - \frac{a_w(1-u_3)\beta_{hw} I_h}{N_h} S_w, && \text{(4.1g)} \\
\frac{dE_w}{dt} &= \frac{a_w(1-u_3)\beta_{hw} I_h}{N_h} S_w - \beta_w E_w - \mu_w E_w, && \text{(4.1h)} \\
\frac{dI_w}{dt} &= \beta_w E_w - \mu_w I_w, && \text{(4.1i)} \\
\frac{dM_w}{dt} &= u_2(t) + (1-\tau)\gamma_w A_w - \mu_m M_w, && \text{(4.1j)}
\end{aligned}$$

$$\frac{dS_h}{dt} = \mu_h N_h - \mu_h S_h - \frac{a_n(1-u_3)\beta_{nh} I_n}{N_h} S_h \tag{4.2a}$$

$$- \frac{a_w(1-u_3)\beta_{wh} I_w}{N_h} S_h, \tag{4.2b}$$

$$\frac{dE_h}{dt} = \frac{a_n \beta_{nh} I_n}{N_h} S_h + \frac{a_w \beta_{wh} I_w}{N_h} S_h - \mu_h E_h - \theta_h E_h, \tag{4.2c}$$

$$\frac{dI_h}{dt} = \theta_h E_h - \mu_h I_h - \beta_h I_h, \tag{4.2d}$$

$$\frac{dR_h}{dt} = \beta_h I_h - \mu_h R_h. \tag{4.2e}$$

subject to the following initial conditions

$$\begin{aligned} &A_n(0) \geq 0, \quad S_n(0) \geq 0, \quad E_n(0) \geq 0, \quad I_n(0) \geq 0, \quad M_n(0) \geq 0, \\ &A_w(0) \geq 0, \quad S_w(0) \geq 0, \quad E_w(0) \geq 0, \quad I_w(0) \geq 0, \quad M_w(0) \geq 0, \\ &S_h(0) \geq 0, \quad E_h(0) \geq 0, \quad I_h(0) \geq 0, \quad R_h(0) \geq 0. \end{aligned} \tag{4.3}$$

and with

$$0 \leq u_1 \leq u_{1max}, \qquad 0 \leq u_2 \leq u_{2max}, \text{and} \qquad 0 \leq u_3 \leq u_{3max} \leq 1. \tag{4.4}$$

Our goal with the optimal control dengue model (4.1) is to minimize the number of infected humans (I_h) and susceptible *Wolbachia*-free mosquitoes S_n along with the cost associated with the implementation of control strategies during the time interval $[0, T]$. To this end, we define the following objective functional, which is also in line with optimal control models considered in the literature on malaria, chikungunya, and dengue [61, 62, 83, 84],

$$J(u_1^*, u_2^*, u_3^*) = \min_{u_1, u_2, u_3 \in \mathcal{U}} \int_0^T A_1 I_h + A_2 S_n + \tfrac{1}{2}\left(B_1 u_1^2 + B_2 u_2^2 + B_3 u_3^2\right) dt, \tag{4.5}$$

subject to the system (4.1a)-(4.2e) and (2.2). The set $\mathcal{U}$ in (4.5) is a measurable control set

and is defined as

$$\mathcal{U} := \left\{ \begin{array}{l} (u_1(t),\, u_2(t),\, u_3(t))\,,\, 0 \leq u_1(t) \leq u_{1\max}, \\ 0 \leq u_2(t) \leq u_{2\max}, 0 \leq u_3(t) \leq u_{3\max}, \\ u_1,\, u_2,\, u_3 \text{ measurable } \forall t \in [0,\, T] \end{array} \right\} \tag{4.6}$$

The positive weight constants A_1 and A_2 in the objective functional (4.5) express the priorities of reducing the number of humans infected with dengue I_h and the number of wild susceptible adult female mosquitoes S_n, whereas the constants $B_1, B_2,\, B_3 \geq 0$ represent the weight (or marginal unit costs) associated with the implementation of controls u_1, u_2 and u_3, respectively. The values of the weight constants are chosen to give each term in the objective functional (4.5) its relative importance. The quadratic terms $\frac{1}{2}B_i u_i^2$ $(i = 1, 2, 3)$ in the objective functional state that the total marginal cost of the control interventions $B_1u_1(t) + B_2u_2(t)+B_3u_3(t)$ depends on the implementation of controlling strategies. Since the marginal cost is the change in total cost, the integrand in the objective functional (4.5) is quadratic with respect to control variables $u_1(t)$, $u_2(t)$, and $u_3(t)$ and commonly used in optimal control epidemic models to avoid convexity and convergence issues [7, 10, 39, 40, 59–63, 78, 84].

Thus, in mathematical terms, we want to find an optimal control strategy $(u_1^*(t),\, u_2^*(t),\, u_3^*(t))$ that minimizes the objective functional (4.5), i.e.

$$J(u_1^*, u_2^*, u_3^*) = \min_{u_1,\, u_2,\, u_3 \in \mathcal{U}} \int_0^T A_1 I_h + A_2 S_n + \tfrac{1}{2}\left(B_1 u_1^2 + B_2 u_2^2 + B_3 u_3^2\right)\, dt, \tag{4.7}$$

where $\mathcal{U}$ is the control set defined in (4.6).

4.3 Existence and characterization of optimal controls

4.3.1 Existence of optimal controls

To prove the existence of the optimal control pair (u_1^*, u_2^*, u_3^*), we use results from (1.1) and also stated in chapter (1) .

Theorem 4.1. *There exists an optimal control pair* (u_1^*, u_2^*, u_3^*) *and the corresponding solution of the system* (4.1a)-(4.2e) *with initial conditions* (4.3) *that minimize the objective functional* (4.5) *over the set* $\mathcal{U}$.

Proof. To show the existence of an optimal control pair (u_1^*, u_2^*, u_3^*), we verify the conditions of the Theorem (1.1):

1. The set of controls $\mathcal{U}$ is nonempty since $u_1 = u_2 = u_3 = 0$ is a solution of the dynamical system (4.1a)-(4.2e).

2. The control set $\mathcal{U}$ is bounded and convex on $[0,\, T]$ by definition.

3. the right hand side of the dynamical system (4.1a)-(4.2e) is continuous, and the state variables and controls are bounded on $[0,\, T]$. Note that the right hand side of the dynamical system (4.1a)-(4.2e) is linear in control variables u_1, u_2, and u_3.

4. The integrand of the objective functional (4.7) is strictly convex in controls by definition.

5. To show condition 5, we write the integrand of the objective functional (4.7) as,

$$\begin{aligned} L(t, I_h, I_n, S_n, u_1, u_2, u_3) &= A_1 I_h + A_2 I_n + A_3 S_n + \tfrac{1}{2}\left(B_1 u_1^2 + B_2 u_2^2 + B_3 u_3^2\right) \\ &\geq \tfrac{1}{2}\left(B_1 u_1^2 + B_2 u_2^2 + B_3 u_3^2\right) \qquad (\text{for } I_h,\, I_n, S_n \geq 0) \\ &\geq \tfrac{\delta_1}{2}\left(\sum_{j=1}^{3} |u_i|^2\right)^{\frac{\phi}{2}} - \delta_2 \end{aligned}$$

   The last inequality is satisfied when $\delta_1 = \min\{B_1, B_2, B_3\}$, $\phi = 2$, and $\delta_2 > 0$.

Since all conditions are satisfied, there exists an optimal control $(u_1^*,\, u_2^*,\, u_3^*)$ for the dynamical system (4.1a)-(4.2e). □

4.3.2 Characterization of the optimal controls

The *Hamiltonian* function $\mathcal{H}$ associated to the dynamical system (4.1a)-(4.2e) and (4.5) is defined by:

$$
\begin{aligned}
\mathcal{H} &= A_1 I_h + A_2 I_n + A_3 S_n + \tfrac{1}{2}\left(B_1 u_1^2 + B_2 u_2^2 + B_3 u_3^2\right) \\
&+ \lambda_{A_n}\rho_n\left(S_n + E_n + I_n\right)\tfrac{M_n}{M_n+M_w}\left(1 - \tfrac{A_n+A_w}{K}\right) \\
&\quad + \lambda_{A_n}(1-\alpha)\rho_n\left(S_n + E_n + I_n\right)\tfrac{M_w}{M_n+M_w}\left(1 - \tfrac{A_n+A_w}{K}\right) \\
&\quad + \lambda_{A_n}\left(\rho_w(1-\epsilon_w)\left(S_w + E_w + I_w\right)\left(1 - \tfrac{A_n+A_w}{K}\right) - \left(\gamma_n + \mu_{na}\right)A_n\right) \\
&+ \lambda_{S_n}\left(\tau\gamma_n A_n - \mu_n S_n - \tfrac{(1-\xi u_3)a_n\beta_{hn}I_h}{N_h}S_n\right) \\
&+ \lambda_{E_n}\left(\tfrac{(1-\xi u_3)a_n\beta_{hn}I_h}{N_h}S_n - \beta_n E_n - \mu_n E_n\right) \\
&+ \lambda_{I_n}\left(\beta_n E_n - \mu_n I_n\right) \\
&+ \lambda_{M_n}\left((1-\tau)\gamma_n A_n - \mu_m M_n\right) \\
&+ \lambda_{A_w}\left(\rho_w\epsilon_w\left(S_w + E_w + I_w\right)\left(1 - \tfrac{A_n+A_w}{K}\right)\right) - \lambda_{A_w}(\gamma_w + \mu_{wa})A_w \\
&+ \lambda_{S_w}\left(u_1(t) + \tau\gamma_w A_w - \mu_w S_w - \tfrac{(1-\xi u_3)a_w\beta_{hw}I_h}{N_h}S_w\right) \\
&+ \lambda_{E_w}\left(\tfrac{(1-\xi u_3)a_w\beta_{hw}I_h}{N_h}S_w - \beta_w E_w - \mu_w E_w\right) \\
&+ \lambda_{I_w}\left(\beta_w E_w - \mu_w I_w\right) \\
&+ \lambda_{M_w}\left(u_2(t) + (1-\tau)\gamma_w A_w - \mu_m M_w\right) \\
&+ \lambda_{S_h}\left(\mu_h N_h - \mu_h S_h - \tfrac{(1-\xi u_3)a_n\beta_{nh}I_n}{N_h}S_h - \tfrac{(1-\xi u_3)a_w\beta_{wh}I_w}{N_h}S_h\right) \\
&+ \lambda_{E_h}\left(\tfrac{(1-\xi u_3)a_n\beta_{nh}I_n}{N_h}S_h + \tfrac{(1-\xi u_3)a_w\beta_{wh}I_w}{N_h}S_h - \mu_h E_h - \theta_h E_h\right) \\
&+ \lambda_{I_h}\left(\theta_h E_h - \mu_h I_h - \beta_h I_h\right) \\
&+ \lambda_{R_h}\left(\beta_h I_h - \mu_h R_h\right),
\end{aligned}
\tag{4.8}
$$

where λ_{A_n}, λ_{S_n}, λ_{E_n}, λ_{I_n}, λ_{M_n}, λ_{A_w}, λ_{S_w}, λ_{E_w}, λ_{I_w}, λ_{M_w}, λ_{S_h}, λ_{E_h}, λ_{I_h}, λ_{R_h} are the adjoint variables (also called co-state variables).

Theorem 4.2 (Pontryagin's Maximum Principle [13]). *If $u^* = (u_1^*, u_2^*, u_3^*)$ is an optimal control pair and*
$(A_n^*, S_n^*, E_n^*, I_n^*, M_n^*, A_w^*, S_w^*, E_w^*, I_w^*, M_w^*, S_h^*, E_h^*, I_h^*, R_h^*)$ is the corresponding solution that minimize the objective functional $J(u_1, u_2, u_3)$ (4.7), then there exists adjoint variables λ_i,

where $i = \{A_n, S_n, E_n, I_n, M_n, A_w, S_w, E_w, I_w, M_w, S_h, E_h, I_h, R_h\}$, *that satisfy:*

$$
\begin{aligned}
\frac{d\lambda_{A_n}}{dt} =& \lambda_{A_n}\left(\mu_{na} + \frac{\rho_n\left(S_n + E_n + I_n\right)\left(M_n + (1-\alpha)M_w\right)}{K(M_n + M_w)}\right) \\
& \gamma_n(\lambda_{A_n} - (1-\tau)\lambda_{M_n} - \tau\lambda_{S_n}) + \frac{\rho_w(S_w + E_w + I_w)\left((1-\epsilon_w)\lambda_{A_n} + \epsilon_w\lambda_{A_w}\right)}{K} \\
\frac{d\lambda_{S_n}}{dt} =& - A_3 - \frac{\lambda_{A_n}\rho_n\ \left(M_n + (1-\alpha)M_w\right)}{K(M_n + M_w)}\left(1 - \frac{A_n + A_w}{K}\right) \\
& + a_n(1-u_3)\beta_{hn}\frac{I_h}{N_h}(\lambda_{S_n} - \lambda_{E_n}) + \mu_n\lambda_{S_n} \\
\frac{d\lambda_{E_n}}{dt} =& - \frac{\lambda_{A_n}\rho_n\ \left(M_n + (1-\alpha)M_w\right)}{K(M_n + M_w)}\left(1 - \frac{A_n + A_w}{K}\right) \\
& + \lambda_{E_n}(\beta_n + \mu_n) - \lambda_{I_n}\beta_n \\
\frac{d\lambda_{I_n}}{dt} =& - A_2 - \frac{\lambda_{A_n}\rho_n\ \left(M_n + (1-\alpha)M_w\right)}{K(M_n + M_w)}\left(1 - \frac{A_n + A_w}{K}\right) \\
& + a_n\beta_{nh}(1-u_3)\frac{S_h}{N_h}(\lambda_{S_h} - \lambda_{E_h}) + \lambda_{I_n}\mu_n \\
\frac{d\lambda_{M_n}}{dt} =& \mu_m\lambda_{M_n} - \rho_n\alpha\lambda_{A_n}\left(S_n + E_n + I_n\right)\frac{M_w}{(M_n + M_w)^2}\left(1 - \frac{A_n + A_w}{K}\right) \\
\frac{d\lambda_{A_w}}{dt} =& \mu + _{wa}\,\lambda_{A_n} + \rho_n\lambda_{A_n}\frac{\left(S_n + E_n + I_n\right)\left(M_n + (1-\alpha)M_w\right)}{K(M_n + M_w)} \\
& + \rho_w\left(S_w + E_w + I_w\right)\frac{(1-\epsilon_w)\lambda_{A_n} + \epsilon\lambda_{A_w}}{K} \\
& + \gamma_w(\lambda_{A_w} - (1-\tau)\lambda_{M_w} - \tau\lambda_{S_n} \\
\frac{d\lambda_{S_w}}{dt} =& \mu_w\lambda_{S_w} + a_w(1-u_3)\beta_{hw}(\lambda_{S_w} - \lambda_{E_w})\frac{I_h}{N_h} \\
& - \rho_w\left(\epsilon_w\lambda_{S_w} + (1-\epsilon_w)\lambda_{A_n}\right)\left(1 - \frac{A_n + A_w}{K}\right) \\
\frac{d\lambda_{E_w}}{dt} =& \mu_w\lambda_{E_w} + \beta_w(\lambda_{E_w} - \lambda_{I_w}) \\
& - \rho_w\left(\epsilon_w\lambda_{A_w} + (1-\epsilon_w)\lambda_{A_n}\right)\left(1 - \frac{A_n + A_w}{K}\right) \\
\frac{d\lambda_{I_w}}{dt} =& \mu_w\lambda_{I_w} + a_w(1-u_3)\beta_{wh}(\lambda_{S_h} - \lambda_{E_h})\frac{S_h}{N_h} \\
& - \rho_w\left(\epsilon_w\lambda_{A_w} + (1-\epsilon_w)\lambda_{A_n}\right)\left(1 - \frac{A_n + A_w}{K}\right) \\
\frac{d\lambda_{M_w}}{dt} =& \mu_m\lambda_{M_w} + \alpha\lambda_{A_n}\rho_n\left(1 - \frac{A_n + A_w}{K}\right)\frac{M_n(S_n + E_n + I_n)}{\left(M_n + M_w\right)^2} \\
\frac{d\lambda_{S_h}}{dt} =& \mu_h\lambda_{S_h} + \frac{(1-u)3)\left(a_n\beta_{nh}I_n + a_w\beta_{wh}I_w\right)(\lambda_{S_h} - \lambda_{E_h})}{N_h} \\
\frac{d\lambda_{E_h}}{dt} =& (\lambda_{E_h} - \lambda_{I_h})\theta_h + \mu_h\lambda_{E_h} \\
\frac{d\lambda_{I_h}}{dt} =& - A_1 + \beta_h(\lambda_{I_h} - \lambda_{R_h}) + \mu_h\lambda_{I_h} + \left((1-u_3)(\lambda_{S_n} - \lambda_{E_n})a_n\beta_{hn}\right)\frac{S_n}{N_h} \\
& + \left((1-u_3)(\lambda_{E_w} - \lambda_{I_w})a_w\beta_{hw}\right)\frac{S_w}{N_h} \\
\frac{d\lambda_{R_h}}{dt} =& \mu_h\lambda_{R_h}.
\end{aligned}
\tag{4.9}
$$

and with transversality conditions

$$\lambda_i(T) = 0 \quad \textit{where} \quad i \in \{A_n, S_n, E_n, I_n, M_n, A_w, S_w, E_w, I_w, M_w, S_h, E_h, I_h, R_h\}. \tag{4.10}$$

The optimality condition is given as

$$\frac{\partial \mathcal{H}}{\partial u_j} = 0, \qquad j = 1,\, 2,\, 3.$$

Furthermore, the optimal controls u_1^*, u_2^* and u_3^* are given as

$$\begin{aligned} u_1^* &= \max\left\{0, \min\{-\tfrac{\lambda_{S_w}}{B_1}, u_{1max}\}\right\}, \\ u_2^* &= \max\left\{0, \min\{-\tfrac{\lambda_{M_w}}{B_2}, u_{2max}\}\right\}, \\ u_3^* &= \max\left\{0, \min\left\{-(\Lambda_1 + \Lambda_2), u_{3max}\right\}\right\}, \end{aligned} \tag{4.11}$$

where

$$\begin{aligned} \Lambda_1 &= \tfrac{a_n}{B_3}\left(\beta_{hn} S_n(\lambda_{S_n} - \lambda_{E_n})\tfrac{I_h}{N_h} + \beta_{nh} S_h(\lambda_{S_h} - \lambda_{E_h})\tfrac{I_n}{N_h}\right), \\ \Lambda_2 &= \tfrac{a_w}{B_3}\left(\beta_{hw} S_w(\lambda_{S_w} - \lambda_{E_w})\tfrac{I_h}{N_h} + \beta_{wh} S_h(\lambda_{S_h} - \lambda_{E_h})\tfrac{I_w}{N_h}\right). \end{aligned}$$

Proof. Using the *Hamiltonian* $\mathcal{H}$ and $\frac{d\lambda_i}{dt} = -\frac{\partial \mathcal{H}}{\partial x_i}$, we obtain the system of adjoint equations in (4.9). Since the state variables are free at the final time T, we get the transversality conditions $\lambda_i(T) = 0$. Using the optimality conditions $\frac{\partial \mathcal{H}}{\partial u_i} = 0$ and the property of the control set $\mathcal{U}$, we have

$$\begin{aligned} \tfrac{\partial \mathcal{H}}{\partial u_1} &= B_1 u_1 + \lambda_{S_w} = 0 && \Longrightarrow\ u_1^* = -\tfrac{\lambda_{S_w}}{B_1} \\ \tfrac{\partial \mathcal{H}}{\partial u_2} &= B_2 u_2 + \lambda_{M_w} = 0 && \Longrightarrow\ u_2^* = -\tfrac{\lambda_{M_w}}{B_2} \\ \tfrac{\partial \mathcal{H}}{\partial u_3} &= B_3 u_3 + (\Lambda_1 + \Lambda_2) = 0 && \Longrightarrow\ u_3^* = -\tfrac{\Lambda_1 + \Lambda_2}{B_3} \end{aligned} \tag{4.12}$$

Now using the definition of the control set $\mathcal{U}$, we get

$$u_1^* = \begin{cases} 0 & \text{if} \quad -\frac{\lambda_{S_w}}{B_1} < 0 \\ -\frac{\lambda_{S_w}}{B_1} & \text{if} \quad 0 < -\frac{\lambda_{S_w}}{B_1} < u_{1max} \\ u_{1max} & \text{if} \quad -\frac{\lambda_{S_w}}{B_1} > u_{1max}. \end{cases} \tag{4.13}$$

$$u_2^* = \begin{cases} 0 & \text{if} \quad -\frac{\lambda_{M_w}}{B_2} < 0 \\ -\frac{\lambda_{M_w}}{B_2} & \text{if} \quad 0 < -\frac{\lambda_{M_w}}{B_2} < u_{2max} \\ u_{2max} & \text{if} \quad -\frac{\lambda_{M_w}}{B_2} > u_{2max}. \end{cases} \tag{4.14}$$

$$u_3^* = \begin{cases} 0 & \text{if} \quad -\frac{\Lambda_1+\Lambda_2}{B_3} < 0 \\ -(\Lambda_1+\Lambda_2) & \text{if} \quad 0 < -\frac{\Lambda_1+\Lambda_2}{B_3} < u_{3max} \\ u_{3max} & \text{if} \quad -\frac{\Lambda_1+\Lambda_2}{B_3} > u_{3max}. \end{cases} \tag{4.15}$$

Writing equations (4.13), (4.14) and (4.15) in compact form, which is also known as characterization of optimal control, we get

$$u_1^* = \max\left\{0, \min\{-\frac{\lambda_{S_w}}{B_1}, u_{1\max}\}\right\}, \tag{4.16}$$

$$u_2^* = \max\left\{0, \min\{-\frac{\lambda_{M_w}}{B_2}, u_{2\max}\}\right\}, \tag{4.17}$$

$$u_3^* = \max\left\{0, \min\left\{-(\Lambda_1+\Lambda_2), u_{3\max}\right\}\right\}, \tag{4.18}$$

□

4.3.3 The optimality system

The optimality system (two-point boundary value problem) consists of state equations (4.1a)-(4.2e) with initial conditions (4.3) along with adjoint equations (4.9) with transversality conditions (4.10) where the control variables u_1, u_2, and u_3 are replaced with their characterizations given in (4.11).

4.4 Numerical results and cost-effectiveness analysis

We numerically solve the optimal control model (4.1a)-(4.2e) using the forward-backward sweep method as discussed in Section 1.2.3 of chapter 1 and investigate the effects of control strategies on the transmission dynamics of the dengue disease.

In all simulations, we used the final time $T = 150$ days (5 months), which is around the

Table 4.1: Seven different combinations of control strategies.

Strategies	**Description**
Strategy F	Releasing only *Wolbachia*-infected female mosquitoes (i.e. control u_1 only)
Strategy M	Releasing only *Wolbachia*-infected male mosquitoes (i.e. control u_2 only)
Strategy FM	Releasing both *Wolbachia*-infected female and male mosquitoes (i.e. controls u_1 and u_2)
Strategy E	Reducing humans-mosquitoes contact through Educational campaigns (i.e. control u_3 only)
Strategy FE	Releasing *Wolbachia*-infected female mosquitoes along with Educational campaigns (i.e. controls u_1 and u_3 only)
Strategy ME	Releasing *Wolbachia*-infected male mosquitoes along with Educational campaigns (i.e. controls u_2 and u_3 only)
Strategy FME	Releasing both *Wolbachia*-infected female and male mosquitoes along with Educational campaigns (i.e. all controls)

average infection season of dengue. Since the top priority of the optimal control is to reduce the number of human infections, we need to put a higher weight for the weight constant A_1. We use the estimate given in [75, 85] that the average medical cost of one dengue infected person is about \$400. Therefore, an average daily cost of one dengue infected person is $A_1 = \frac{400}{\beta_h} = \frac{400}{8} = \$50$, where $\frac{1}{\beta_h} = \frac{1}{8}$ is the length of infectious period in humans. The weight constant A_2, which is associated with the societal unit cost of one susceptible mosquitoes, is taken 10 times less than the average cost of one dengue infected individual (i.e. $A_2 = \frac{A_1}{10}$) [75, 85]. The values of the control weights B_1, B_2 and B_3 are taken as $B_1 = B_2 = 0.06$ and $B_3 = 10^3$. Since the magnitude of the state and control variables in the objective functional (4.5) are on a different scale, we chose the values of the control weights to balance the state and control variables in the objective function (4.5). Since educational campaigns and protective measures are generally more expensive, we set the cost of educational campaigns higher than the cost of producing and releasing *Wolbachia*-infected mosquitoes. The values of other parameters are shown in Table 3.1 in chapter 3. We analyze the model (4.1a)-(4.2e) for the seven different control strategies based on the combination of the three controls u_1, u_2, and u_3.

4.4.1 Only *Wolbachia*-infected mosquitoes as control interventions

The numerical results in Figure (4.1) show the dynamics of infected humans (upper left panel) and infected mosquitoes (upper right panel) when only *Wolbachia*-infected mosquitoes are used as control strategies: strategy F (releasing *Wolbachia*-infected female mosquitoes only), strategy M (releasing *Wolbachia*-infected male mosquitoes only), and Strategy FM (releasing both *Wolbachia*-infected female and male mosquitoes). In Figure (4.1a), we see that the number of infected individuals (I_h) significantly reduced compared to uncontrol model under strategies FM and F, whereas under the strategy M we do not see a significant deviation from the uncontrolled system. It is also evident from Figure (4.1a) that the number of infected individuals (I_h) is lower under strategy FM compared to strategy F. In Figure (4.1c), the optimal control plots for $u_1^*(t)$ (middle left panel) show that the number of *Wolbachia*-infected female mosquitoes required to release under strategy F and FM is almost the same for the first two weeks, and after that release rate of *Wolbachia*-infected female is higher under the strategy F compared to strategy FM. The numerical results in Figure (4.1d) (middle right panel) show the optimal control variable $u_2^*(t)$ under control interventions F, M, and FM. The plots in Figure (4.1d) show that a large number of *Wolbachia*-infected male mosquitoes is required to be released daily for a longer time under the control strategy M compared to strategy FM. The plots in Figure (4.1e) (lower left panel) show the total cost under the control interventions F, M, or FM, whereas the plots in Figure (4.1f) (lower right panel) show the total health benefits (averted infections) associated with the control interventions F, M, or FM. The numerical results in Figure (4.1e) show that the strategy F is the cheapest compared to strategies M and FM, whereas the strategy FM is the most expensive compared to strategies, F and M. We also observe that the control intervention FM dominates the other two control interventions, F and M, in terms of maximum health benefits.

4.4.2 Release of *Wolbachia*-infected mosquitoes along with educational campaigns

In Figure (4.2), we also observe that the number of infected humans reduced significantly under the control interventions E, FE, ME, and FME, compared to the uncontrol model, but the number of infected individuals remain almost the same when any of the control interventions E, FE, ME, and FME are implemented. The optimal control profiles for $u_1^*(t)$ and $u_2^*(t)$ look similar as when control interventions F, M, and FM were implemented. The optimal control profile for $u_3^*(t)$ shows that educational campaigns required for longer time under control interventions E and ME compared to control interventions FE and FME for motivating people to use personal protection, such as bed nets and mosquito repellents, in order to reduce human-mosquitoes contact. The plots in Figure (4.2f) (lower right panel) show the total cost under the control interventions E, FE, and FME. In terms of costs, the results in Figure (4.2f) show that the strategy ME (releasing *Wolbachia*-infected males along with educational campaigns) is the most expensive strategy, while the strategy FME (i.e. using all controls) is the least expensive strategy.

4.5 Cost-effectiveness analysis

In section 4.4, we presented the numerical results of seven different optimal control strategies as listed in Table (4.1). However, it is not clear from these results, which strategy will provide better results if applied in practice. Therefore, we perform the cost-effectiveness analysis that allows assessing the costs of each control intervention and the benefits associated with the control intervention. For the cost-effectiveness analysis, we use and define two standard indexes: (i) average cost-effectiveness ratio (ACER), and (ii) incremental cost-effectiveness ratio (ICER).

- Average cost-effectiveness ratio (ACER) evaluates the performance of a single control strategy X with respect to the baseline option (i.e. without control) and is defined as

$$\text{ACER} = \frac{\text{Cost of a strategy X}}{\text{Benefits from the strategy X}}. \tag{4.19}$$

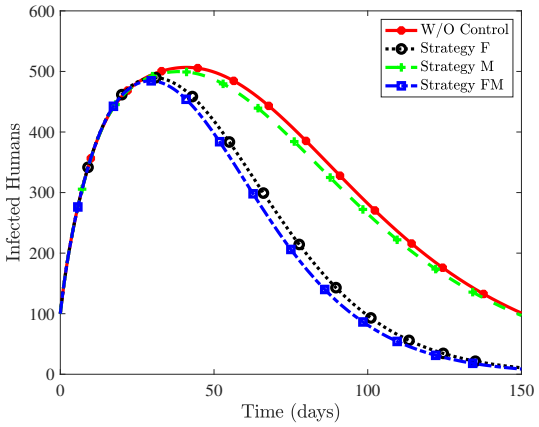

(a) Optimal trajectories of Infected humans (I_h).

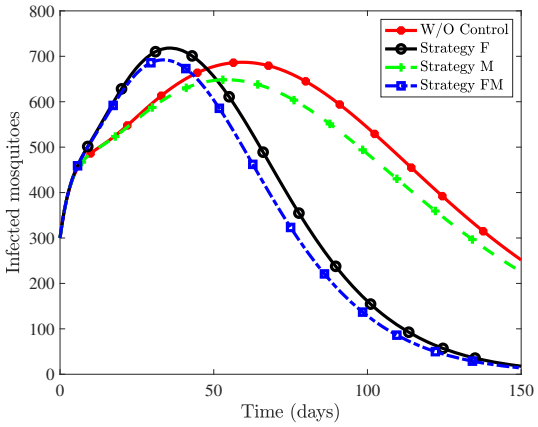

(b) Optimal trajectories of Infected mosquitoes ($I_n + I_w$).

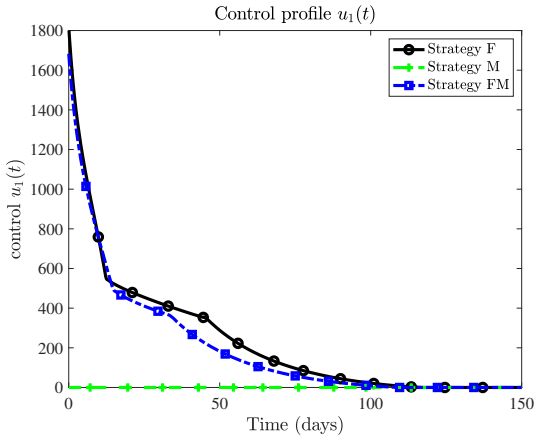

(c) Optimal control profile $u_1^*(t)$.

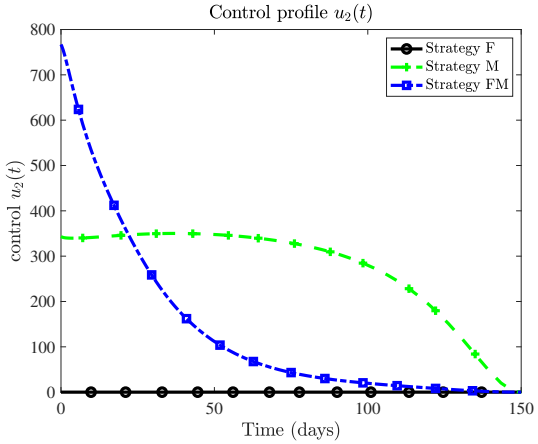

(d) Optimal control profile $u_2^*(t)$.

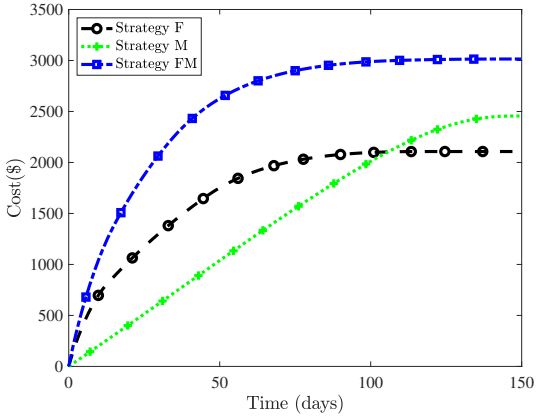

(e) Cost under control interventions F, M, and FM.

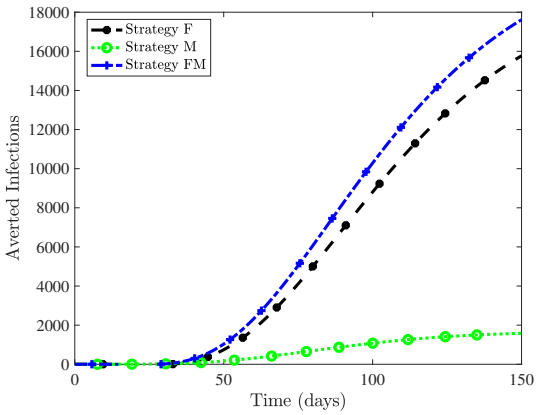

(f) Health benefits (averted infections) under control interventions F, M, and FM.

Figure 4.1: Optimal solutions when control strategies F , M , and FM are implemented.

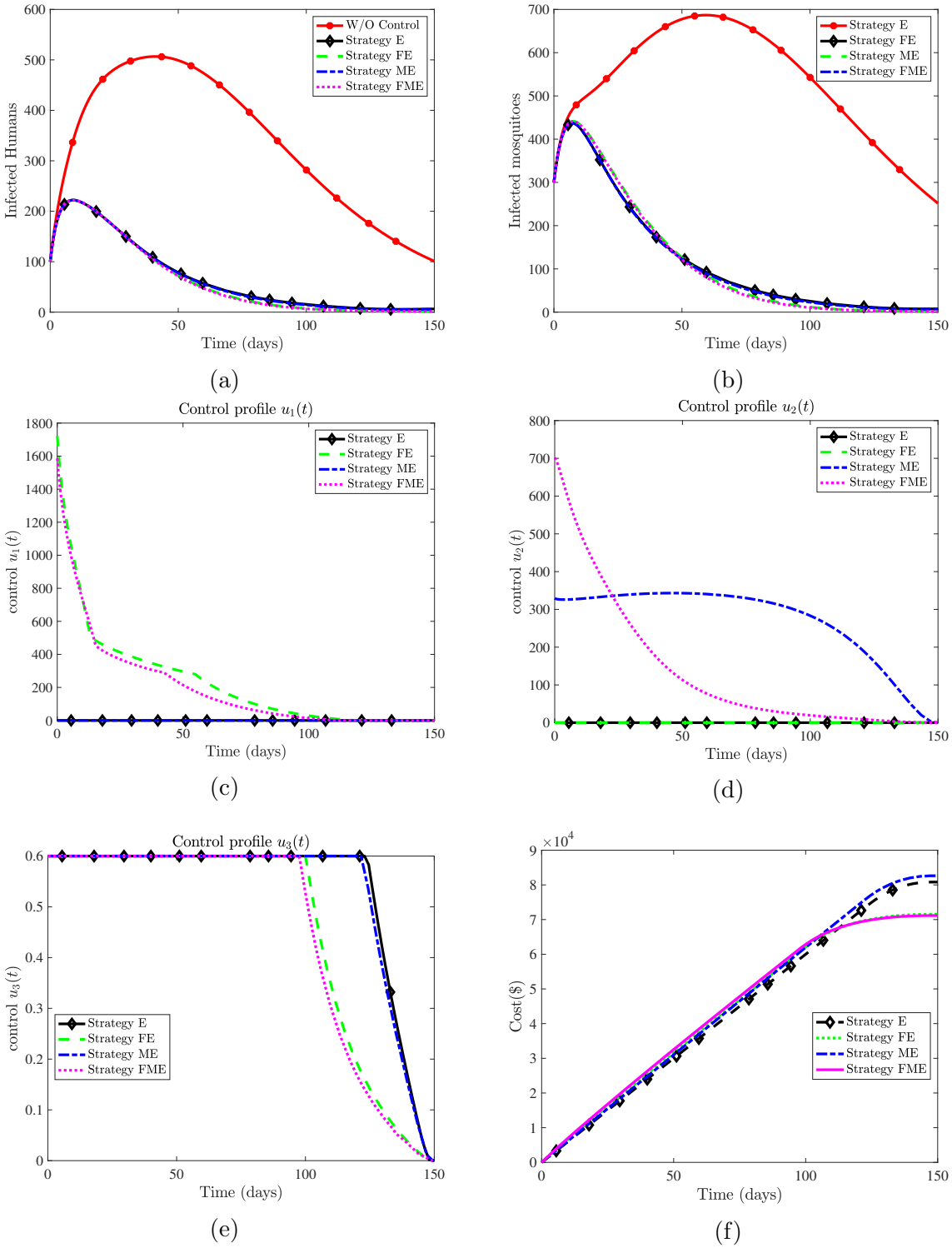

Figure 4.2: Optimal solutions when the control strategies E, FE, ME, and FME are implemented.

In our case, X represents a strategy listed in Table 4.1. From Eq. (4.19), we can observe that an individual strategy with more health benefits and low cost is more desirable control strategy. Thus, the strategy that has lowest ACER is considered the most cost-effective strategy.

- Incremental cost-effectiveness ratio (ICER) [61,86,87] is used to compare two different strategies (X and Y) and is defined as

$$\begin{aligned} ICER(X) =& \frac{\text{Cost(X)}}{\text{Benefits(X)}}, \\ ICER(X,Y) =& \frac{\text{Cost(X) - Cost(Y)}}{\text{Benefits(X) - Benefits(Y)}}. \end{aligned} \tag{4.20}$$

The numerator and denominator in the ICER Eq. (4.20) represent the difference in intervention costs and health benefits, respectively.

To use Eq. (4.19) or (4.20) for cost-effectiveness analysis, we first need to find the total cost of a strategy and the health benefits from the strategy during the time $[0, T]$. To find the total cost of a control strategy and the health benefits from the strategy, we define the cost and health benefits functionals as follows:

$$\text{Cost of a control strategy} = \int_0^T \left(B_1 u_1^*(t) + B_2 u_2^*(t) + B_3 u_3^*(t)\right) dt, \tag{4.21}$$

$$\text{Benefits from a control strategy} = \int_0^T \left(I_0(t) - I^*(t)\right) dt, \tag{4.22}$$

where $u_1^*(t), u_2^*(t)$, and $u_3^*(t)$ stand for the optimal control variables obtained by applying a particular control strategy, I_0 is the state trajectory of infected humans without controls (i.e. when $u_1(t) = u_2(t) = u_3(t) = 0$), whereas $I^*(t)$ stands for the number of infected humans when controls $u_1^*(t)$, $u_2^*(t)$, $u_3^*(t)$ are implemented. We want to point out here that in many studies, for example [61,84,86,88,89] , the authors considered the same cost functional as the objective functional for finding optimal control solutions. However, there are few models, for example [75, 90–92] , where the authors considered the cost functional consists of the terms that have only control variables. We also define the cost functional (4.21) that only

Table 4.2: The cost($) of each control strategy in increasing order, health benefits, ACER, and the ranking of each control strategy based on ACER index.

Strategies	Cost (USD)	Averted Infections	ACER
Strategy F	2.1×10^3	1.58×10^4	0.13
Strategy M	2.45×10^3	0.15×10^4	1.55
Strategy FM	3.01×10^3	1.77×10^4	0.17
Strategy FME	7.12×10^4	4.12×10^4	1.73
Strategy FE	7.15×10^4	4.11×10^4	1.74
Strategy E	8.08×10^4	4.04×10^4	1.99
Strategy ME	8.26×10^4	4.05×10^4	2.04

depends on the control variables, which is inline with [75, 90–92] . Thus, the optimal control solutions that we obtain satisfy the objective functional (4.5) that penalizes high level of controls, whereas the cost functional (4.21) incorporate the economic cost of applying the control strategies.

To calculate the ACER index, we sort all the strategies in ascending order of costs. The ACER index of all the strategies is calculated using Eq. (4.19) and the results are presented in Table 4.2. Based on the ACER index for all strategies given in Table 4.2, we observe that Strategy F (releasing only female *Wolbachia*-infected mosquitoes) is the most cost-effective strategy, $0.0011 per averted infection when compared to all other strategies. We also note that the averted infections are largest under the control strategy FME, but it also entails the highest costs ($\$2.29 \times 10^5$) when compared with the strategy F.

Next, we want to investigate the most cost-effective strategy using the ICER index. To determine the most cost-effective strategy using ICER index, we use the following process:

1. Rank the control strategies in the ascending order of costs.

2. Compute the ICER value for the first strategy in the sorted list and the ICER value between the first and second strategies using Eq. (4.20).

3. If the ICER between the two strategies is positive, then eliminate the strategy that has higher ICER value.

4. If the ICER between the two strategies is negative, eliminate the second strategy: the second strategy has higher cost and lower averted levels.

5. Repeat the process until only one strategy is left in the sorted list.

Following the above procedure, we start with the strategies M and FM, and calculate the ICER index using Eq. (4.20).

$$\begin{aligned} \text{ICER (F)} &= \frac{2.1\times10^3}{1.58\times10^4} &&= 0.13 \\ \text{ICER(Strategy F, Strategy M)} &= \frac{2.46\times10^3-2.1\times10^3}{1.58\times10^3-1.57\times10^4} &&= -0.024 \end{aligned}$$

The negative ICER index between strategy F and strategy M suggests that strategy M has a higher cost and lower averted infections when compared with strategy F. Therefore, we exclude strategy M and continue to compare strategy F with FM, the next strategy in the sorted list.

$$\begin{aligned} \text{ICER(F)} &= 0.13 \\ \text{ICER(F, FM)} &= \frac{3.01\times10^3-2.1\times10^3}{1.76\times10^4-1.57\times10^4} &&= 0.49 \end{aligned}$$

The lower ICER index for strategy F compared with Strategy FM suggests Strategy FM is more expensive and less effective compared with strategy F. Thus, we exclude strategy FM. Using the similar procedure, we now compare strategy F with all the next strategies in the sorted list.

$$\begin{aligned} \text{ICER(F)} &= 0.13 \\ \text{ICER(F, FME)} &= 2.71 \\ \text{ICER(F, FE)} &= 2.74 \\ \text{ICER(F, E)} &= 3.19 \\ \text{ICER(F, ME)} &= 3.25 \end{aligned}$$

We observe that strategies FME, FE, E, and ME are more expensive and less effective compare to strategy F. Therefore, we conclude that strategy F (releasing female *Wolbachia*-

infected mosquitoes) is the most cost-effective strategy among all other strategies.

Both, ACER and ICER, indexes conclude that releasing *Wolbachia*-infected female mosquitoes in the wild is the most cost-effective strategy for the control of dengue virus, whereas the strategy FM, releasing both *Wolbachia*-infected female and male mosquitoes in the wild, is the second-best strategy. We also observe that the difference between the ACER index of the strategy F and FM is minimal (0.03), which can also be implemented instead of the strategy F.

4.6 Conclusion

In this chapter, we formulated an optimal control model for the transmission of dengue virus disease in humans that incorporates three control interventions, namely, releasing *Wolbachia*-infected female mosquitoes only, releasing *Wolbachia*-infected male mosquitoes only, and preventive measures to reduce humans-mosquitoes contact induced by educational campaigns. Using the numerical results, we investigated the effects of single control intervention as well as combinations of different control interventions on the transmission of dengue virus. We observed that when strategy F is implemented, the total cost is $\$2.1 \times 10^3$, and the number of averted infections is 1.58×10^4. Similarly, the costs of implementing control interventions M and FM are $\$2.45 \times 10^3$ and $\$3.01 \times 10^3$, respectively, and the averted infections are 1.58×10^3 and 0.15×10^4, respectively. To determine the most cost-effective strategy among all control strategies, we used two common cost-effective indexes, namely, average cost-effectiveness ratio (ACER) and incremental cost-effectiveness ratio (ICER). Based on the ACER and ICER indexes, we conclude that releasing *Wolbachia*-infected female mosquitoes only is the most cost-effective strategy among all strategies for controlling dengue disease. Releasing both female and male *Wolbachia*-infected mosquitoes is the second-best strategy for controlling dengue disease.

CHAPTER 5

A MODEL OF *DAPHNIA* EPIDEMICS WITH SPATIAL DISTRIBUTION OF SPORES AND ALGAE IN WELL-MIXED WATER COLUMN

5.1 Introduction

Phytoplankton is a generic name for microorganisms found in marine and freshwater ecosystems [93] and is the base of several aquatic food webs, e.g., zooplankton (such as *Daphnia*) eat phytoplankton (Algae) and then smaller fish eat zooplankton (*Daphnia*) which are then eaten by larger fish. The importance of phytoplankton in the aquatic ecosystem has long been recognized and has been widely studied [94–99]. Phytoplankton, like other plants, utilizes solar energy (light) and carbon dioxide to produce biomass during photosynthesis [100]. Several factors such as light intensity, available nutrients, sinking velocity (sinking due to higher density than water), and mixing (due to waves, wind, and storm) affect the phytoplankton profile in a water column. Thus, we focus on the following two questions:

1. How does the phytoplankton population persist?

2. What helps the sinking phytoplankton population to remain in the upper well lit and well-mixed layer of shallow lakes where light intensity and turbulent diffusion is high?

Many authors have studied Spatio-temporal models of phytoplankton in water columns. Condie and Bormans [101], and Hodges and Rudnick [98] studied the dynamics of phytoplankton in the presence of sinking, but they neglect the light effects on the phytoplankton growth rate. Huismann and Sommeijer [96, 102], Huisman et al. [103], and Bhutiani et al. [104] considered the light effects on the growth of phytoplankton, but they did not consider the effects of nutrients in their studies. Paul et al. [105] considered only the effects of nutrients to model the distribution of the phytoplankton population in the water column. Ryabob et al. [99] analyzed an advection-diffusion-reaction for phytoplankton in which

the growth rate depends on the light intensity as well as on nutrients in a water column. Yoshiyama and Nakajima [106] considered the variation of phytoplankton population density in surface and deep layers with growth rate depending on light intensity and concentration of nutrients in each layer. Mellard et al. [107], Yoshiyama et al. [108], and Klausmeier and Litchman [97] considered the advection-diffusion-reaction model of phytoplankton density in a stratified water column with a well-mixed surface layer on top of a poorly mixed deep layer in the presence of light intensity and nutrients. Hsu et al. [109] studied a spatio-temporal model arising from the dynamics of harmful algae and zooplankton in flowing-water habitats and neglected vertical stratification and light limitation.

The focal host *Daphnia dentifera* is a lake zooplankton and filter-feed algae. While filter-feeding on algae, the susceptible *Daphnia* get infected by accidentally ingesting fungal spores (*Metschnikowia bicuspidata*) [30] because they can not differentiate between algae and fungal spores. Thus, *Daphnia*-spores interaction forms a host-parasite system and has been studied using ordinary differential equations (ODEs) to describe the dynamics of the hosts (*Daphnia*) and parasites (spores) [32, 33, 110, 111]. Due to weight density, free living spores and algae can also sink in a water column and can diffuse due to temperature gradient and wind effects on the water surface.

A model has not been studied yet that incorporates sinking and turbulent-diffusion rates of phytoplankton (Algae) and fungal spores (*Metschnikowia bicuspidata*) along with their interaction with zooplankton (*Daphnia dentifera*). A partial differential equations model is needed where we can incorporate convective terms as well as diffusive terms in algae and spores classes. To this end, we formulate and analyze an advection-diffusion-reaction partial differential equations (PDEs) epidemic model of phytoplankton (algae), fungal spores (*Metschnikowia bicuspidata*), and zooplankton (*Daphnia*) to investigate the effects of sinking and turbulent-diffusion of algae and spores in a well-illuminated shallow lake. We also want to investigate how the water column depth, algal carrying capacity, and advection speed of algae effects the disease dynamics of *Daphnia*.

5.2 Advection-diffusion *Daphnia*-spore-algae epidemic model

Following the work of [32], we denote the population of susceptible *Daphnia* by S, infected *Daphnia* by I), density of free living spores with Z, and algal biomass with A. We extend the model studied in [32] by considering the sinking and diffusion of algae and free living fungal spores in a well-illuminated water column of depth $0 \leq z \leq L$ with $z = 0$ at the top and $z = L$ at the bottom of the water column. We want to model the dynamics of host, algae and spores in a shallow water with maximum depth around $z_{max} = 10$ meters. Since the water column we consider is well-illuminated, we consider uniform light intensity in the water column.Therefore, the system of partial differential equations (PDEs) that governs the dynamics of the model is given by

$$\begin{aligned}
\frac{\partial S}{\partial t} &= \overbrace{e_s f_s(A)(S+\rho I)}^{\text{Births}} - \underbrace{(d+p_s(z))S}_{\text{Death + Predation}} - \overbrace{\mu f_s(A) S \frac{Z}{A}}^{\text{Infection}} \\
\frac{\partial I}{\partial t} &= \overbrace{\mu f_s(A) S \frac{Z}{A}}^{\text{Infection}} - \underbrace{(d+v+\theta p_s(z))I}_{\text{Death + Predation}} \\
\frac{\partial Z}{\partial t} &= \underbrace{D_z \frac{\partial^2 Z}{\partial z^2}}_{\text{Diffusion}} - \overbrace{v_z \frac{\partial Z}{\partial z}}^{\text{Advection}} + \overbrace{\sigma\,(d+v)\,I}^{\text{Spore release from dead infected hosts}} - \underbrace{\lambda Z}_{\text{Spore loss}} \\
\frac{\partial A}{\partial t} &= \underbrace{D_a \frac{\partial^2 A}{\partial z^2}}_{\text{Diffusion}} - \overbrace{v_a \frac{\partial A}{\partial z}}^{\text{Advection}} + \overbrace{r(z)\left(1-\frac{A}{K}\right)A}^{\text{Logistic growth}} - \underbrace{f_s(A)(S+I)}_{\text{Grazing on Algae}},
\end{aligned} \tag{5.1}$$

Boundary conditions:

$$\begin{aligned} D_z\frac{\partial Z}{\partial z}(0,t) - v_z Z(0,t) = 0, \qquad & D_z\frac{\partial Z}{\partial z}(L,t) - v_z Z(L,t) = 0 \\ D_a\frac{\partial A}{\partial z}(0,t) - v_a A(0,t) = 0, \qquad & D_a\frac{\partial A}{\partial z}(L,t) - v_a A(L,t) = 0. \end{aligned} \tag{5.2}$$

The increase in the S class is due to births from the susceptible *Daphnia* and infected *Daphnia* with rate $e_s f_s(A)$, where $f_s(A)$ represents host feeding rate and e_s denotes the conversion efficiency of algal biomass to *Daphnia* biomass and $0 < \rho < 1$ [32] accounts for reduction in birth rate of infected hosts due to infection. The decrease in the S class is due to mortality at rate d and predation at rate p_s. The susceptible class also decreases when susceptible hosts become infected and move into the infected host class at rate $\mu\frac{f_s(A)}{A}$, where μ denotes the per spore infectivity. The infection rate of the susceptible hosts depends on the feeding rate $f_s(A)$, the density of the susceptible hots S, per spore infectivity μ, and the relative density of spores to algae biomass Z/A.

The number of infected hosts (I) increases when susceptible hosts (S) become infected and move into the infected class. The decrease in the infected class is due to mortality at rate d, disease-induced mortality at rate ν, and predation at rate θp_s. To account for the fact that infected hosts become opaque and their vulnerability to predation increases, we use the host selectivity parameter $\theta \geq 1$. The host selectivity parameter $\theta > 1$ implies that predators prefer to prey on the infected hosts, whereas $\theta = 1$ implies no preference among hosts.

The density of spores (Z) in the water column increases when infected hosts die and release spores $\sigma(d+\nu)I$ back in the water column, where $(d+\nu)$ denotes the death rate of infected *Daphnia* and σ denotes the number of spores released per dead infected host. Spores are removed from the water column at rate λ. The density of spores in the water column is also affected due to sinking at a rate v_z and mixing with turbulent-diffusion coefficient D_z. We used an advection-diffusion equation to model the sinking and diffusion process of spores in the water column. We also want to point out that we do not assume that spore biomass depends on the host growth rate $e_s f_s(A)$, and neither host consumes spores, both were assumed in the model [32].

Finally, algae (A) grows logistically with intrinsic growth rate r and carrying capacity K and decreases due to the consumption by the susceptible and infected *Daphnia* at rate $f_s(A)$. The algal biomass also changes due to sinking at rate v_a and mixing with turbulent-diffusion coefficient D_a, which we modeled using an advection-diffusion equation for algae class. To model the feeding rate of *Daphnia*, we consider the following Holling Type-II functional response

$$f_s(A) = \frac{f_{s0}A}{h_s + A}, \tag{5.3}$$

where f_{s0} is the maximum feeding rate and h_s is a half-saturation constant.

We want to point out that our model (5.1) matches with the model studied in [32] except that

- We assume that spore biomass does not depend on the host growth rate $e_s f_s(A)$. In our model, the spore biomass only depends on the density of infected host I and is modeled as $\sigma(d+\mu)I$, where $(d+\mu)I$ I represents the density of infected host per unit time and σ is the number of spores released per dead infected host.

- We do not consider the term $f_s(A)(S+I)\frac{Z}{A}$ in our model.

- In our model (5.1), we also consider the sinking and diffusion of algae and spores in the water column, which we modeled using an advection-diffusion partial differential equation (PDE) for both algae and spore classes. Therefore, our model turns into a PDE model.

Our main focus in this work is to investigate the effects of sinking speeds (v_a, v_z), diffusion coefficients D_a, D_z, algal carrying capacity K, and water column maximum depth z_{max} on the dynamics of the model (5.1). To make model (5.1) simple, we assume that the turbulent-diffusion coefficients (D_z and D_a) and sinking velocities (v_z and v_a) of algae and spores are constant and do not vary with water column depth z. Also, the positive direction of v_z and v_a are oriented downward, in the direction of increasing z.

Table 5.1: Variables and parameters [32] .

Symbol	Description	Value	Unit
Variables:			
S	Density of susceptible hosts	...	mgC/L
I	Density of infected hosts	...	mgC/L
Z	Density of spores	...	mgC/L
A	Density of Algae	...	mgC/L
z	Depth	...	meters (m)
t	Time	...	days
Parameters:			
λ	Loss rate of spores	0.2	day^{-1}
d	Background mortality rate of host	0.03	day^{-1}
p_s	Predation rate on susceptible host	constant for low K and depth dependent for high K	day^{-1}
p_i	Predation rate on infected host	θp_s	day^{-1}
ν	Disease-induced mortality rate	0.05	day^{-1}
r	Algal growth rate	constant for low K and depth dependent for high K	day^{-1}
f_{s0}	Maximum feeding rate	0.32	day^{-1}
μ	Host susceptibility	10	mgC/mgC
K	Algal carrying capacity	$0-6$	mgC/L
ρ	Fecundity reduction due to infection	0.9	
σ	Spore release parameter	4	days$\times$ mgC/mgC
e_s	Conversion efficiency	0.6	
h_s	Half saturation constant	0.3	mgC/L
L	Depth of the water column	10	meters (m)
v_z	Spore sinking rate	$0.05-0.95$	meters per day
D_z	Spore diffusivity coefficient	8	square meters per day
v_a	Algae sinking rate	$0.05-0.95$	meters per day
D_a	Algae diffusivity coefficient	8	square meters per day

5.3 Disease-free equilibrium states

The steady states equations of the model (5.1) are given by the following equations:

$$0 = e_s f_s(A)(S + \rho I) - (d + p_s(z))S - \mu \frac{f_s(A)}{A} SZ, \tag{5.4}$$

$$0 = \mu \frac{f_s(A)}{A} SZ - (d + v + \theta p_s(z))I, \tag{5.5}$$

$$0 = D_z Z'' - v_z Z' + \sigma (d + v) I - \lambda Z, \tag{5.6}$$

$$0 = D_a A'' - v_a A' + r(z) \left(1 - \frac{A}{K}\right) A - f_s(A)(S + I). \tag{5.7}$$

For the disease-free steady states, it holds that $I = 0 = Z$ and from equation (5.4) and (5.7), we have the following steady states:

1. $S = 0$ leads to the existence of trivial equilibrium state $E_0 = (0, 0, 0, 0)$ and algae-only equilibrium state $E_1 = (0, 0, 0, A^*(z))$, where $A^*(z)$ is the solution of the following nonlinear boundary value problem:

$$\begin{aligned} D_a A'' - v_a A' + r(z) \left(1 - \tfrac{A}{K}\right) A &= 0, \\ \text{BCs:} \qquad D_a A'(0) - v_a A(0) &= 0, \\ D_a A'(L) - v_a A(L) &= 0. \end{aligned} \tag{5.8}$$

2. $S \neq 0$ implies the existence of a disease-free equilibrium state $E_2 = (S^*(z), 0, 0, A^*(z))$, where S^* and A^* are solutions of the following steady state equations

$$e_s f_s(A)S - (d + p_s(z))S = 0, \tag{5.9}$$

$$D_a A'' - v_a A' + r(z) \left(1 - \frac{A}{K}\right) A - f_s(A)S = 0. \tag{5.10}$$

$$\begin{aligned} \text{BCs:} \qquad D_a\, A'(0) - v_a\, A(0) &= 0, \\ D_a\, A'(z_m) - v_a\, A(z_m) &= 0 \end{aligned}$$

5.4 Basic reproduction number $\mathcal{R}_0^{SIZA}$

To find the basic reproduction number $\mathcal{R}_0^{SIZA}$ for the model (5.12), we make use of the theorems proved in [112] and stated below. The method discussed in [112] is similar to the next-generation matrix approach but for the parabolic system of partial differential equations that do not have advection and diffusion terms present in all equations. Note that in our model (5.1) the advection and diffusion terms are also absent in the susceptible and infected host classes; hence the results proved in [112] are also applicable for our model.

Theorem 5.1 ([112]). *Assume that there exists $d_0 > 0$ such that $d_i(z) \geq d_0$ for $1 \leq i \leq m$. If the elliptic eigenvalue problem*

$$\begin{aligned} -\nabla.(d_I(z)\nabla\psi) + \mathcal{V}(z)\psi &= \lambda\mathcal{F}(z)\psi, \qquad z \in \Omega \\ \frac{\partial\psi}{\partial n} &= 0, \quad z \in \partial\Omega, \end{aligned} \tag{5.11}$$

admits a unique positive eigenvalue λ_0 with a positive eigenfunction, then

$$\mathcal{R}_0^{SIZA} = r(-\mathcal{F}B^{-1}) = r(-B^{-1}\mathcal{F}) = 1/\lambda_0$$

.

Theorem 5.2 ([112]). *Assume that $s(-\mathcal{V}_{22}) < 0$. Let $B_1 := \nabla.(d_{i_1}\nabla) - \mathcal{V}_1$, where $\mathcal{V}_1 := \mathcal{V}_{11} - \mathcal{V}_{12}\mathcal{V}_{22}^{-1}\mathcal{V}_{21}$. Then the following statements are valid:*

1. *If $\mathcal{F}_{12} = 0$ and $\mathcal{F}_{22} = 0$, then $\mathcal{R}_0^{SIZA} = r(-B^{-1}\mathcal{F}) = r(-B_1^{-1}\mathcal{F}_1)$, where $\mathcal{F}_1 := \mathcal{F}_{11} - \mathcal{V}_{12}\mathcal{V}_{22}^{-1}\mathcal{F}_{21}$.*

2. *If $\mathcal{F}_{21} = 0$ and $\mathcal{F}_{22} = 0$, then $\mathcal{R}_0^{SIZA} = r(-B^{-1}\mathcal{F}) = r(-B_1^{-1}\mathcal{F}_2)$, where $\mathcal{F}_2 := \mathcal{F}_{11} - \mathcal{F}_{12}\mathcal{V}_{22}^{-1}\mathcal{V}_{21}$.*

First, we linearize the system (5.1) around the disease-free equilibrium (DFE) state $E_2 = (S^*, 0, 0, A^*)$ by setting

$$\tilde{S} = S - S^*, \qquad \tilde{I} = I, \qquad \tilde{Z} = Z, \qquad \tilde{A} = A - A^*,$$

into the system (5.1) and keeping only first order terms, we get the following linearized system

$$\begin{aligned}
\frac{\partial \tilde{S}}{\partial t} &= \left(e_s f_s(A^*) - (d+p_s)\right)\tilde{S} + \rho e_s f_s(A^*)\tilde{I} \\
&\quad -\mu \frac{f_s(A^*)}{A^*} S^* \tilde{Z} + \frac{e_s f_{s0} h_s S^*}{(h_s+A^*)^2}\tilde{A} \\
\frac{\partial \tilde{I}}{\partial t} &= \mu \frac{f_s(A^*)}{A^*} S^* \tilde{Z} - (d+v+p_i)\tilde{I} \\
\frac{\partial \tilde{Z}}{\partial t} &= D_z \frac{\partial^2 \tilde{Z}}{\partial z^2} - v_z \frac{\partial \tilde{Z}}{\partial z} + \sigma\,(d+v)\,\tilde{I} - \lambda \tilde{Z} \\
\frac{\partial \tilde{A}}{\partial t} &= D_a \frac{\partial^2 \tilde{A}}{\partial z^2} - v_a \frac{\partial \tilde{A}}{\partial z} + \left(r - \frac{2rA^*}{K} - \frac{f_{s0} h_s S^*}{(h_s+A^*)^2}\right)\tilde{A} \\
&\quad -f_s(A^*)\tilde{S} - f_s(A^*)\tilde{I}.
\end{aligned} \tag{5.12}$$

In our model (5.1), the infected classes are I and Z. Therefore, the transmission matrix $\mathcal{F}$, which describes the generation of secondary infections in the infected classes, and transition matrix $\mathcal{V}$, which describes how individuals move in and out of the infected classes, at the disease-free equilibrium state $E_2 = (S^*(z), 0, 0, A^*(z))$ are given by

$$\mathcal{F} = \begin{bmatrix} 0 & 0 \\ \mu \frac{f_s(A^*)}{A^*} S^* & 0 \end{bmatrix} \qquad \text{and} \qquad \mathcal{V} = \begin{bmatrix} \lambda & -\sigma(d+\nu) \\ 0 & d+\nu+\theta p_s(z) \end{bmatrix}. \tag{5.13}$$

$$\mathcal{F}_1 = \mathcal{F}_{11} - \mathcal{V}_{12}\mathcal{V}_{22}^{-1}\mathcal{F}_{21} \Rightarrow \mathcal{F}_1 = \frac{\sigma f_s(A^*)(d+\nu)\mu S^*}{A^*(d+\nu+\theta p_s(z))},$$

$$\mathcal{V}_1 = \mathcal{V}_{11} - \mathcal{V}_{12}\mathcal{V}_{22}^{-1}\mathcal{V}_{21} \Rightarrow \mathcal{V}_1 = \lambda,$$

$$B_1 := D_z \frac{\partial^2}{\partial z^2} - v_z \frac{\partial}{\partial z} - \mathcal{V}_1 \Rightarrow B_1 = D_z \frac{\partial^2}{\partial z^2} - v_z \frac{\partial}{\partial z} - \lambda.$$

To find $\mathcal{R}_0^{SIZA}$, we used the following results obtained by Wang and Zhao [112]:

Finally, we write the infected classes, which in our case are I and Z, in terms of eigenvalue problem by setting

$$\tilde{I} = e^{\eta t}\phi(z), \qquad \tilde{Z} = e^{\eta t}\psi(z)$$

into the second and third equation of the linearized system (5.12), we get the following

eigenvalue problem:

$$\mu\frac{f_s(A^*)}{A^*}S^*\psi(z) - (d+v+\theta p_s(z))\phi(z) = \eta\phi(z), \tag{5.14}$$

$$D_z\frac{d^2\psi}{dz^2} - v_z\frac{d\psi}{dz} + \sigma(d+v)\phi(z) - \lambda\psi(z) = \eta\psi(z), \tag{5.15}$$

Solving for $\phi(z)$ from (5.14) and substituting into (5.15), we can write

$$-B_1\psi = \lambda\mathcal{F}_1\psi, \tag{5.16}$$

where $B_1\psi = D_z\frac{d^2\psi}{dz^2} - v_z\frac{d\psi}{dz} - \lambda\psi$ and $\mathcal{F}_1\psi = \frac{\sigma f_s(A^*)(d+\nu)\mu S^*}{A^*(d+\nu+\theta p_s(z))}\psi$.

Lemma 5.1. *Let η_1 be the principle positive eigenvalue of the eigenvalue problem*

$$\begin{aligned} -D_z\frac{d^2\psi}{dz^2} + v_z\frac{d\psi}{dz} + \lambda\psi &= \eta\frac{\sigma f_s(A^*)(d+\nu)\mu S^*}{A^*(d+\nu+\theta p_s(z))}\psi, \\ D_z\,\psi'(0) - v_z\,\psi(0) = 0, &\qquad D_z\psi'(L) - v_z\psi(L) = 0 \end{aligned} \tag{5.17}$$

with a positive eigenfunction. Then $\mathcal{R}_0^{SIZA} = 1/\eta_1$.

Using the transformation $\psi(z) = e^{\frac{v_z}{D_z}z}\Psi(z)$, Eq. 5.17 takes the following form,

$$\begin{aligned} -\left(D_z e^{\frac{v_z}{D_z}z}\Psi'(z)\right)' + \lambda e^{\frac{v_z}{D_z}z}\Psi(z) &= \eta\frac{\sigma f_s(A^*)(d+\nu)\mu S^*}{A^*(d+\nu+\theta p_s(z))}e^{\frac{v_z}{D_z}z}\Psi(z), \\ \Psi'(0) &= 0, \\ \Psi'(L) &= 0. \end{aligned} \tag{5.18}$$

5.5 Numerical results

The nonlinear advection-diffusion-reaction model (5.1) with boundary conditions can not be solved analytically. We solve the model (5.1) numerically using the method of lines [113]. In all numerical simulations, we consider uniform initial conditions for state variables and use the parameter values given in Table 5.1 unless otherwise stated. We assume that the algal growth rate and predation rate are constant when the algae carrying capacity is low (e.g.

$0 < K \leq 2$), whereas growth and predation rates vary with depth when the algal carrying capacity is high (e.g. $4 \leq K \leq 6$). To incorporate this assumption, we consider

$$\text{growth rate} = \begin{cases} 0.2 & 0 < K \leq 2 \\ r(z) & 4 \leq K \leq 6 \end{cases}$$

$$\text{predation rate} = \begin{cases} 0.1 & 0 < K \leq 2 \\ p(z) & 4 \leq K \leq 6 \end{cases},$$

where $r(z)$ and $p(z)$ vary with depth and their variation with respect to depth is shown in Figure 5.1.

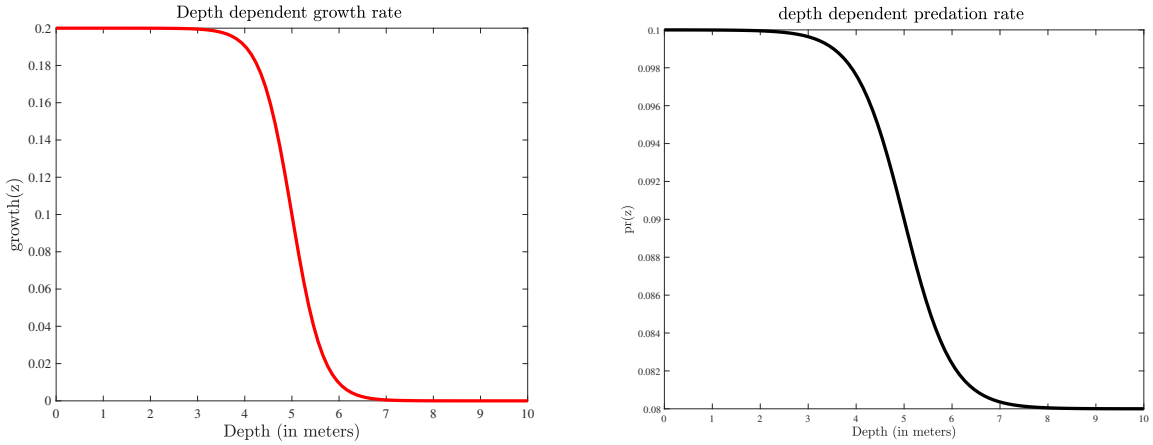

(a) (b)

Figure 5.1: Qualitative shape of algae growth rate function $r(z)$ (left panel) and host predation rate function $p_s(z)$ (right panel) when the carrying capacity K is high ($4 \leq K \leq 6$).

In all simulations, we also assume that algae and spore sink with the same speed (i.e. $v_a = v_z$), positive v_a and v_z are oriented downward, in the direction of increasing z.

5.5.1 Dependence of steady states on the carrying capacity K

To understand how the algal carrying capacity K affects the dynamics of the model (5.1), we fix the water column maximum depth $z_{\max} = 10$ meters (m), sinking rates $v_z = v_a = 0.1\, m/day$, turbulent-diffusion coefficients $D_z = D_a = 8\, m^2/day$, and solve the model (5.1)

numerically using low and high values of the carrying capacity K. The numerical results in Figure 5.2 show that Algae-only steady state exists when the carrying capacity is $K = 0.8$, whereas disease-free steady state exists only when the carrying capacity is $K = 1.2$. The results in Figure 5.2 reveal that algae-only or disease-free steady states exist when the the carrying capacity is low $0 < K \leq 2$. However, the endemic equilibrium state exists when the carrying capacity is high (e.g. $K = 5$ and $K = 5.5$), as shown in Figure 5.3. The numerical results in Figure 5.3 also reveal that

- algal biomass is high for large K and low for small K, as expected,
- there is more algae in the upper layer than at the bottom of the water column,
- most of the *Daphnia* are (on average) deep but not exactly at the bottom of the lake. Similar behavior is also observed for the infected *Daphnia* as well,
- the number of susceptible and infected *Daphnia* is maximum at $z = 6.55\,m$, which is 1.55 meters below the inflection point on the growth and predation rates curve shown in Figure 5.1,
- the number of spores increases up to the depth $z = 7.2$ meters, and then starts decreasing until the bottom of the lake $z = 10$.

It is worth mentioning that the decrease in spores density after a certain depth is due to i) decrease in infected *Daphnia*, which are the only source for the spores, and ii) zero flux boundary conditions along with the presence of diffusion and advection in spores equation. Through numerical experiments, we also observe that spores sink to the bottom of the lake when advection time scale $\frac{L}{v_z}$ is much smaller than the diffusion time scale $\frac{L}{D_z}$.

Overall, the results in Figures 5.2 and 5.3 show that under fix $v_z = v_a = 0.1$, $z_{\max} = 10$, and carrying capacity K increases from $K = 0.8$ through 1.5 to 5, we observe the same behavior as in the system without advection and diffusion and was studied in [32]. Namely, we see the transition from the algae-only to the disease-free, and finally, the endemic steady state when we only change the carrying capacity K while keeping the sinking rates and water column maximum depth constant.

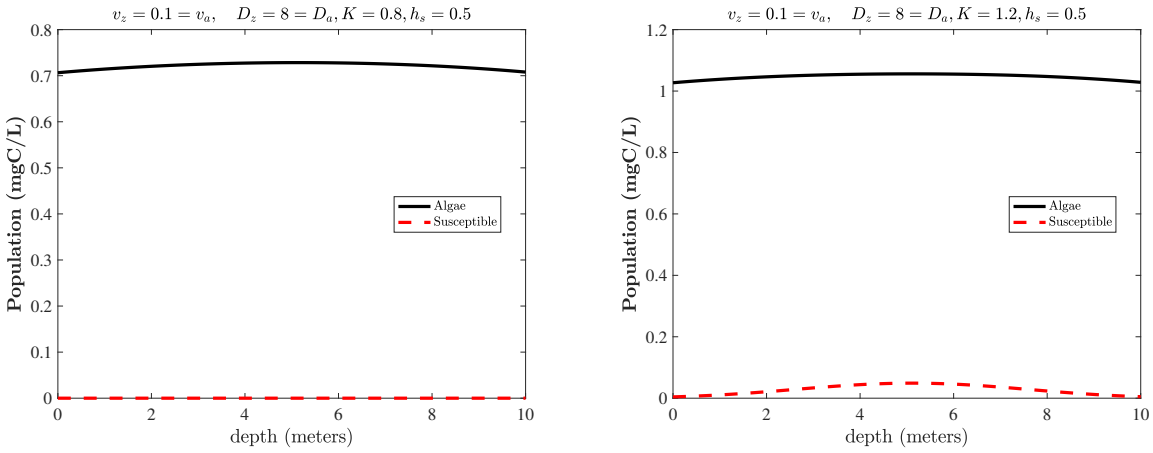

(a) (b)

Figure 5.2: Algae-only steady state exists when $K = 0.8$ (left panel) and disease-free steady state exists when $K = 1.2$ (right panel). The basic reproduction number when $K = 1.2$ is $\mathcal{R}_0^{SIZA} = 0.2$.

5.6 Dependence of steady states on the carrying capacity K, sinking rates $v_z = v_a$, and water column depth $z_{\max}$.

To investigate how the sinking rates and the water column maximum depth $z_{\max}$ affect the dynamics of the system (5.1), we consider

- two water columns of different depths $z_{\max} = 5,\ 10$ meters (m),
- low and high values of the algal carrying capacity $K = 0.8,\ 1.2,\ 5,\ 5.5$ mgC/L,
- different sinking rates with values in range $v_z = v_a = 0.1 - 0.9$ m/day,

and solve the model (5.1) numerically by taking different combinations of the cases mentioned above. In the numerical results that follow, the plots in the left column represent the dynamics of the model (5.1) for $z_{\max} = 5$, whereas the plots in the right column represent the dynamics for $z_{\max} = 10$. Within each column, left and right, the variation of sinking rates is also shown. The effects of the carrying capacity are shown by taking different K for each figure; that is, each figure corresponds to a fixed value of K.

In Figure 5.4, we observe that Algae-only steady state exists for low carrying capacity ($K = 0.8$) and $z_{\max} = 10$ (right panels) for different sinking rates, whereas only trivial steady state exists when the advection speed exceeds 0.5 for the same carrying capacity

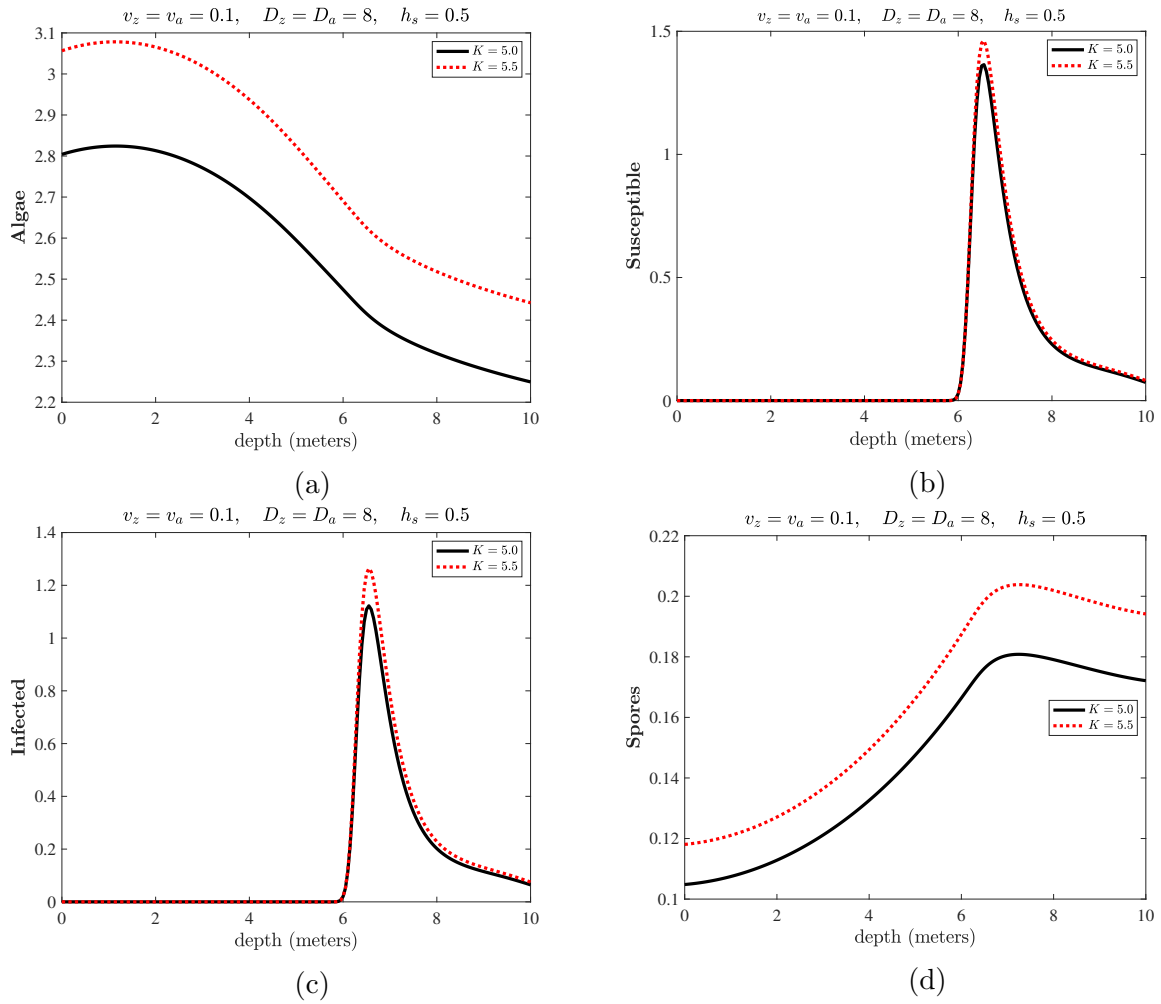

Figure 5.3: Endemic steady state exists when the carrying capacity is high and $v_z = v_a = 0.1$ and $D_z = D_a = 8$. The solid black lines correspond to $K = 5$, whereas the red dotted lines correspond to $K = 5.5$. The basic reproduction number is $\mathcal{R}_0^{SIZA} = 1.13$ when $K = 5$ and $\mathcal{R}_0^{SIZA} = 8.29$ when $K = 5.5$.

(i.e., $K = 0.8$) but the maximum depth is small $z_{\max} = 5$ (left panels). In Figure 5.4, we also observe that algal biomass decreases when the sinking speed of algae increases.

The results in Figures 5.5 and 5.6 correspond to the carrying capacity $K = 1.2$. For the case where maximum depth $z_{\max} = 10$ (right panels), we observe disease-free equilibrium state as long as sinking speed is less than 0.1 and algae-only equilibrium state when sinking speed exceeds 0.1. For the case where maximum water column depth $z_{\max} = 5$ (left panels), algae-only steady state exists as long as sinking speed is less than 0.5 and when sinking speed exceeds 0.5 we observe only trivial equilibrium steady state.

The numerical results in Figures 5.7–5.8c correspond to the high carrying capacity value $K = 5$ where we observe either trivial, algae-only, disease-free, or endemic steady states depending on the water column maximum depth $z_{\max}$ and algae sinking speed v_a.

Based on the numerical results presented in Figures 5.4–5.8c, we observe that steady-state equilibrium states of the model (5.1) not only depend on the algal carrying capacity K, as we see in Figures 5.2–5.3, but also depend on the sinking speed of algae v_a and the water column maximum depth $z_{\max}$. These numerical results suggest that there exists a critical water column maximum depth $z_{c\max}$, which also depends on the sinking speed, such that if the water column maximum depth is less than $z_{c\max}$ algae do not persist and if greater than the critical length algae persist.

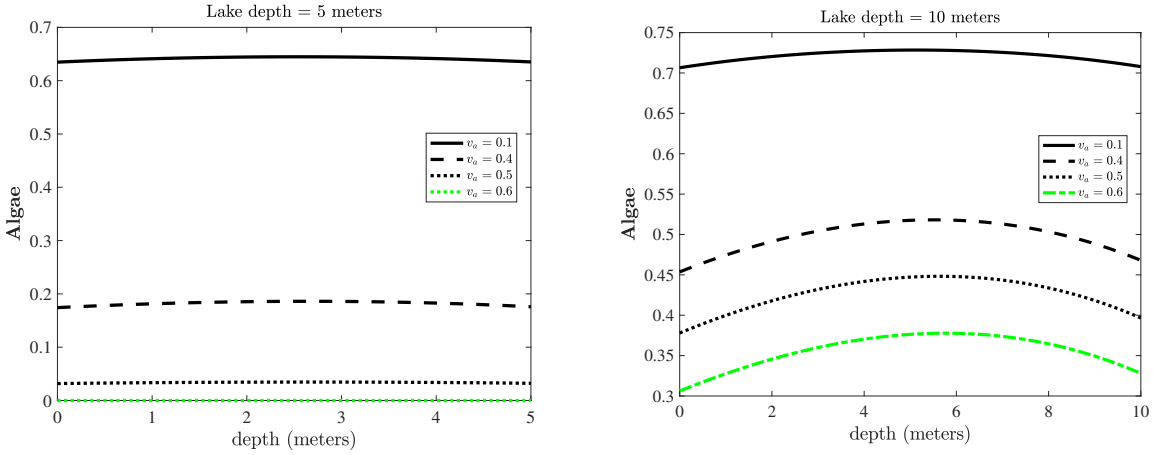

(a) (b)

Figure 5.4: Numerical results when $K = 0.8$ and $z_{max} = 5$ (left column) vs $z_{max} = 10$ (right column). For $z_{\max} = 5$ (left column), algal density decreases as sinking rate increases and finally becomes zero when sinking rate exceeds 0.5, whereas for $z_{\max} = 10$ (right column) algae persists even when the sinking speed exceeds 0.5.

5.7 Conclusion

In this chapter, we formulated an advection-diffusion-reaction *Daphnia* epidemic model where the susceptible hosts (*Daphnia*) become infected by accidentally ingesting fungal spores (*Metschnikowia bicuspidata*) in a water column. The feeding rate of the host on algae is modeled using Holling type-II functional response. Due to weight density and tem-

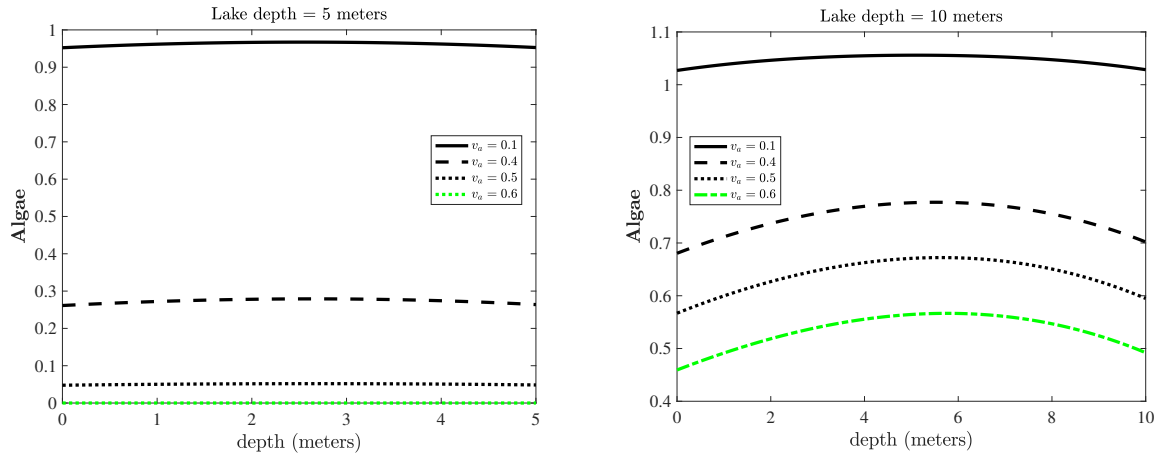

(a) (b)

Figure 5.5: Numerical simulations when $K = 1.2$ and $z_{\max} = 5$ (left panels) vs $z_{\max} = 10$ (right panels).

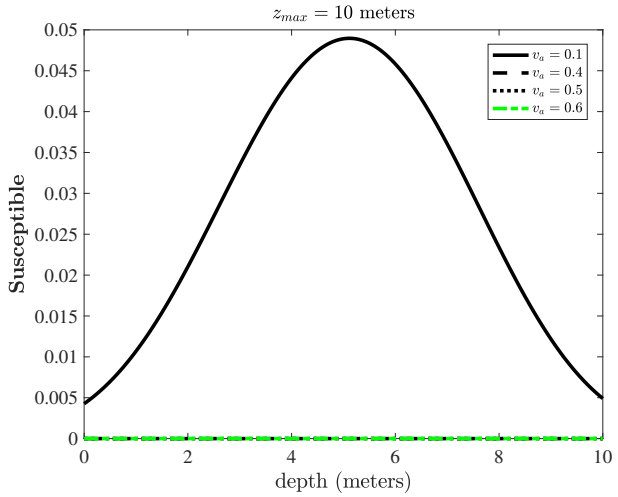

Figure 5.6: Numerical results show that disease-free steady state exist only when $K = 1.2$, $v_a = 0.1$, and $z_{\max} = 10$.

perature gradient, the spore and algae sink as well as diffuse in the water column, which we modeled by incorporating the advection and diffusion terms in the equations that correspond to algae and spores. We assume that the host (susceptible and infected *Daphnia* neither sink nor diffuse; hence the host's equations do not have advection and diffusion terms in them. Using the numerical results, we observed that steady states of the PDE model depend on the carrying capacity, algae sinking speed, and water column maximum depth. Numerical results suggest that corresponding to each algae sinking speed, there exists a critical water

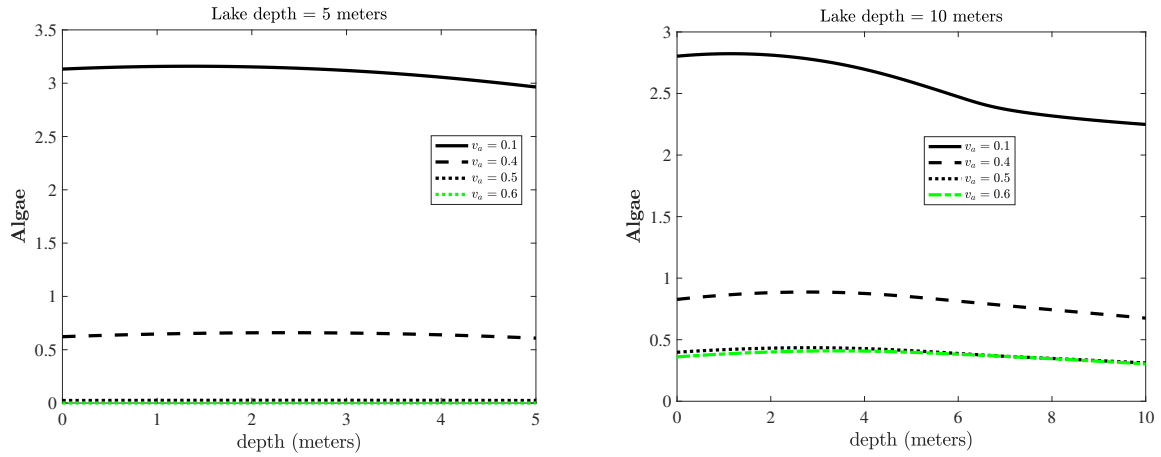

(a) (b)

Figure 5.7: Numerical results when $K = 5$ and $z_{\max} = 5$ (left column) vs $z_{\max} = 10$ (right column).

column maximum depth such that if the water column maximum depth is below the critical depth, algae do not persist, and if above the critical length algae persist. Also, using the dimensional analysis on algae equation in appendix (C), we observe that algae persist if the advection time scale $\frac{z_{max}}{v_a}$ is large compared to algae growth time scale $\frac{1}{r(z)}$, that is algae grows faster than it sinks. However, when the algae growth time scale dominates advection time scale (i.e. algae grows slower and sink fast) then algae does not persist. It is clear that advection time scale depends on the water column depth z_{max} and the algae sinking rate $v_a\, m/day$, and the advection time scale is small for small z_{max} and large v_a. Our numerical results are consistent with the dimensional analysis and we also observe numerically that for small water column depth and large advection, algae does not persist.

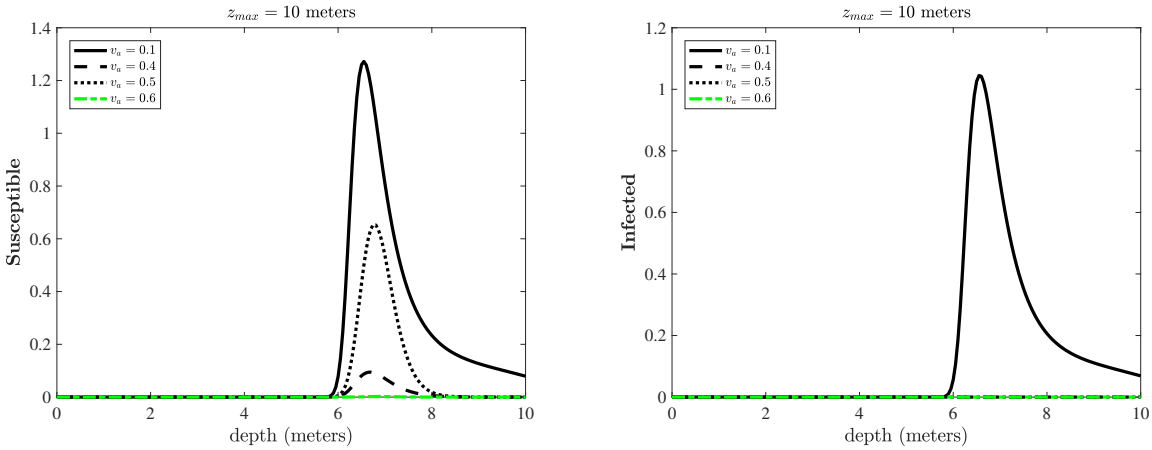

(a) Susceptible host

(b) Infected host

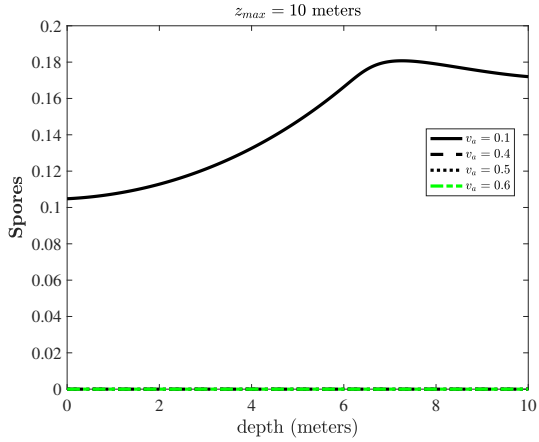

(c) Spores

Figure 5.8: Numerical results when $K = 5$ and $z_{\max} = 10$ for susceptible and infected hosts and spores.

APPENDIX A

DEFINITIONS AND STATEMENT OF THEOREMS

In this appendix, we define important terms and state theorems that we used in this thesis.

Definition A.1. *A set $\mathcal{C}$ is called convex if $\forall\, z_1,\, z_2 \in \mathcal{C}$ and $\eta \in [0,1]$ then $\eta z_1 + (1-\eta) z_2 \in \mathcal{C}$.*

Definition A.2. *A function $f : \mathcal{C} \to \mathbb{R}$ is called convex if $\mathcal{C}$ is a convex set and $\forall\, z_1,\, z_2 \in \mathcal{C}$, and all $\eta \in [0,1]$, we have $f(\eta z_1 + (1-\eta) z_2) \leq \eta f(z_1) + (1-\eta) f(z_2)$.*

Definition A.3. *A function f is called Lipschitz if $\exists$ a constant κ such that $|f(z_1) - f(z_2)| \leq \kappa |z_1 - z_2|$ for all $z_1,\, z_2$ in the domain of f.*

Theorem A.1 (Pontryagin's Maximum Principle [13])**.** *Let u^* be an admissible control and y^* be the corresponding trajectory, then there exists adjoint variable $\lambda_y : [0,T] \to \mathbb{R}$, such that*

$$\frac{dy}{dt} = \frac{\partial \mathcal{H}}{\partial \lambda_y} \qquad \text{and} \qquad \frac{d\lambda_y}{dt} = -\frac{\partial \mathcal{H}}{\partial y} \tag{A.1}$$

where the Hamiltonian $\mathcal{H}$ = integrand of the objection functional + $\lambda_y \frac{dy}{dt}$

$$\mathcal{H}(t, y^*(t), u^*(t), \lambda_y(t)) \leq \mathcal{H}(t, y^*(t), u, \lambda_y(t)) \quad \forall u \in \mathcal{U}, \tag{A.2}$$

and the transversality condition

$$\lambda_y(T) = 0 \tag{A.3}$$

APPENDIX B

LOCAL STABILITY ANALYSIS OF IT WOLBACHIA-FREE EQUILIBRIUM (WFE) POINT

In this appendix, we prove the stability of the it Wolbachia-free equilibrium point $E_1 = (A_{1n}, F_{1n}, F_{1n}, 0, 0, 0)$ discussed in section 2.3.3 of chapter 2.

The Jacobian of (2.1a)-(2.1f) at the WFE point E_1 is

$$J_{E_1} = \begin{pmatrix} -(\gamma_n + \mu_{na}) + \frac{(1-\mathscr{R}_{0n})\tau\gamma_n\rho_n}{\mu_n\mathscr{R}_{0n}} & \frac{\rho_n}{\mathscr{R}_{0n}} & 0 & \frac{(1-\mathscr{R}_{0n})\tau\gamma_n\rho_n}{\mu_n\mathscr{R}_{0n}} & \frac{(1-\epsilon_w)\rho_w}{\mathscr{R}_{0n}} & \frac{-\tau\mu_{mn}\rho_n}{R_{0n}(1-\tau)\mu_n} \\ \tau\gamma_n & -\mu_n & 0 & 0 & 0 & 0 \\ (1-\tau)\gamma_n & 0 & -\mu_{mn} & 0 & 0 & 0 \\ 0 & 0 & 0 & -(\gamma_w + \mu_{wa}) & \frac{\epsilon_w\rho_w}{\mathscr{R}_{0n}} & 0 \\ 0 & 0 & 0 & \tau\gamma_w & -\mu_w & 0 \\ 0 & 0 & 0 & (1-\tau)\gamma_w & 0 & -\mu_m \end{pmatrix}.$$

Eigenvalues of J_{E_1} are $-\mu_w$, $-\mu_m$, and the roots of the following quadratic equations

$$\Lambda^2 + \zeta_1\Lambda + \zeta_2 = 0, \tag{B.1}$$

$$\Lambda^2 + \zeta_3\Lambda + \zeta_4 = 0, \tag{B.2}$$

where

$$\begin{aligned} \zeta_1 &= (\gamma_n + \mu_n + \mu_{na}) + (1 - \frac{1}{\mathscr{R}_{0n}})\frac{\tau\gamma_n\rho_n}{\mu_n}, \\ \zeta_2 &= \mu_n(\gamma_n + \mu_{na})(\mathscr{R}_{0n} - 1), \\ \zeta_3 &= (\gamma_w + \mu_w + \mu_{wa}), \\ \zeta_4 &= \gamma_w(\mu_w + \mu_{wa})(1 - \mathscr{R}_0^{wolb}). \end{aligned}$$

Using the Routh-Hurwitz criteria, the solutions of the (B.1) have negative real part if all

the coefficients are positive. ζ_1 and ζ_2 are positive provided $\mathscr{R}_{0n} > 1$. Hence, the real part of all the roots of (B.1) is negative if $\mathscr{R}_{0n} > 1$. The roots of (B.2) have negative real part if $\zeta_3 > 0$ and $\zeta_4 > 0$. ζ_3 is always positive while ζ_4 is positive if $\mathscr{R}_0^{wolb} < 1$. Therefore, the real part of all the roots of (B.2) is negative if $\mathscr{R}_0^{wolb} < 1$.

Theorem B.1. *If $\mathscr{R}_{0n} > 1$ and $\mathscr{R}_0^{wolb} < 1$ then the it Wolbachia-free equilibrium point $E_1 = (A_{1n}, F_{1n}, M_{1n}, 0, 0, 0)$ is locally stable and unstable if $\mathscr{R}_0^{wolb} > 1$.*

APPENDIX C

PERSISTENCE/EXTINCTION OF ALGAE

In this appendix, we analyze the algae equation in the absence of *Daphnia* and spores and discuss the dynamics of algal biomass in terms of advection and growth time scales.

In the absence of *Daphnia* and spores, the dynamics of algal biomass is governed by the following partial differential equation;

$$\frac{\partial A}{\partial t} = D_a \frac{\partial^2 A}{\partial z^2} - v_a \frac{\partial A}{\partial z} + r\left(1 - \frac{A}{K}\right) A, \tag{C.1}$$

with zero flux boundary conditions

$$\begin{aligned} D_a \tfrac{\partial A(0,t)}{\partial z} - v_a A(0,t) &= 0, \\ D_a \tfrac{\partial A(L,t)}{\partial z} - v_a A(L,t) &= 0, \end{aligned} \tag{C.2}$$

where L denotes the maximum length of water column, that is $L = z_{\max}$. Using the non-dimensional variables $\tilde{A} = \frac{A}{K}$, $\tilde{z} = \frac{z}{L}$, and $\tilde{t} = \frac{t}{t_s}$, Eq. (C.1) becomes

$$\frac{1}{t_s}\frac{\partial \tilde{A}}{\partial \tilde{t}} = \frac{D_a}{L^2}\frac{\partial^2 \tilde{A}}{\partial \tilde{z}^2} - \frac{v_a}{L}\frac{\partial \tilde{A}}{\partial \tilde{z}} + r\left(1 - \tilde{A}\right)\tilde{A}, \tag{C.3}$$

with zero flux boundary conditions

$$\begin{aligned} \tfrac{D_a}{L} \tfrac{\partial \tilde{A}(0,t)}{\partial z} - v_a \tilde{A}(0,t) &= 0, \\ \tfrac{D_a}{L} \tfrac{\partial A(L,t)}{\partial z} - v_a \tilde{A}(L,t) &= 0. \end{aligned} \tag{C.4}$$

Let $t_d = \frac{L^2}{D_a}$, $t_a = \frac{L}{v_a}$, and $t_r = \frac{1}{r}$ denote the diffusion, advection, and growth time scales. In terms of these time scales, Eq. (C.3) becomes

$$\frac{1}{t_s}\frac{\partial \tilde{A}}{\partial \tilde{t}} = \frac{1}{t_d}\frac{\partial^2 \tilde{A}}{\partial \tilde{z}^2} - \frac{1}{t_a}\frac{\partial \tilde{A}}{\partial \tilde{z}} + \frac{1}{t_r}\left(1 - \tilde{A}\right)\tilde{A}, \tag{C.5}$$

with zero flux boundary conditions

$$\begin{aligned} \frac{D_a}{L}\frac{\partial \tilde{A}(0,t)}{\partial z} - v_a \tilde{A}(0,t) &= 0, \\ \frac{D_a}{L}\frac{\partial A(1,t)}{\partial z} - v_a \tilde{A}(1,t) &= 0. \end{aligned} \tag{C.6}$$

From Eq. (C.5), we observe that when advection time is large compared to the growth time ($t_a >> t_r$), we expect the existence of algae as algae grow faster than it sinks to the bottom. However, when advection time is small compared to the growth time (i.e $t_a << t_r$), the algae sink to the bottom and do not grow.

REFERENCES

[1] O. Diekmann, J. A. P. Heesterbeek, and J. A. J. Metz, "On the definition and the computation of the basic reproduction ratio R_0 in models for infectious diseases in heterogeneous populations," *Journal of Mathematical Biology*, vol. 28, pp. 365 – 382, 1990.

[2] B. Buonomo, "A note on the direction of the transcritical bifurcation in epidemic models," *Nonlinear Anal Model Control*, vol. 20, pp. 38–55, 2015.

[3] K. P. Hadeler and P. Van den Driessche, "Backward bifurcation in epidemic control," *Mathematical Biosciences*, vol. 146, no. 1, pp. 15–35, 1997.

[4] A. Gumel, "Causes of backward bifurcations in some epidemiological models," *Journal of Mathematical Analysis and Applications*, vol. 395, no. 1, pp. 355–365, 2012.

[5] S. Garba, A. Gumel, and M. Bakar, "Backward bifurcations in dengue transmission dynamics," *Mathematical Biosciences*, vol. 215, no. 1, pp. 11–25, 2008.

[6] C. Castillo-Chavez and B. Song, "Dynamical models of tuberculosis and their applications," *Mathematical Biosciences and Engineering*, vol. 1, pp. 361 – 404, 2004.

[7] K. W. Blayneh, A. B. Gumel, S. Lenhart, and T. Clayton, "Backward bifurcation and optimal control in transmission dynamics of west nile virus," *Bulletin of Mathematical Biology*, vol. 72, no. 4, pp. 1006–1028, 2010.

[8] A. A. Lashari, K. Hattaf, G. Zaman, and X.-Z. Li, "Backward bifurcation and optimal control of a vector borne disease," *Applied Mathematics & Information Sciences*, vol. 7, no. 1, pp. 301–309, 2013.

[9] R. Ross, "The prevention of malaria, 2nd edn london," *UK: John Murray*, 1911.

[10] S. Lenhart and J. T. Workman, *Optimal control applied to biological models.* New York: CRC Press, 2007.

[11] S. P. Sethi, *Optimal Control Theory.* Springer, 2019.

[12] W. H. Fleming and R. W. Rishel, *Deterministic and stochastic optimal control.* New York: Springer-Verlag, 1975.

[13] L. S. Pontryagin, V. G. Boltyanskii, R. V. Gamkrelidze, and E. Mishchenko, *The mathematical theory of optimal processes*. New York: Interscience, 1962.

[14] D. L. Smith, T. A. Perkins, R. C. Reiner Jr, C. M. Barker, T. Niu, L. F. Chaves, A. M. Ellis, D. B. George, A. Le Menach, J. R. Pulliam et al., "Recasting the theory of mosquito-borne pathogen transmission dynamics and control," *Transactions of the Royal Society of Tropical Medicine and Hygiene*, vol. 108, no. 4, pp. 185–197, 2014.

[15] M. Kraemer, M. Sinka, K. Duda, A. Mylne, F. Shearer, C. Barker, and G. Hendrickx, "The global distribution of the arbovirus vectors *Aedes aegypti* and *Aedes albopictus*," *eLife*, vol. 4, p. e08347, 2015.

[16] S. Halstead, "Dengue haemorrhagic fever – a public health problem and a field for research," *Bulletin of the World Health Organization*, vol. 58, no. 1, p. 1, 1980.

[17] M. Derouich, A. Boutayeb, and E. Twizell, "A model of dengue fever," *BioMedical Engineering OnLine*, vol. 2, no. 1, p. 4, 2003.

[18] L. R. Bowman, S. Donegan, and P. J. McCall, "Is dengue vector control deficient in effectiveness or evidence?: Systematic review and meta-analysis," *PLoS Neglected Tropical Diseases*, vol. 10, no. 3, p. e0004551, 2016.

[19] K. Hilgenboecker, P. Hammerstein, P. Schlattmann, A. Telschow, and J. H. Werren, "How many species are infected with *Wolbachia*- a statistical analysis of current data," *FEMS Microbiology Letters*, vol. 281, pp. 215 – 220, 2008.

[20] S. P. Sinkins, H. R. Braig, and S. L. O'Neill, "*Wolbachia pipientis*: bacterial density and unidirectional cytoplasmic incompatibility between infected populations of *Aedes albopictus*," *Experimental Parasitology*, vol. 81, pp. 284–291, 1995.

[21] D. A. Joubert and S. L. O'Neill, "Comparison of stable and transient *Wolbachia* infection models in *Aedes aegypti* to block dengue and west nile viruses," *PLoS Neglected Tropical Diseases*, vol. 11, p. e0005275, 2017.

[22] T. J. Walker, P. H. Johnson, L. A. Moreira, I. Iturbe-Ormaetxe, F. D. Frentiu, C. J. McMeniman, Y. S. Leong, Y. Dong, J. Axford, and P. Kriesner, "The *wMel Wolbachia* strain blocks dengue and invades caged *Aedes aegypti* populations," *Nature*, vol. 476, pp. 450 – 453, 2011.

[23] A. A. Hoffmann, B. Montgomery, J. Popovici, I. Iturbe-Ormaetxe, P. Johnson, F. Muzzi, M. Greenfield, M. Durkan, Y. Leong, Y. Dong et al., "Successful establishment of *Wolbachia* in *Aedes* populations to suppress dengue transmission," *Nature*, vol. 476, no. 7361, p. 454, 2011.

[24] A. F. Van den Hurk, S. Hall-Mendelin, A. T. Pyke, F. D. Frentiu, K. McElroy, A. Day, S. Higgs, and S. L. O'Neill, "Impact of *Wolbachia* on infection with chikungunya and yellow fever viruses in the mosquito vector *Aedes aegypti*," *PLoS Neglected Tropical Diseases*, vol. 6, no. 11, p. e1892, 2012.

[25] A. A. Hoffmann, I. Iturbe-Ormaetxe, A. G. Callahan, L. B. Phillips, K. Billington, J. K. Axford, B. Montgomery, A. P. Turley, and S. L. O'Neill, "Stability of the *wMel Wolbachia* infection following invasion into *Aedes aegypti* populations," *PLoS Neglected Tropical Diseases*, vol. 8, p. e3115, 2014.

[26] H. L. C. Dutra, L. M. B. D. Santos, E. P. Caragata, J. B. L. Silva, D. A. M. Villela, R. M. de Freitas, and L. A. Moreira, "From lab to field: the influence of urban landscapes on the invasive potential of *Wolbachia* in brazilian *Aedes aegypti* mosquitoes," *PLoS Neglected Tropical Diseases*, vol. 9, p. e0003689, 2015.

[27] J. A. Jerrery, N. T. Nguyen, V. S. Nam, A. A. Hoffmann, B. H. Kay, and P. A. Ryan, "Characterizing the *Aedes aegypti* population in a vietnamese village in preparation for a *Wolbachia*-based mosquito control strategy to eliminate dengue," *PLoS Neglected Tropical Diseases*, vol. 3, p. e552, 2009.

[28] T. H. Nguyen, H. L. Nguyen, T. Y. Nguyen, S. N. Vu, N. D. Tran, T. N. Le, Q. M. Vien, T. Bui, H. T. Le, and S. Kutcher, "Field evaluation of the establishment potential of *wMelPop Wolbachia* in Australia and Vietnam for dengue control," *Parasites & Vectors*, vol. 8, p. 563, 2015.

[29] L. O'Connor, C. Plichart, A. C. Sang, C. L. Brelsfoard, H. C. Bossin, and S. L. Dobson, "Open release of male mosquitoes infected with a *Wolbachia* biopesticide: field performance and infection containment," *PLoS Neglected Tropical Diseases*, vol. 6, p. e1797, 2012.

[30] D. Ebert, *Ecology, epidemiology, and evolution of parasitism in Daphnia*. National Library of Medicine, 2005.

[31] B. E. Miner, L. De Meester, M. E. Pfrender, W. Lampert, and N. G. Hairston Jr, "Linking genes to communities and ecosystems: *Daphnia* as an ecogenomic model," *Proceedings of the Royal Society B: Biological Sciences*, vol. 279, no. 1735, pp. 1873–1882, 2012.

[32] C. E. Cáceres, G. Davis, S. Duple, S. Hall, A. Koss, P. Lee, and Z. Rapti, "Complex *Daphnia* interactions with parasites and competitors," *Mathematical Biosciences*, vol. 258, pp. 148–161, 2014.

[33] S. R. Hall, A. J. Tessier, M. A. Duffy, M. Huebner, and C. E. Cáceres, "Warmer does not have to mean sicker: temperature and predators can jointly drive timing of epidemics," *Ecology*, vol. 87, no. 7, pp. 1684–1695, 2006.

[34] P. A. Bliman, M. S. Aronna, F. C. Coelho, and M. A. D. Silva, "Ensuring successful introduction of *Wolbachia* in natural populations of *Aedes aegypti* by means of feedback control," *Journal of Mathematical Biology*, vol. 76, pp. 1269–1300, 2018.

[35] H. Hughes and N. F. Britton, "Modeling the use of *Wolbachia* to control dengue fever transmission," *Bulletin of Mathematical Biology*, vol. 75, pp. 796 – 818, 2013.

[36] M. Keeling, F. Jiggins, and J. Read, "The invasion and coexistence of competing *Wolbachia* strains," *Heredity*, vol. 9191, p. 382, 2003.

[37] M. Z. Ndii, R. I. Hickson, and G. N. Mercer, "Modelling the introduction of *Wolbachia* into *Aedes aegypti* mosquitoes to reduce dengue transmission," *The ANZIAM Journal*, vol. 53, pp. 213–227, 2012.

[38] M. Z. Ndii, R. I. Hickson, D. Allingham, and G. N. Mercer, "Modelling the transmission dynamics of dengue in the presence of *Wolbachia*," *Mathematical Biosciences*, vol. 262, pp. 157–166, 2015.

[39] D. Campo-Duarte, D. Cardona-Salgado, and O. Vasilieva, "Establishing *wMelPop Wolbachia* infection among wild *Aedes aegypti* females by optimal control approach," *Appl. Math*, vol. 11, pp. 1011–1027, 2017.

[40] D. Campo-Duarte, O. Vasilieva, D. Cardona-Salgado, and M. Svinin, "Optimal control approach for establishing *wMelPop Wolbachia* infection among wild *Aedes aegypti* populations," *Journal of Mathematical Biology*, vol. 76, pp. 1907–1950, 2018.

[41] Z. Qu, L. Xue, and J. M. Hyman, "Modeling the transmission of *Wolbachia* in mosquitoes for controlling mosquito-borne diseases," *SIAM Journal on Applied Mathematics*, vol. 78, pp. 826–8520, 2018.

[42] L. Xue, C. A. Manore, P. Thongsripong, and J. M. Hyman, "Two-sex mosquito model for the persistence of *Wolbachia*," *Journal of Biological Dynamics*, vol. 11, pp. 216 – 237, 2017.

[43] M. Huang, J. Luo, L. Hu, B. Zheng, and J. Yu, "Assessing the efficiency of *Wolbachia* driven *Aedes* mosquito suppression be delay differential equations," *Journal of Theoretical Biology*, vol. 440, pp. 1 – 11, 2018.

[44] J. Y. B. Zheng, M. Tang, "Modeling *Wolbachia* spread in mosquitoes through delay differential equations," *SIAM Journal of Applied Mathematics*, vol. 74, pp. 743–770, 2014.

[45] L. Hu, M. Huang, M. Tang, J. Yu, and B. Zheng, "*Wolbachia* spread dynamics in stochastic environments," *Theoretical Population Biology*, vol. 106, pp. 32 – 44, 2015.

[46] M. Huang, M. Tang, and J. Yu, "*Wolbachia* infection dynamics by reaction-diffusion equations," *Sci. China Math.*, vol. 58, pp. 77 – 96, 2015.

[47] M. Huang, M. Tang, L. Hu, and B. Zheng, "Qualitative analysis for a *Wolbachia* infection model with diffusion," *Sci. China Math.*, vol. 59, pp. 1249 – 1266, 2016.

[48] M. Turelli and N. Barton, "Deploying dengue-suppressing *Wolbachia*: Robust models predict slow but effective spatial spread in *Aedes aegypti*," *Theoratical Population Biology*, vol. 115, pp. 45–60, 2017.

[49] P. Ross, I. Wiwatanaratanabutr, J. Axford, V. White, N. Endersby-Harshman, and A. Hoffmann, "*Wolbachia* infections in *Aedes aegypti* differ markedly in their response to cyclical heat stress," *PLoS Pathog.*, vol. 13, p. e1006006, 2017.

[50] B. Zheng, M. Tang, J. Yu, and J. Qiu, "*Wolbachia* spreading dynamics in mosquitoes with imperfect maternal transmission," *Journal of Mathematical Biology*, vol. 11, pp. 216–237, 2017.

[51] B. Zheng, W. Guo, L. Hu, M. Huang, and J. Yu, "Complex *Wolbachia* infection dynamics in mosquitoes with imperfect maternal transmission," *Mathematical Biosciences and Engineering*, vol. 15, pp. 523–541, 2018.

[52] B. Zheng and J. Yu, "Characterization of *Wolbachia* enhancing domain in mosquitoes with imperfect maternal transmission," *Journal of Biological Dynamics*, vol. 12, pp. 596–610, 2018.

[53] J. Z. Farkas and P. Hinow, "Structured and unstructured continuous models for *Wolbachia* infections," *Bulletin of Mathematical Biology*, vol. 72, pp. 2067–2088, 2010.

[54] P. V. den Driessche and J. Watmough, "Reproduction numbers and sub-threshold endemic equilibria for compartmental models of disease transmission," *Mathematical Biosciences*, vol. 180, pp. 29–48, 2002.

[55] C. Castillo-Chavez, J. X. Velasco-Hernandez, and S. Fridman, "Modeling contact structures in biology," *Frontiers in Mathematical Biology*, pp. 454–491, 1994.

[56] J. Guckenheimer and P. Holmes, *Nonlinear oscillations, dynamical systems, and bifurcations of vector fields.* New York: Springer-Verlag, 1983.

[57] J. Dushoff, W. Huang, and C. Castillo-Chavez, "Backwards bifurcations and catastrophe in simple models of fatal diseases," *Journal of Mathematical Biology*, vol. 36, pp. 227–248, 1998.

[58] J. Carr, *Applications of centre manifold theory.* New York: Springer-Verlag, 1982.

[59] R. Thomé, H. Yang, and L. Esteva, "Optimal control of *Aedes aegypti* mosquitoes by the sterile insect technique and insecticide," *Mathematical Biosciences*, vol. 223, no. 1, pp. 12–23, 2010.

[60] W. Bock and Y. Jayathunga, "Optimal control of a multi-patch dengue model under the influence of *Wolbachia* bacterium," *Mathematical Biosciences*, p. 108219, 2019.

[61] K. O. Okosun, O. Rachid, and N. Marcus, "Optimal control strategies and cost-effectiveness analysis of a malaria model," *BioSystems*, vol. 111, no. 2, pp. 83–101, 2013.

[62] F. Agusto, "Optimal isolation control strategies and cost-effectiveness analysis of a two-strain avian influenza model," *Biosystems*, vol. 113, no. 3, pp. 155–164, 2013.

[63] O. Sharomi and T. Malik, "Optimal control in epidemiology," *Annals of Operations Research*, vol. 251, no. 1-2, pp. 55–71, 2017.

[64] N. M. Ferguson, D. T. H. Kien, H. Clapham, R. Aguas, V. T. Trung, T. N. B. Chau, J. Popovici, P. A. Ryan, S. L. O'Neill, E. A. McGraw et al., "Modeling the impact on virus transmission of *Wolbachia*-mediated blocking of dengue virus infection of *Aedes aegypti*," *Science Translational Medicine*, vol. 7, pp. 279ra37–279ra37, 2015.

[65] P. Hancock, S. Sinkins, and H. Godfray, "Population dynamic models of the spread of *Wolbachia*," *The American Naturalist*, vol. 177, no. 3, pp. 323–333, 2011.

[66] J. Koiller, M. D. Silva, M. Souza, A. Iggidr, and G. Sallet, "*Aedes, Wolbachia* and dengue," *Inria Nancy-Grand Est*, 2014.

[67] M. Chan and P. Kim, "Modelling a *Wolbachia* invasion using a slow fast dispersal reaction diffusion approach," *Bulletin of Mathematical Biology*, vol. 75, no. 9, pp. 1501–1523, 2013.

[68] Y. Dumont, F. Chiroleu, and C. Domerg, "On a temporal model for the chikungunya disease modeling theory and numerics," *Mathematical Biosciences*, vol. 213, no. 1, pp. 80–91, 2008.

[69] H. Yang, "The basic reproduction number obtained from jacobian and next generation matrices–a case study of dengue transmission modelling," *Biosystems*, vol. 126, pp. 52–75, 2014.

[70] J. Kamgang and G. Sallet, "Global asymptotic stability for the disease free equilibrium for epidemiological models," *Comptes Rendus Mathematique*, vol. 341, no. 7, pp. 433–438, 2005.

[71] H. Chu, T. Chan, and F. Jao, "Gis-aided planning of insecticide spraying to control dengue transmission," *International Journal of Health Geographics*, vol. 12, no. 1, p. 42, 2013.

[72] E. Esu, A. Lenhart, L. Smith, and O. Horstick, "Effectiveness of peridomestic space spraying with insecticide on dengue transmission; systematic review," *Tropical Medicine & International Health*, vol. 15, no. 5, pp. 619–631, 2010.

[73] P. Luz, C. Codeco, J. Medlock, C. Struchiner, D. Valle, and A. Galvani, "Impact of insecticide interventions on the abundance and resistance profile of *Aedes aegypti*," *Epidemiology & Infection*, vol. 137, no. 8, pp. 1203–1215, 2009.

[74] N. Alphey, L. Alphey, and M. B. Bonsall, "A model framework to estimate impact and cost of genetics-based sterile insect methods for dengue vector control," *PLoS One*, vol. 6, no. 10, p. e25384, 2011.

[75] L. S. Sepulveda and O. Vasilieva, "Optimal control approach to dengue reduction and prevention in Cali, Colombia," *Mathematical Methods in the Applied Sciences*, vol. 39, no. 18, pp. 5475–5496, 2016.

[76] M. A. L. Caetano and T. Yoneyama, "Optimal and sub-optimal control in dengue epidemics," *Optimal Control Applications and Methods*, vol. 22, no. 2, pp. 63–73, 2001.

[77] H. S. Rodrigues, M. T. T. Monteiro, and D. F. Torres, "Dynamics of dengue epidemics when using optimal control," *Mathematical and Computer Modelling*, vol. 52, no. 9-10, pp. 1667–1673, 2010.

[78] A. Camacho, F. Saldaña, I. Barradas, and S. Jerez, "Modeling public health campaigns for sexually transmitted infections via optimal and feedback control," *Bulletin of Mathematical Biology*, pp. 1–24, 2019.

[79] W. O. Dias, E. F. Wanner, and R. T. Cardoso, "A multiobjective optimization approach for combating *Aedes aegypti* using chemical and biological alternated step-size control," *Mathematical Biosciences*, vol. 269, pp. 37–47, 2015.

[80] H. O. Florentino, D. R. Cantane, F. L. Santos, and B. F. Bannwart, "Multiobjective genetic algorithm applied to dengue control," *Mathematical Biosciences*, vol. 258, pp. 77–84, 2014.

[81] M. Rafikov, E. Rafikova, and H. M. Yang, "Optimization of the *Aedes aegypti* control strategies for integrated vector management," *Journal of Applied Mathematics*, vol. 2015, 2015.

[82] S. A. Carvalho, S. O. da Silva, and I. da Cunha Charret, "Mathematical modeling of dengue epidemic: control methods and vaccination strategies," *Theory in Biosciences*, pp. 1–17, 2015.

[83] D. Moulay, M. Aziz-Alaoui, and H.-D. Kwon, "Optimal control of chikungunya disease: larvae reduction, treatment and prevention," *Mathematical Biosciences & Engineering*, vol. 9, no. 2, pp. 369–392, 2012.

[84] F. B. Agusto, "Optimal control and cost-effectiveness analysis of a three age-structured transmission dynamics of chikungunya virus," *Discrete & Continuous Dynamical Systems-B*, vol. 22, no. 3, pp. 687–715, 2017.

[85] D. Lasluisa, E. Barrios, and O. Vasilieva, "Optimal strategies for dengue prevention and control during daily commuting between two residential areas," *Processes*, vol. 7, no. 4, p. 197, 2019.

[86] K. O. Okosun, R. Ouifki, and N. Marcus, "Optimal control analysis of a malaria disease transmission model that includes treatment and vaccination with waning immunity," *Biosystems*, vol. 106, no. 2-3, pp. 136–145, 2011.

[87] J. D. Cape, J. M. Beca, and J. S. Hoch, "Introduction to cost-effectiveness analysis for clinicians," *University of Toronto Medical Journal*, vol. 90, no. 3, 2013.

[88] H. S. Rodrigues, M. T. T. Monteiro, and D. F. Torres, "Vaccination models and optimal control strategies to dengue," *Mathematical Biosciences*, vol. 247, pp. 1–12, 2014.

[89] S. K. Nandi, S. Jana, M. Mandal, and T. Kar, "Mathematical analysis of an epidemic system in the presence of optimal control and population dispersal," *Biophysical Reviews and Letters*, vol. 13, no. 01, pp. 1–17, 2018.

[90] P. Rodrigues, C. J. Silva, and D. F. Torres, "Cost-effectiveness analysis of optimal control measures for tuberculosis," *Bulletin of Mathematical Biology*, vol. 76, no. 10, pp. 2627–2645, 2014.

[91] G. T. Tilahun, O. D. Makinde, and D. Malonza, "Modelling and optimal control of pneumonia disease with cost-effective strategies," *Journal of Biological Dynamics*, vol. 11, no. sup2, pp. 400–426, 2017.

[92] G. T. Tilahun, O. D. Makinde, and D. Malonza, "Co-dynamics of pneumonia and typhoid fever diseases with cost effective optimal control analysis," *Applied Mathematics and Computation*, vol. 316, pp. 438–459, 2018.

[93] C. Hoek, D. Mann, and H. M. Jahns, *Algae: an introduction to phycology*. Cambridge, Cambridge University Press, Cambridge, 1995.

[94] C. S. Reynolds, *The ecology of freshwater phytoplankton*. Cambridge University Press, 1984.

[95] J. Huisman, P. van Oostveen, and F. J. Weissing, "Species dynamics in phytoplankton blooms: incomplete mixing and competition for light," *The American Naturalist*, vol. 154, no. 1, pp. 46–68, 1999.

[96] J. Huisman and B. Sommeijer, "Population dynamics of sinking phytoplankton in light-limited environments: simulation techniques and critical parameters," *Journal of Sea Research*, vol. 48, no. 2, pp. 83–96, 2002.

[97] C. A. Klausmeier and E. Litchman, "Algal games: The vertical distribution of phytoplankton in poorly mixed water columns," *Limnology and Oceanography*, vol. 46, no. 8, pp. 1998–2007, 2001.

[98] B. A. Hodges and D. L. Rudnick, "Simple models of steady deep maxima in chlorophyll and biomass," *Deep Sea Research Part I: Oceanographic Research Papers*, vol. 51, no. 8, pp. 999–1015, 2004.

[99] A. B. Ryabov, L. Rudolf, and B. Blasius, "Vertical distribution and composition of phytoplankton under the influence of an upper mixed layer," *Journal of Theoretical Biology*, vol. 263, no. 1, pp. 120–133, 2010.

[100] J. T. Kirk, *Light and photosynthesis in aquatic ecosystems*. Cambridge university press, 1994.

[101] S. A. Condie and M. Bormans, "The influence of density stratification on particle settling, dispersion and population growth," *Journal of Theoretical Biology*, vol. 187, no. 1, pp. 65–75, 1997.

[102] J. Huisman and B. Sommeijer, "Maximal sustainable sinking velocity of phytoplankton," *Marine Ecology Progress Series*, vol. 244, pp. 39–48, 2002.

[103] J. Huisman, M. Arrayás, U. Ebert, and B. Sommeijer, "How do sinking phytoplankton species manage to persist?" *The American Naturalist*, vol. 159, no. 3, pp. 245–254, 2002.

[104] R. Bhutiani, D. Khanna, and K. S. Chandra, "Light-limited population dynamics of phytoplankton: modeling light and depth effects," *The Environmentalist*, vol. 29, no. 1, pp. 93–105, 2009.

[105] J. T. Paul, N. Ramaiah, and S. Sardessai, "Nutrient regimes and their effect on distribution of phytoplankton in the Bay of Bengal," *Marine Environmental Research*, vol. 66, no. 3, pp. 337–344, 2008.

[106] K. Yoshiyama and H. Nakajima, "Catastrophic transition in vertical distributions of phytoplankton: alternative equilibria in a water column," *Journal of Theoretical Biology*, vol. 216, no. 4, pp. 397–408, 2002.

[107] J. P. Mellard, K. Yoshiyama, E. Litchman, and C. A. Klausmeier, "The vertical distribution of phytoplankton in stratified water columns," *Journal of Theoretical Biology*, vol. 1, pp. 16–30, 2011.

[108] K. Yoshiyama, J. P. Mellard, E. Litchman, and C. A. Klausmeier, "Phytoplankton competition for nutrients and light in a stratified water column," *The American Naturalist*, vol. 174, no. 2, pp. 190–203, 2009.

[109] S. Hsu, F. Wang, and X. Zhao, "Global dynamics of zooplankton and harmful algae in flowing habitats," *Journal of Differential Equations*, vol. 255, no. 3, pp. 265–297, 2013.

[110] M. Scheffer, *Ecology of shallow lakes*. Springer Science & Business Media, 1997, vol. 22.

[111] Z. Rapti, T. E. S. Merrill, B. Mueller-Brennan, J. H. Kavouras, and C. E. Cáceres, "Indirect effects in a planktonic disease system," *Theoretical Population Biology*, vol. 130, pp. 132–142, 2019.

[112] W. Wang and X. Zhao, "Basic reproduction numbers for reaction-diffusion epidemic models," *SIAM Journal on Applied Dynamical Systems*, vol. 11, no. 4, pp. 1652–1673, 2012.

[113] W. E. Schiesser and G. W. Griffiths, *A compendium of partial differential equation models: method of lines analysis with Matlab*. Cambridge University Press, 2009.